

# Behavior stability and individual differences in Pavlovian extended conditioning

Gianluca Calcagni

Instituto de Estructura de la Materia, CSIC, Serrano 121, 28006 Madrid, Spain

Ernesto Caballero-Garrido

National Association of Researchers, Twenty-First Century, Facultad de Psicología, UNED, Calle de Juan del Rosal, 10, Madrid, Spain

Ricardo Pellón

28040 Madrid, Spain

May 27, 2018

How stable and general is behavior once reached maximum learning? To answer this question and understand post-acquisition behavior and its related individual differences, we propose a psychological principle that naturally extends the basic associative single-cue Rescorla–Wagner model (which may also be called Hull model) of Pavlovian conditioning to (i) a framework of *dynamical models* predicting resistance to learning in the first few sessions followed by an over-optimal response peak. In turn, (ii) the theory can be further extended to describe response fluctuations by the laws of *quantum mechanics*. (iii) We also introduce an independent model characterized by the presence of a *stochastic noise* of cognitive origin. We ran an unusually long experiment with 32 rats over 3960 trials, where we excluded habituation and other well-known phenomena as sources of variability in the subjects' performance. There is weak to positive evidence that Hull model is the best nonlinear regression to averaged data only for a minority of the subjects, while its dynamical extension (i) can explain the totality of data. The noise encountered in all individual responses is white, thus confirming the simplest version of model (iii) but standing in contrast with the colored-noise findings in human performance. Finally, data are compatible with the quantum extension (ii), although experimental uncertainties dominate the result. On the other hand, data do not favor models with (iv) a long-memory effect or (v) where response variability is solely described by a random fractal.

*Keywords:* Pavlovian conditioning, Hull/Rescorla–Wagner model, Extended training, Inhibition with reinforcement, Individual differences, Bayes information criterion, Stochastic learning models,  $1/f$  noise

## Contents

		Discussion . . . . .	12
<b>INTRODUCTION</b>	<b>2</b>	<b>DYNAMICAL MODELS OF INDIVIDUAL BEHAVIOR</b>	<b>13</b>
<b>HULL MODEL: SINGLE-CUE RESCORLA–WAGNER</b>	<b>4</b>	Motivation: least-action principle and fine tuning . . . . .	13
<b>A LONG EXPERIMENT ON PAVLOVIAN CONDITIONING</b>	<b>5</b>	Theory . . . . .	15
Subjects . . . . .	5	Data analysis: comparison with Hull model . . . . .	15
Materials . . . . .	5	Discussion . . . . .	16
Experimental design . . . . .	6	<b>COLORED STOCHASTIC MODEL OF INDIVIDUAL BEHAVIOR</b>	<b>16</b>
Procedure . . . . .	6	Motivation and spectral analysis . . . . .	16
Results . . . . .	6	Theory . . . . .	19
		Data analysis: comparison with Hull model . . . . .	20
		Discussion . . . . .	21
		<b>QUANTUM HULL MODEL</b>	<b>21</b>
		Theory . . . . .	22
		Empirical evidence of predictions . . . . .	23

E-mail: g.calcagni@csic.es, ernesto.caballero@psi.uned.es

arXiv:1806.01778v2 [q-bio.NC] 26 Aug 2018

Discussion . . . . . 24

**GENERAL CONCLUSIONS** . . . . . **25**

**Appendix A DYNAMICAL HULL MODEL WITH FRICTION** . . . . . **26**

**Appendix B MULTI-CUE AND VARIABLE-SALIENCE MODELS** . . . . . **27**

Classical dynamics of the Rescorla–Wagner model . . . . . 28

Classical dynamics of the Mackintosh model and its nonlinear approximation . . . . . 28

**Appendix C OTHER MODELS OF FLUCTUATING RESPONSE** . . . . . **30**

Fractional stochastic model . . . . . 30

Random-fractal model . . . . . 31

**Appendix D SPECTRAL ANALYSIS** . . . . . **32**

**Appendix E CONSTRUCTION OF THE QUANTUM HULL MODEL** . . . . . **32**

Preliminaries: classical setting . . . . . 32

Quantization . . . . . 34

Predictions . . . . . 35

**Appendix F POTENTIAL WITH INFINITE BARRIERS** . . . . . **37**

**References** . . . . . **38**

**INTRODUCTION**

How stable is behavior when there is nothing more to learn? Much debate has been flourished around this basic question since the earliest studies of animal conditioning (Pavlov, 1927), especially after the first efforts to make the discipline theoretically quantitative with a mathematical approach (Hull, 1943). Observations point towards an instability of the response in extended training. In the context of discrimination experiments of operant conditioning, extended training was studied in relation with behavioral contrast and the peak-shift effect. Pigeons trained for 60 days with interspersed generalization testing showed a gradual response decrease (Terrace, 1966). In an experiment lasting 64 sessions, Hearst (1971) did not observe this decrease from peak responding, sometimes called overtraining effect (as a reduction in behavioral contrast), inhibition with reinforcement, or post-peak depression (see Kimmel and Burns, 1975, for an early review and other references). Extending the training to 105-125 days, the response decrease was found to be a subject-dependent and transient effect, giving way to a greater variety of patterns characterized by apparently random response fluctuations and, in general, remarkable individual differences (Dukhayil and Lyons, 1973). An attenu-

ated conditioned responding with extended reinforced training has been observed also in the case of Pavlovian conditioning, where is modulated by the context (Bouton et al., 2008; Overmier et al., 1979; Urcelay et al., 2012). Post-peak depression is a rather short-scale phenomenon usually achieved within a few sessions and not too many trials. For instance, the experiments with dogs by Overmier et al. (1979) showed response decrease on a time scale of 300 trials. In the experiments of Bouton et al. (2008), the groups of subjects received about two weeks of training. In the case of Urcelay et al. (2012), they were given 5 to 6 sessions of 5 to 60 trials, for a maximum of about 360 trials. For acquisition of fear conditioning, 100 pairings during 10 days are sufficient (Pickens et al., 2009). However, longer-term cases are known, such as the first documented case of inhibition with reinforcement. Pavlov (1927, Lecture XIV) reported experiments with a dog that spanned several years and that showed a progressive decrease in the conditioned response when the same type of stimuli were applied. On the other extreme of the spectrum, response fluctuations have been registered also on the very short time scale of trial by trial (Ayres et al., 1979).

The prototypical learning curve of Pavlovian conditioning in the presence of a single cue was described by Hull in his renown book (Hull, 1943), while a few years later Estes (1950) and Bush and Mosteller (1951a) wrote down a precise mathematical model (somewhat implicit in Hull’s discussion) in terms of response probability, and that gave rise to a linear incremental equation. For operational reasons, the latter was replaced by the association strength  $v$  by Rescorla and Wagner (1972). Due to this complicated genesis, the resulting single-cue model in terms of  $v$  has received several names: Hull, Hull–Spence, Estes, Bush–Mosteller, and single-cue Rescorla–Wagner, among others (Le Pelley, 2004; Wagner & Vogel, 2009). For brevity, we will call it *Hull model* here.

Including Hull’s, most conditioning models are about learning, which means that their simulation of the execution or reaction of the subject once the asymptote is reached has not been validated extensively. A classic problem consists in that, when one has learned everything, it is not convenient to keep giving attention to the stimuli of the task and there is a transition to a more automatic mode of execution. In order to explain this transition, many Pavlovian models (e.g., the Pearce–Hall model, 1980) distinguish between automatic and controlled processing. Still, this difference plays a role in the first few sessions of training and it does not address the issue of what happens after thousand of trials. Going beyond associative models, the opponent-processes theory (Solomon and Corbit, 1974) and the SOP model (Wagner, 1981) provide a partial, but not entirely comprehensive, explanation of post-peak depression and related phenomena.

These studies also highlight the parallel issue of individual

differences. An obvious feature of individual plots is their non-smoothness and erratic nature, to the point where any vestige of the clean, smooth learning curve of averaged data may be completely lost. When averaging, information on individuals is usually lost. This concern is not new and it was voiced already in early days of the discipline (Hayes, 1953; Merrill, 1931; Sidman, 1952) and retaken into consideration in recent years (Blanco and Moris, 2017; Gallistel, 2012; Gallistel et al., 2004; Glautier, 2013; Jaksic et al., 2018; Young, 2018; see especially the refreshing point of view of Smith and Little, 2018). As Sidman (1952) pessimistically put it, “[i]ntra-organism variability may be so great as to obscure any lawful relation.” Smooth group-learning curves have even been stigmatized as an artifact, since step-like sudden acquisition has been observed in several experiments (Gallistel et al., 2004). Despite these warnings, however, averaging the data can be a useful procedure (Estes, 1956) and is still commonly employed in the great majority of publications, even those where individual responses are analyzed (Mazur and Hastie, 1978).

All this literature helps to refocus the question we proposed in the opening and to give the term “stability” two different meanings. One corresponds to intra-subject behavior stability: the variability of the individual response throughout the experiment. The other is inter-subject stability, in the sense of the range and variety of patterns that individual differences can take when the performance of experimental subjects is compared. Both intra- and inter-subject stability can refer to phenomena spanning trials (short-term stability) or sessions (long-term stability). Short-term stability usually pertains to the initial acquisition stage of conditioning, where the subjects are in the process of acquiring maximal learning but have not quite reached the asymptote of their learning curve. Long-term stability is more related to response at the asymptote. Response variations in the form of random fluctuations may be regarded both as short-term effects (they occur as gradients from one session to another) and as long-term, since they can span several sessions (or when one detects oscillation-like features with a long period).

To the best of our knowledge, the mainstream of mathematical associative models starting from Hull’s predicts an indefinitely long asymptotic permanence of execution in the learning process, for each and any subject. Neither individual differences nor response fluctuations are considered in most analytic treatments of the theories, notwithstanding the number of exceptions to this generalized trend, some of which we have mentioned above. A reversion of this trend has been seen recently, when new models have arisen that give more importance to individual differences. The multiple-state learning model of Blanco and Moris (2017) and the MECA model of Glautier (2013) are examples. Also, Estes’s stimulus sampling theory (1950) is one of the earliest attempts to quantify and explain variability in learning

progress, as due to fluctuations in environmental and internal factors. The issue at stake here is not just whether there exist superior *ad hoc* fits to averaged data than that provided by Hull model with one cue. It is already known that other types of learning curves can fare better than the exponential profile (see Eq. (4) below), even at the individual level. A power-law curve (Newell and Rosenbloom, 1981) or the accumulation model (Mazur and Hastie, 1978) are two instances. Rather, here we are interested in the problem of stability in the double sense specified above and, moreover, any new model should arise as an underlying theory rather than just a tailor-made learning curve.

With the aim to study both very long-term stability and individual differences, we present the results of an experiment of Pavlovian conditioning that ran through a total of 3960 trials. The first goal of this paper is to check how variable is behavior in the long-term post-acquisition phase. We do find fluctuations around the asymptote, both on a trial-by-trial and a session-by-session basis, but not statistically significant. In other words, behavior is fairly stable even when the subject is no longer learning. This provides a validation of Hull (Rescorla–Wagner single-cue) associative model even in the not-so-often explored plateau region of the learning curve, far away from initial acquisition. However, the fit of the data of individual subjects is much more unstable and one may wonder whether there exist a quantitative model accounting for this variability. Our second goal is to explore several associative models extending Hull’s and Rescorla–Wagner’s in a most natural way, introducing a psychological principle that, in analogy with the same tool used in classical<sup>1</sup> mechanics physics, we will call of *least action*. This principle states that learning processes must be described as dynamical systems, where *dynamical* means that there exists a quantity (the *action*) that must be minimized when the association strength is changed during conditioning. Independently, we will also introduce a model governed by a random noise. Through a detailed statistical and spectral analysis, we show that, despite the large fluctuations of the subjects’ behavior, Hull model is still a good fit to data, except in 4 out of 15 experimental subjects. An extension (not a competitor) of Hull model based on the principle of least action and predicting resistance to learning in the first sessions provides a better fit to the data of this 20% of the sample, according to both Bayesian and Akaike Information Criteria. Although the existence of a learning asymptote has been questioned in the past (Gallistel et al., 2004), we find its presence to be a robust feature of all the models. The formalism we propose can be extended to the multi-cue and varying-salience cases and can account for the non-normative performance of some

<sup>1</sup>To avoid an otherwise inevitable confusion, in this paper we use the term “classical” always in the sense of physics, calling the traditional associative models of conditioning “Pavlovian.”

subjects.

One of the main novelties of this work is that traditional associative models are not extended in an *ad hoc* way, but by using a rigorous top-down procedure leading to a natural (in the sense of logic-based) conclusion, closer to a theory rather than a phenomenological model. To that aim, we need mathematics more advanced than those available to a large portion of the readership in psychology, but the payback offered in terms of explanation of the data may be worthwhile. In order to keep the presentation simple, we will introduce all models in a pedagogical way, confining the most rigorous parts to appendices.

The plan of the article is the following. We first review Hull's associative model in section *Hull model: single-cue Rescorla–Wagner* and clarify whether it should be applied to individual subjects or to their average. In order to clarify the type of phenomena we would like to explore, in section *A long experiment on Pavlovian conditioning*, we present a 3960-trial-long experiment, with a first analysis centered on the average learning curve. Two alternative models of individual conditioning are discussed in sections *Dynamical models of individual behavior* (a general framework where we reformulate Hull model and introduce a new model where subjects initially show resistance to learning) and *Colored stochastic model of individual behavior*, where we formulate a descriptive model and contrast it with the data, finding that the latter are always characterized by white noise. In section *Quantum Hull model*, we present a predictive theory where random fluctuations of the subject response are described by the mathematics of quantum mechanics. Data neither rule out nor confirm this theory and one cannot discard the interpretation of response variability as quantum fluctuations. Final remarks are collected in section *General conclusions*. The Appendices are devoted to material that would disrupt the flow of the main text. Appendix A presents dynamical associative models and, in particular, the Hull model with friction. In Appendix B, we consider relevant applications of the dynamical approach for future checks of the theory, especially to the Rescorla–Wagner and Mackintosh models. In Appendix C, we consider scenarios which are excluded, or at least not confirmed, by the data: one encoding a long-memory effect and one where response variability is described by a random fractal. The basics of spectral analysis are discussed in Appendix D. In Appendix E, we present the detailed mathematical construction of the quantum model, while in Appendix F some technical considerations related to it are collected.

### HULL MODEL: SINGLE-CUE RESCORLA–WAGNER

According to the model developed by C. L. Hull, the association between the conditioned stimulus (CS) and the unconditioned stimulus (US) in Pavlovian training can be mea-

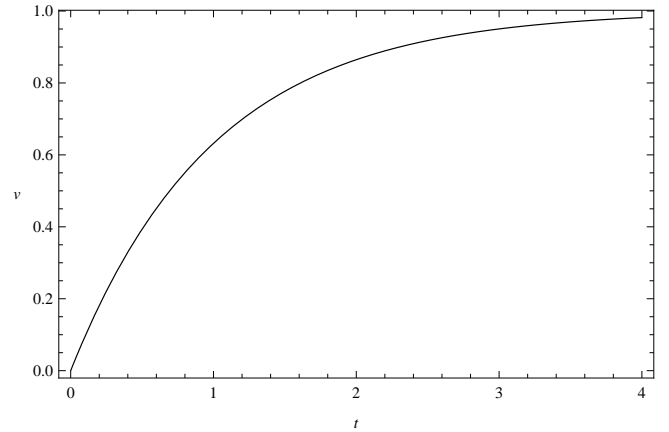


Figure 1. Learning curve: the solution (3)  $v(t)$  (vertical axis) of Hull's conditioning model (2) as a function of time  $t$  (horizontal axis), for  $c = \lambda = 1$  and  $\alpha\beta = 1$  (excitatory conditioning).

sured, at the  $n$ -th trial or session, by the operational variable  $v_n$ , called association strength. Usually in the literature, this is denoted with  $V_n$ , but here we use a small letter to avoid confusion with the potentials introduced below. The change  $\Delta v_n := v_n - v_{n-1}$  in the strength of the association at the  $n$ -th trial is

$$\Delta v_n = \alpha\beta(\lambda - v_{n-1}), \quad n = 1, 2, 3, \dots, \quad (1)$$

where  $0 \leq \alpha \leq 1$  is the salience of the CS,  $0 \leq \beta \leq 1$  is the salience of the US, and  $0 \leq \lambda \leq 1$  is the magnitude of the US. For convenience, we promote the trial sequence  $n = 1, 2, 3, \dots$  to a continuous time process described by a continuous time variable  $t$ . This approximation is valid as long as we consider many trials or sessions. In this way, we can recast Eq. (1) as the first-order differential equation

$$\dot{v} = \alpha\beta(\lambda - v), \quad (2)$$

where a dot denotes a derivative with respect to time,  $\dot{v} := dv(t)/dt$ . Its general solution is

$$v(t) = \lambda - ce^{-\alpha\beta t}, \quad (3)$$

where  $c$  is a constant. The initial condition at  $t = 0$  of this solution is  $v(0) = \lambda - c$ , while  $v(+\infty) = \lambda$ . Therefore, for excitatory conditioning  $c = \lambda > 0$  (Fig. 1), while for extinction  $\lambda = 0$  and  $c < 0$ , so that  $v = |c| \exp(-\alpha\beta t)$  decreases in time.

In this article, we will consider only excitatory conditioning and attempt, among other possibilities, to fit data with the monotonic learning curve

$$v_{\text{excit}}(t) = \lambda \left(1 - e^{-\alpha\beta t}\right). \quad (4)$$

This theoretical curve has two free parameters:  $\lambda$  and the product  $\alpha\beta$ . In the experiment below, we will not be able to determine the salience of the CS and US separately.

At the risk of stating the obvious, it should be noted that there are two ways in which to interpret Eqs. (2) and (4). One is as an associative model for individuals, in which case  $v(t)$  is the association strength at a given time  $t$  of a given subject. If Hull model were a reliable description of reality, all subjects should obey the model with reasonable accuracy and differ in their behavior only in the value of the parameters  $\lambda$ ,  $\alpha$ , and  $\beta$  in the aforementioned equations. However, this interpretation is too restrictive and does not allow for individual differences in the learning process, something that any experimentalist would recognize as inevitable. However, if the majority of subjects obeyed Hull model, then the latter could be regarded as valid in average, in which case we will make it explicit that the association strength appearing in Eqs. (2) and (4) should be replaced by the average  $\langle v \rangle := \sum_{i=1}^N v_i / N$  over the subjects:

$$\dot{\langle v \rangle} = \alpha\beta(\lambda - \langle v \rangle), \quad \langle v \rangle_{\text{excit}}(t) = \lambda(1 - e^{-\alpha\beta t}). \quad (5)$$

As we will see in this article, Hull model is a good description of Pavlovian learning both for individuals and in average. However, we do find individual differences which can be better described by an extension of the model which we will dub “dynamical,” and which does not improve averaged data significantly. Therefore, we will strictly keep the distinction between models for individuals ( $v$ ) and in average ( $\langle v \rangle$ ).

## A LONG EXPERIMENT ON PAVLOVIAN CONDITIONING

### Subjects

32 male Wistar Han non-naïve rats (Charles River Laboratories) were used. These rats proceeded from three different operant-conditioning experiments conducted in the same laboratory, but they had no prior overt training in Pavlovian conditioning nor they had been trained in the same apparatus. The characteristics of previous experiments were such that any significant influence on the present work is most unlikely.

Four subjects began the experiment with 43 weeks of age and ended 15 weeks later. 18 subjects started with 39 weeks and 10 subjects with 21 weeks; all of them ended 10 weeks later. The average age at the beginning and end of the experiment was of, respectively,  $33.9 \pm 8.8$  and  $44.5 \pm 9.5$  weeks.

The subjects were kept in individual identical cages of size 19 (h)  $\times$  23.5 (w)  $\times$  35.5 (l) cm (non-enriched environment) with unrestricted water supply and a restricted diet of food to maintain 100% of their theoretical body weight. The average theoretical weight was of  $418 \pm 25$  g. In theory, therefore, animals were neither food nor water deprived.

This study received approval by the local research ethics committee.

### Materials

Four identical conditioning boxes were used. Each experimental box was 35.5 cm in length by 29 cm in height and 24.5 cm in depth, and was enclosed within a sound-attenuating chest, equipped with a fan, which provided ventilation and masking noise, a fluorescent lamp (20 W), which served as houselight, and a window for observation in the frontal part. The front panel of each experimental chamber was of aluminum, the posterior panel was of black metal, and the remaining walls were made of transparent plexiglass.

Two syringes connected to water bombs were installed in the back of the front panel. The water-bomb device was designed at the Department of Basic Psychology I at UNED and made by CIBERTEC (Madrid, Spain). It consisted in a 24 V DC pinch-type electrovalve by ASCO placed between a 60 ml depot and a capillary exit, connected by a silicon tube (1.74 mm external diameter, approximately 10 cm length). The exit was connected to a metal water tube, 5 mm of diameter, which protruded 4 cm into the experimental chamber. Each water tube was located at the sides of the front panel (10 cm from the food magazine). Throughout the experiment, only one tube was active, the other one being inert. The contact of the tongue of the rats with the water tube resulted in the activation of the bomb during 0.1 s, whenever this response was reinforced; otherwise licks were registered and the liquid was not delivered.

As for the US, we prepared two solutions of water and saccharin (sodium saccharin hydrate, Sigma-Aldrich, St. Louis, MO) at 0.1% (1 g/l) and 0.2% (2 g/l), respectively, less than aversive concentrations ( $\gtrsim 0.3\%$ ), much less than toxic dosage (14.2 g/Kg for rats), and for a much shorter time inducing liver inflammation (0.3 g/l for six months for mice; Bian et al., 2017); see also Fujita et al. (2009). The 0.1% concentration was strong enough for subjects to discriminate it from plain water (saccharin concentrations as low as 0.05% have been used in the literature; see Swithers and Hall, 1994). A 0.2% concentration was successfully used in the literature as an appetitive stimulus (Bernal et al., 2008; Scalfani and Ackroff, 1994). The solutions were conserved in two one-liter jars in a laboratory fridge at constant temperature and were freshly remade weekly according to consumption by the subjects during the experimental sessions. The jars were taken out of the fridge to reach laboratory temperature (21°C) before the start of the first session of the day.

Experimental and control programs were written in PASCAL language and executed in the boxes via MED-PC IV® (Med Associates Inc., Fairfax, VT), which also recorded the responses. Data analysis was performed with Microsoft Excel and Wolfram Mathematica.

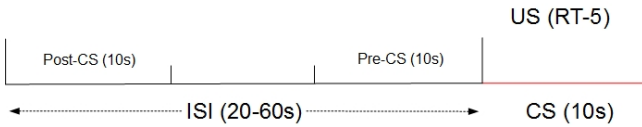


Figure 2. Structure of a trial for the experimental groups as described in the text.

## Experimental design

The experiment was divided into three phases. In the first phase of *pre-training*, subjects were exposed to the basic functioning of the liquid dispenser in the conditioning boxes. Drops of saccharin solution of the concentration corresponding to the rat's group were delivered according to a variable-time 5 s schedule (VT-5), implemented as a uniform random distribution between 3 and 7 s with steps of 1 s. Each lick was reinforced by the delivery of another drop via a fixed-ratio schedule (FR-1). Each session of pre-training lasted 10 minutes and was preceded by 30 s of darkness, lasting in total 10'30".

The second phase (*training*) consisted in sessions of total duration of 2259 s (about 37'40"). After 30 s of darkness, each box was lighted and the session went through for 44 trials, ending with 10 s of inactivity. Figure 2 is a scheme of a trial for the experimental groups. An inter-trial interval (ITI) of variable length averaging 40 s, realized by a uniform random distribution between 20 and 60 s with steps of 4 s, was followed by the CS, a tone of 85 db, 600 Hz, and a fixed 10 s duration. The intensity of the tone was well above the average ambient noise inside each box (65 db). During the CS, a US consisting in one drop of saccharin solution was delivered at random intervals of 5 s (RI-5). A random-interval schedule (Millenson, 1963) establishes a fixed non-zero chance of US delivery every second. In particular, an RI-5 has a 20% chance per second to deliver one drop, hence one drop falls every  $1\text{ s}/0.2 = 5\text{ s}$  in average, i.e., twice per CS. Thus, an average of 88 US per session were delivered, roughly ranging between 70 and 110 drops. Each session ended 10 s after the end of the last CS.

The structure of the trials for control groups was the same except for the schedule of delivery of the US: an RI-25 spanning the whole duration of the trial, so that a US could equally occur during the CS and at any other moment of the trial. This corresponds to the delivery of the same amount of solution per trial as for the experimental groups: one drop every 25 seconds in average, 4% chance of delivery per second, average of 2 drops per trial.

The third and last phase was *extinction*, the only difference with respect to previous training sessions being the absence of liquid in the drinking dispensers.

## Procedure

The subjects were distributed into four groups of 8 rats: *Group 1* (subjects 1-1, 1-2, ..., 1-8) for a US consisting in one drop of 0.1% saccharin solution, *Group 2* (subjects 2-1 to 2-8) for a US consisting in one drop of 0.2% saccharin solution and two control groups with the same concentration (*Group 1C*, subjects 1C-1 to 1C-8, 0.1%; *Group 2C*, subjects 2C-1 to 2C-8, 0.2%) but randomized US delivery as explained in the previous subsection. Although the subjects were naïve in terms of Pavlovian explicit training, their provenance from three operant experiments was counterbalanced in each group as an extra measure of precaution to minimize the effect of uncontrollable variables due to their past history.

On the first day, all subjects went through the phase of pre-training, consisting in two consecutive sessions of the pre-training described in the previous subsection. On the same day or the day after, session 1 of the training phase was run upon the subjects. The total duration of the experiment was 90 sessions, run once or twice per day with an inter-session interval ranging from a minimum of 1 hour and 30 minutes to about 3 hours and 30 minutes. The day after session 90, we moved all subjects through two consecutive sessions of extinction.

## Results

To compare data with the theoretical model, one has to be careful about the identification of the association strength. In our experimental design, the US is presented simultaneously with the CS and one must account for the responses directly due to the US. For this reason, we subtract the number of US (which varies from trial to trial and from session to session), to the total number of licks per session and we identify

$$v = (\text{number of licks during CS}) - (\text{number of US}). \quad (6)$$

Thus, whenever we talk about licks during the CS *in session-by-session* data, we always imply that the number of unconditioned responses (responses following the delivery of an US) has been discounted. In this way, at the beginning of training animals responded only upon presentation of the US and the total number of licks is of the same order of magnitude as the number of US presented. A minor issue is that under-response generates negative values of  $v$ , but this does not correspond to inhibition. While under-response at the beginning of training means that the animal does not know that the CS predicts the US, inhibition would imply that the animal knows that the CS predicts the no-US. Since negative  $v$ 's appear only in the very first sessions, this feature does not influence whatsoever the focus of our research on the rest of the data.

In Eq. (6), we defined unconditioned responses as those occurring in the presence of the US and assumed that the

number of US is equivalent to the number of unconditioned responses. However, this assumption does not account for the following situation. It could be that, sometimes, the subject did not lick upon delivery of the US and that it licked instead afterwards, in the absence of the US (vacuum licking). Although a single drop stayed clung to the dispenser, the short delivery of two US could make the merger of the first and second drop fall before the animal could lick, at which point vacuum licking would take place. All these fine details are not important for the final interpretation of the results, because replacing (6) with a different operational definition of  $v$  would lead to very small quantitative differences. For example, we checked that considering, in alternative, the number of licks during the CS (not discounting the number of US), the number of licks per reinforcer (number of licks during CS)/(number of US), or the number of CS licks minus the number of post-CS licks does not change the plots qualitatively, and response variability remains at the same levels.

In *trial-by-trial* data, we will not subtract the number of US to the actual response by the animal. The reason is that we will be interested in these data when considering the noise component of the signal (see below for details). A randomized US delivery would produce a white noise averaging to zero and of much smaller amplitude than any other source of noise (statistical error or some intrinsic effect to be checked upon).

Before commenting on the main data, some general remarks about the experimental design are in order.

- Unrestricted access to water away from experimental sessions and a controlled diet set at 100% of the theoretical body weight guaranteed that the response of the subjects was not driven by either thirst or hunger. This was done to isolate purely associative effects beyond Hull model.

- The choice of a tone was made to avoid sign tracking and reduce alternative activities inside the box.

- Randomization of the inter-trial interval prevents the subject to use the latter as a predictor of the US, thus guaranteeing that the association is made between the CS and the US only.

- The design of simultaneous conditioning (US delivered during the CS instead of after) was forced upon us by some unavoidable technical characteristics of the available conditioning boxes. When the electrovalve open to release the drop of saccharin solution, the mechanism produces a click sound. We checked in a pilot experiment with delayed conditioning that rats are, in general, much more sensitive to sudden noises than continuous ones, and that the click sound of the electrovalve overshadowed the tone. While in the pilot experiment the subjects waited for the click to lick, and licked only enough to collect the US, in the experiment with simultaneous conditioning design they waited for the auditory CS, since they could only predict that the electrovalve would click during the tone. Qualitative observations showed

that the rats licked also before the click, and that overall they licked much more than in the pilot experiment. As we will see below, simultaneous conditioning is as effective as the delayed one.

- The present design allows one to exclude behavioral changes due to non-associative factors such as satiation and fatigue. The subjects had daily access only to a very limited amount of reinforcer (about 100 drops per session), much lower than the quantity they can assume in a session of the same duration when free access is granted (several thousands of drops, as we checked in a pilot experiment conducted with a different set of animals).

- We checked explicitly that week-end or bank-holiday breaks did not have any impact on the subjects' performance, nor did variations of the time of the day at which sessions were executed. In a pilot experiment conducted with other rats, we checked that inter-session intervals below 40 minutes could have an effect on the response, hence the conservative lower bound of 90 minutes.

Also, concerning the animals:

- We found no correlation between the starting or final age of the subjects and their response. This excludes spurious effects due to the subjects not coming from the same batch.

- The data of one rat (subject 1-8) were eliminated from the analysis due to its poor health.

Figures 3 and 4 show the average of the raw (non-normalized) data for all groups. Notice that we did not subtract the US in the pre-CS, CS, and post-CS trendlines of control data, since they are equally affected by the unconditioned response (the US are evenly distributed in the whole session).

Using Hull model (5) on the raw averaged data, we obtain the fits (Fig. 3):

$$\text{Group 1: } \quad \lambda = 540.1 \pm 7.1, \quad \alpha\beta = 0.129 \pm 0.011, \\ r^2 = 0.99, \quad \sigma = 55.8, \quad (7a)$$

$$\text{Group 2: } \quad \lambda = 687.6 \pm 8.1, \quad \alpha\beta = 0.182 \pm 0.017, \\ r^2 = 0.99, \quad \sigma = 68.0, \quad (7b)$$

where  $r^2$  is the coefficient of determination and  $\sigma$  is the estimated standard deviation of the fit.

At this point, we would like to comment on the fact that the raw average presented in Fig. 3 hides a caveat. Assuming Hull model for the time being, each subject has a particular asymptote  $\lambda$  and a learning rate  $\alpha\beta$ , with great variability among different rats. Therefore, one might doubt about the legitimacy of averaging the data without taking these differences into account. This point was discussed in the early literature and especially acknowledged by Sidman (1952), after which it has gone almost forgotten (but see Gallistel, 2012; Gallistel et al., 2004) because, after all, average data do turn out to be useful in a number of experimental situa-

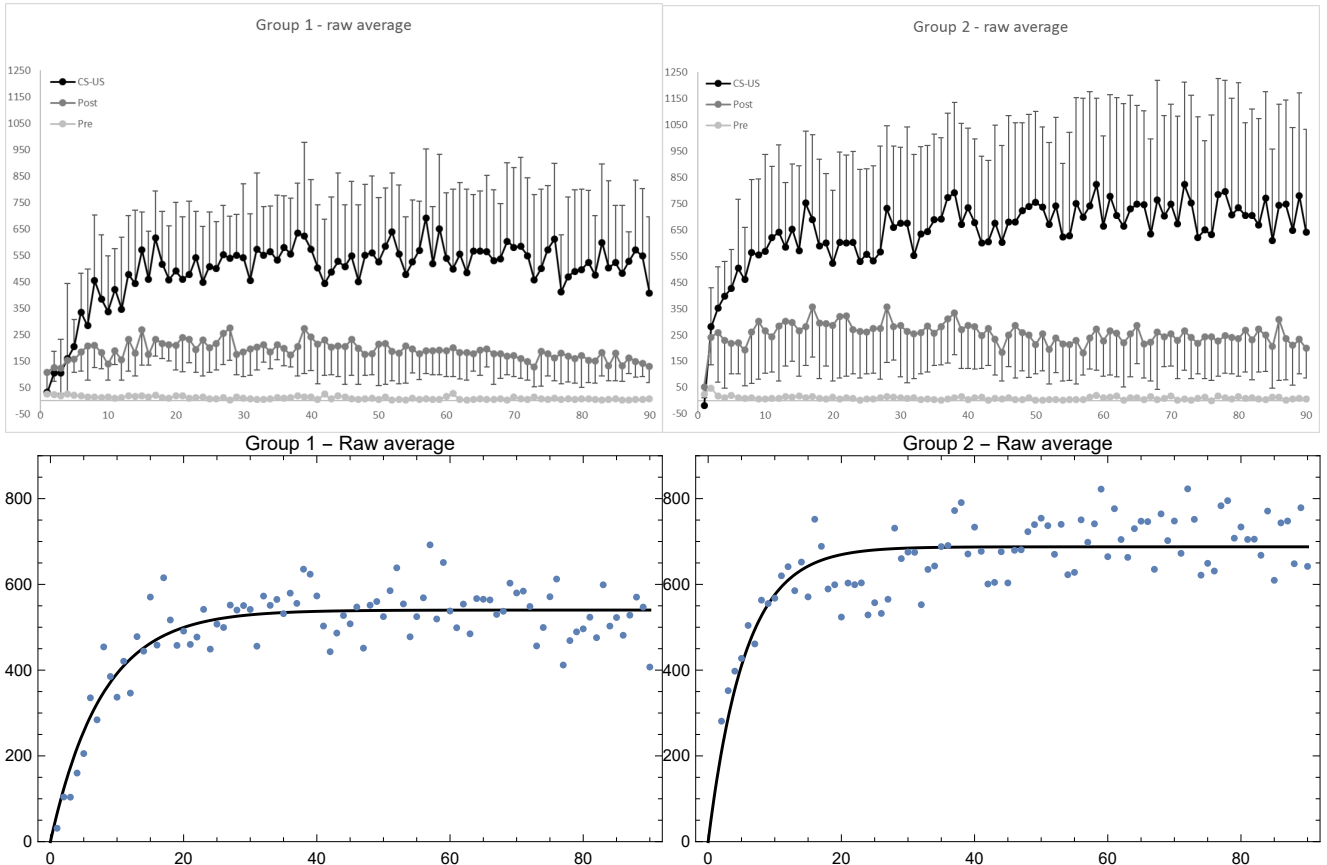


Figure 3. Average of raw (non-normalized) data, for Group 1 (top left) and 2 (top right), together with the best fit with Hull model for Group 1 (bottom left) and 2 (bottom right). Sessions are on the horizontal axis, number of licks on the vertical axis. Light gray, dark gray, and black data points (connected by lines of the same colors) are the licks in the 10 s respectively before, during, and after the CS. The number of US has been subtracted from the during-CS licks of each individual before taking the average, and the upper and lower error bars at the 68% confidence level of CS and post-CS data are shown.

tions. Nevertheless, we tackle the issue explicitly again, with some elementary but not-often-used techniques.

Let us then normalize the data *before* averaging. We do so with two independent methods that will yield the same result. The first method (“averaging procedure”) is model-independent but assumes that there exists an asymptote of learning. To determine it, we remove the first and last 15 to 20 data points and make a linear regression of the remainder. As a general observation, the transient acquisition phase occupied the first 15 to 20 sessions, while in some cases the last 10 sessions were not as stable as intermediate ones. Thus, we took different intervals: sessions 16-90, 16-80, 16-70, 21-90, 21-80, and 21-70. The chosen interval is based on a qualitative observation of the data and we selected the one giving the line with slope closest to zero within one standard deviation. Once selected the session range, we took the average of the data (linear regression with zero slope). The result is reported in Tab. 1.

The second method (“best-fit procedure”) consists in assuming Hull model and use it to fit the individual data. For

each subjects, a nonlinear regression yields an estimate for  $\lambda$  (Tab. 1) and  $\alpha\beta$ . As one can see, the values of  $\lambda$  obtained by both methods are very similar (the estimated standard deviation of the fits ranges from 80 to 240 licks, much larger than the difference  $|\lambda_{\text{average}} - \lambda_{\text{best fit}}|$ ) and, in fact, they have a linear correlation with  $r^2 \approx 0.98$  both in Group 1 and Group 2 (Fig. 1 of *Supplemental Material*). Therefore, the determination of  $\lambda$  for each subject is quite robust and one can choose either method. In what follows, we take the values obtained by the nonlinear fit (last row of Tab. 1). Note that the value of the average  $\lambda$  for each Group is close to the one obtained from the best fit of the raw average data via Hull model, Eq. (7), but the associated standard deviation is much larger. Group 1:  $\langle \lambda_{\text{average}} \rangle = 542 \pm 209$ ,  $\langle \lambda_{\text{best fit}} \rangle = 554 \pm 222$ ; Group 2:  $\langle \lambda_{\text{average}} \rangle = 687 \pm 337$ ,  $\langle \lambda_{\text{best fit}} \rangle = 727 \pm 369$ . This error is a measure of the dispersion of the  $\lambda$  estimates around the average within each group, while the estimated standard deviation  $\sigma$  in Eq. (7) is the mean dispersion of the data with respect to the theoretical curve.

Having thus determined the asymptote of learning for

	1-1	1-2	1-3	1-4	1-5	1-6	1-7	1-8
$\lambda_{\text{average}}$	332	488	860	426	856	493	336	
$\lambda_{\text{best fit}}$	299	565	869	425	889	503	331	
$(\alpha\beta)_{\text{best fit}}$	$0.26 \pm 0.16$	$0.05 \pm 0.01$	$0.11 \pm 0.02$	$0.67 \pm 0.38$	$0.09 \pm 0.01$	$0.09 \pm 0.02$	$0.21 \pm 0.09$	
	2-1	2-2	2-3	2-4	2-5	2-6	2-7	2-8
$\lambda_{\text{average}}$	361	599	769	762	225	546	1417	815
$\lambda_{\text{best fit}}$	362	604	775	778	234	682	1553	827
$(\alpha\beta)_{\text{best fit}}$	$0.22 \pm 0.07$	$0.16 \pm 0.06$	$0.27 \pm 0.07$	$0.30 \pm 0.07$	$0.74 \pm 0.47$	$0.03 \pm 0.01$	$0.06 \pm 0.00$	$0.23 \pm 0.03$

Table 1

Asymptote  $\lambda$  (average number of licks during the CS minus number of US, after acquisition) determined by the averaging and best-fit procedures described in the text for session-by-session data. The association rate  $\alpha\beta$  obtained by the best fit is also shown.

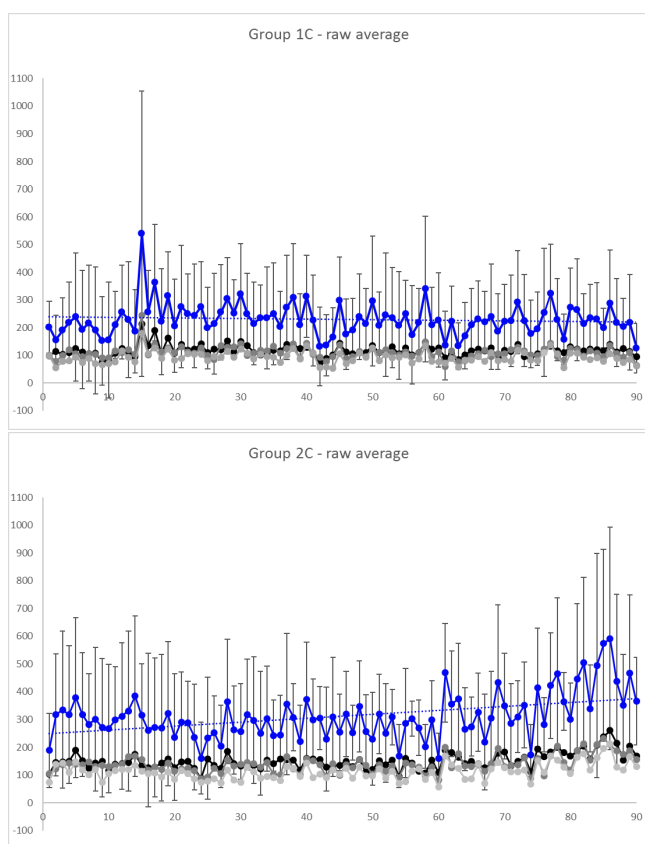


Figure 4. Average of raw (non-normalized) data, for Group 1C (top) and 2C (bottom). Sessions are on the horizontal axis, number of licks on the vertical axis. Light-gray, dark-gray, and black data are, respectively, pre-CS, CS, and post-CS licks, *without* US subtraction. As an added elaboration of the data, we also show the sum of pre-CS, CS, and post-CS licks (blue trendline; darkest gray in B/W rendering), where the number of US has been subtracted from the total licks of each individual before taking the average, and the upper and lower error bars at the 68% confidence level of CS and post-CS data are shown. The dashed line is the regression line of the “summed” data.

each subject, we normalized the data by dividing the number of licks by the estimate of  $\lambda$ . The average of normalized data is shown in Fig. 5. In comparison to Fig. 3, we do not notice any qualitative change in the experimental trendline. However, error bars are considerably smaller. Also, while the estimated standard deviation  $\sigma$  of the best fit of raw data was greater in Group 2 (Eq. (7)), after normalization it is smaller:  $\sigma = 0.13$  for Group 1 and  $\sigma = 0.11$  for Group 2.

The plots showing the data and Hull’s best fit of  $v/\lambda$  for representative subjects in the experimental groups are in Figs. 6 and 7; the figures for all the experimental and control subjects can be found in Figs. 2–7 in the *Supplemental Material*. The advantage of these plots with respect to non-normalized data (not shown) is that one can directly compare the fluctuations in response of different individuals.

The averaged data of the two sessions of extinction are shown in Fig. 8 for the experimental groups (see Fig. 8 in the *Supplemental Material* for controls).

Now we are in a position to comment on the results. First of all, both the pre-CS and post-CS response in the experimental groups were much smaller than the response during the CS, respectively by a factor of 10 and of 2. At the 68% confidence level, none of the curves overlap. This means that the subjects clearly discriminated between the possibility to obtain the US during the tone and in its absence. The higher post-CS response with respect to the pre-CS is easily explained on the grounds of a natural inertia in licking that extended for a few seconds after the tone was switched off. This interpretation is confirmed by calculating Pearson’s correlation coefficient for CS and post-CS licks (non-subtracted and non-normalized data) of individual subjects, which is  $|r| \geq 0.45$  except in two cases (1-6 and 2-7).<sup>2</sup> The corre-

<sup>2</sup>This relatively high correlation might suggest that a better indicator than (6), stripped of micro-motivational or attentional fluctuations, could be obtained if we subtract the number of post-CS licks instead of the number of US. However, as we noted before, we verified that the results of this section do not change.

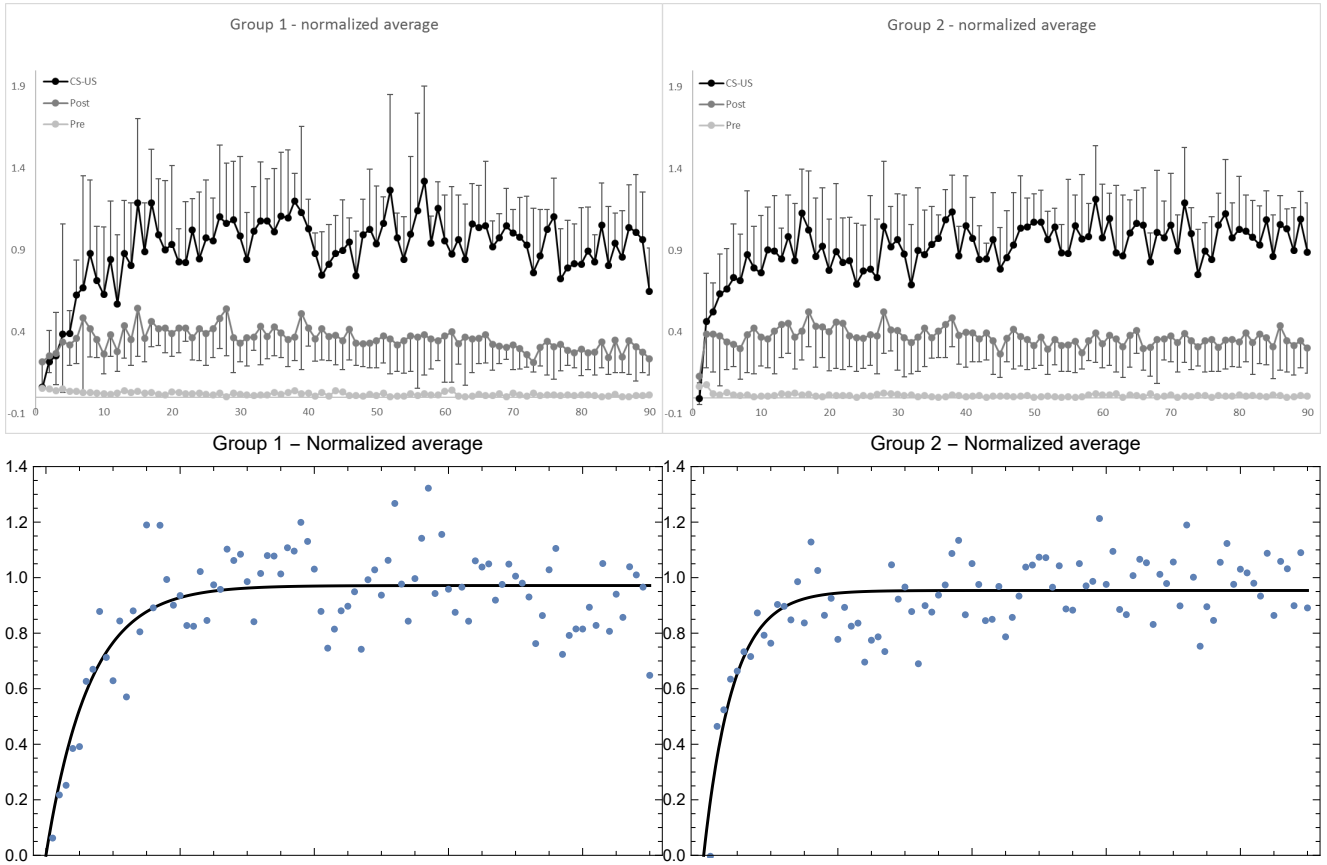


Figure 5. Average of normalized data for Group 1 (top left) and 2 (top right), together with the best fit with Hull model (bottom). Sessions are on the horizontal axis, number of licks on the vertical axis. Light gray, dark gray, and black data points (connected by lines of the same colors) are the licks in the 10 s respectively before, during, and after the CS. The number of US has been subtracted from the during-CS licks of each individual before taking the average, and the upper and lower error bars at the 68% confidence level of CS and post-CS data are shown.

lation between CS and pre-CS licks is smaller,  $|r| < 0.38$ . On the other hand, the control subjects displayed about the same response level before, during, and after the CS, indicating that there was no discrimination and no acquisition of association between the CS and the US.<sup>3</sup> Moreover, the average asymptotes of learning of Groups 1 and 2 reported in Eq. (7) before normalizing the data are significantly different: the rats did respond differentially to 0.1% and 0.2% concentrations. Finally, the data of extinction show a very quick

decrease in response of experimental subjects, likely due to overtraining (Finger, 1942). The flat response of control subjects during the CS reflects the absence of association. Also, control subjects showed extinction to the whole “apparatus + tone + electrovalve click” stimulus (light gray trendlines). Overall, these results indicate that simultaneous conditioning was effective and they validate the experimental design.

Other possible effects of overtraining can be looked for in the long-term trend of post-CS data. A linear regression of post-CS normalized data of Group 1 yields a slightly negative slope  $-0.0010 \pm 0.0002$  and an intercept  $0.41 \pm 0.01$  (the post-CS response is approximately 40% the response during the CS), while for Group 2 the slope is  $-0.0006 \pm 0.0002$  and the intercept  $0.40 \pm 0.01$ . In both cases, the “inertia” after the tone tends to decrease, but at a low rate.

A last type of analysis tackles a subtle point about averaging, which we cover for the sake of rigorousness. It plays no part in the rest of the discussion and the uninterested reader may skip this paragraph. We have seen that averaging of nor-

<sup>3</sup>The total response of control subjects in Group 1C was flat throughout the experiment: a linear fit of the total licks yields a slope  $-0.23 \pm 0.24$  and a correlation  $r^2 = 0.01$ . We did register a slight positive trend in Group 2C: a linear fit of the total licks yields a slope  $1.43 \pm 0.31$  and a correlation  $r^2 = 0.20$ . This trend was driven by subjects 2C-2, 2C-5, and 2C-8. Possibly, this means that subjects developed a liking (unrelated to any CS-US associative process) for the saccharin solution at 0.2% more pronounced than for the less concentrated solution.

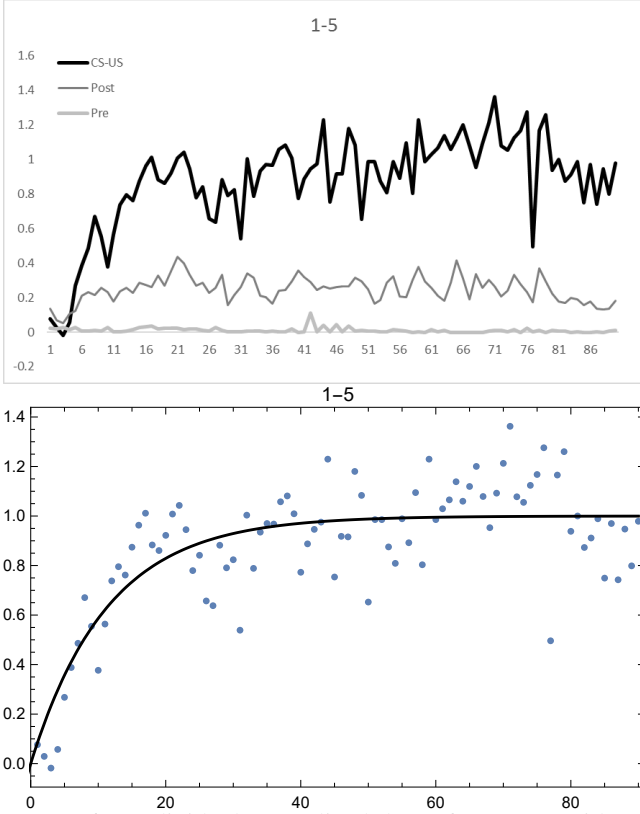


Figure 6. Individual normalized data of Group 1 without (top) and with the best Hull-model fit (bottom): licks before (light gray trend), during (black trend) and after (dark gray trend) the CS, divided by the best-fit  $\lambda$ . The number of US has been subtracted to the licks during the CS. Sessions are on the horizontal axis.

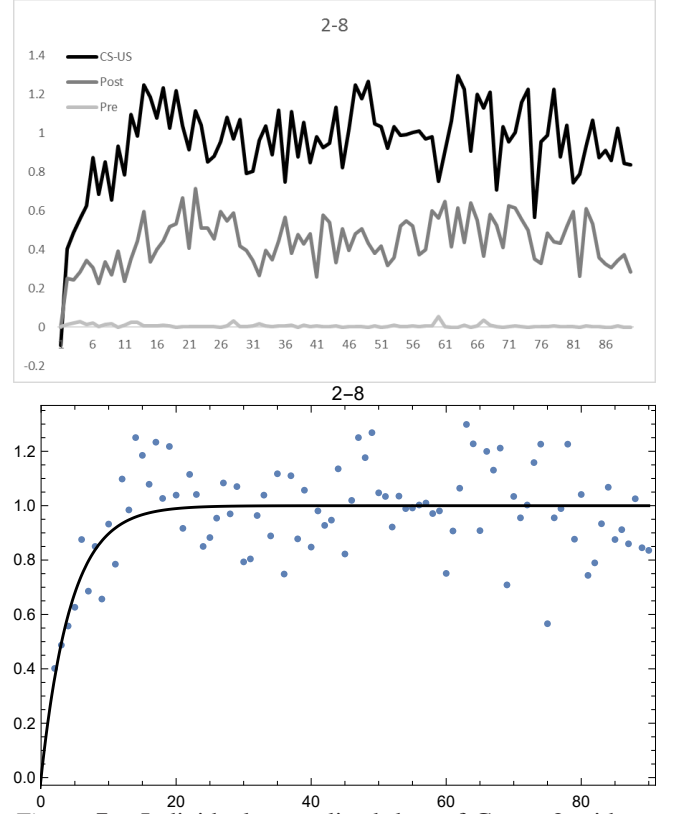


Figure 7. Individual normalized data of Group 2 without (top) and with the best Hull-model fit (bottom): licks before (light gray trend), during (black trend) and after (dark gray trend) the CS, divided by the best-fit  $\lambda$ . The number of US has been subtracted to the licks during the CS. Sessions are on the horizontal axis.

malized data is not very different from averaging of raw data, apart from a decrease of error bars. However, one might still question the validity of the normalized averaging in the acquisition phase, due to the fact that the acquisition rate  $\alpha\beta$  can be very different from subject to subject (Tab. 1). Some rats reached the asymptote of learning very quickly, while others did so only towards the end of the experiment. Therefore, averaging over raw or normalized data does not take into account variability in the acquisition rate. To check whether this introduces unwanted artifacts, we can rescale the “time” of each rat to normalize also the acquisition rate  $\alpha\beta$ . To illustrate the point, assume that Hull model (4) holds and consider two subjects with learning curve  $v_1(t) = \lambda_1[1 - \exp(-\alpha_1\beta_1t)]$  and  $v_2(t) = \lambda_2[1 - \exp(-\alpha_2\beta_2t)]$ . Normalizing the asymptote yields two curves  $v_1(t)/\lambda_1 = 1 - \exp(-\alpha_1\beta_1t)$  and  $v_2(t)/\lambda_2 = 1 - \exp(-\alpha_2\beta_2t)$  that differ only in the learning rate. Calling  $\tilde{t}_1 := \alpha_1\beta_1t$  and  $\tilde{t}_2 := \alpha_2\beta_2t$ , one ends up with a single profile  $w(\tilde{t}) = 1 - \exp(-\tilde{t})$  evaluated at two different “times”  $\tilde{t}_1$  and  $\tilde{t}_2$ . Doing this for all subjects, we obtained the cloud of points shown in Fig. 9 in the *Supplemental Ma-*

*terial*. Since we used Hull model on individual data sets to normalize the asymptote and the learning rate, it should come as no surprise that this cloud of points is fit by Hull model with good accuracy, albeit data are rather dispersed (Group 1:  $\lambda = 1.00 \pm 0.02$ ,  $\alpha\beta = 1.00 \pm 0.10$ ,  $r^2 = 0.88$ ,  $\sigma = 0.34$ ; Group 2:  $\lambda = 1.00 \pm 0.01$ ,  $\alpha\beta = 1.00 \pm 0.07$ ,  $r^2 = 0.92$ ,  $\sigma = 0.27$ ).

Let us now turn to individual response differences. Without the pretense of being exhaustive, we registered the following two pairs of patterns:

- *Wildly fluctuating response* (e.g., subjects 1-1, 1-4, 1-7, 2-1, 2-2, 2-5, 2-6, 1C-1, 1C-3, 1C-6, 2C-1, 2C-4). For experimental subjects, the shape of the learning curve is almost completely lost into noise.

- *Less fluctuating response* (e.g., subjects 1-2, 1-3, 1-5, 1-6, 2-3, 2-4, 2-7, 2-8, 1C-2, 1C-4, 1C-7, 1C-8, 2C-2, 2C-3), where strong fluctuations are less frequent. Experimental subjects follow more clearly the learning curve.

The difference between “wild” and “mild” fluctuations can be quantified by considering the estimated standard deviation

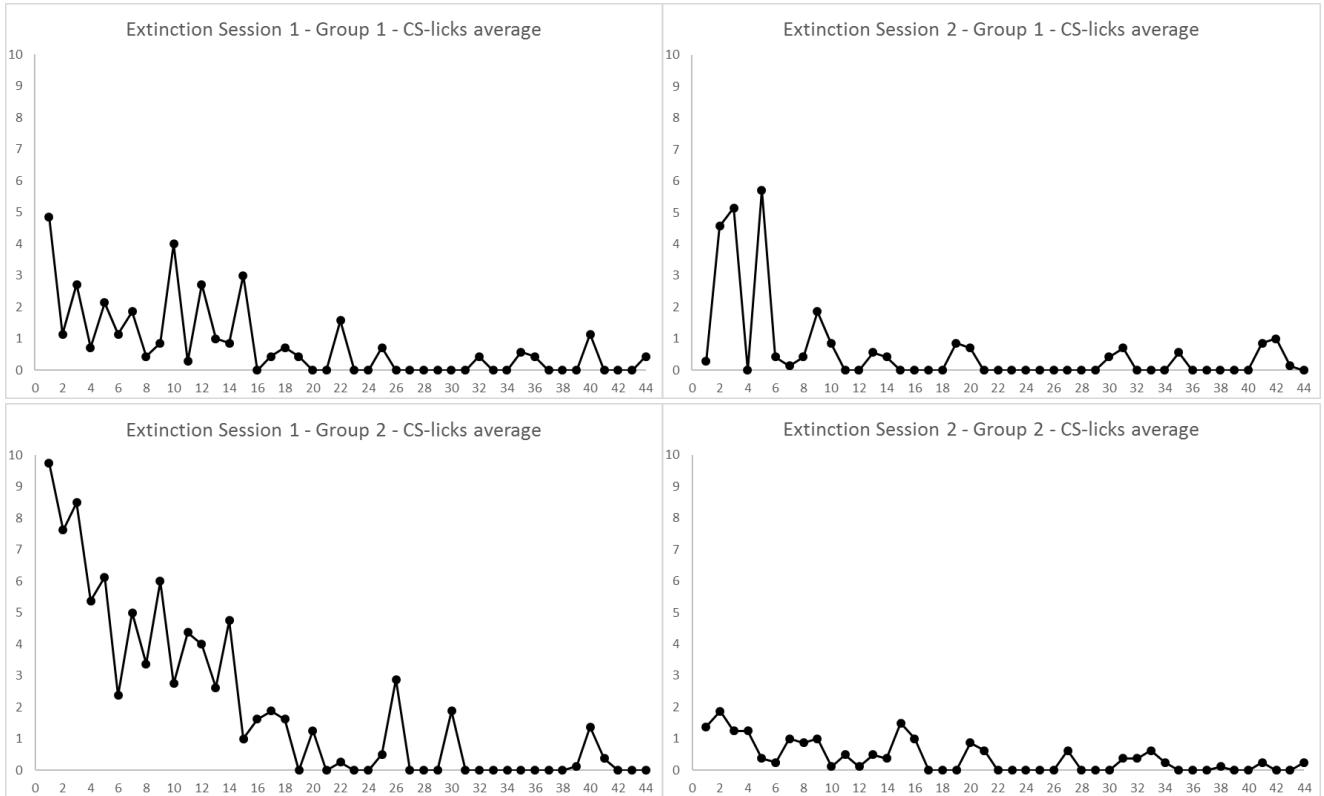


Figure 8. Average of raw (non-normalized) data of the two extinction sessions for experimental groups. Trials are on the horizontal axis and licks are on the vertical axis.

1-1	1-2	1-3	1-4	1-5	1-6	1-7	1-8
0.59	0.29	0.19	0.33	0.16	0.24	0.43	
2-1	2-2	2-3	2-4	2-5	2-6	2-7	2-8
0.32	0.40	0.22	0.20	0.36	0.30	0.10	0.15

Table 2

Estimated standard deviation  $\sigma$  of the Hull-model best fit of normalized session-by-session data.

of data with respect to the nonlinear fit with Hull’s learning curve (Tab. 2). We took as a criterion for “wild fluctuations” variations greater than or equal to 30% of the peak response ( $\sigma \geq 0.30$ ). This criterion is arbitrary (one could have taken, e.g.,  $\sigma = 0.50$  as a threshold) but illustrates the point. Some subjects are somewhat in between these two categories, since they showed a stable response during a long time followed by wildly fluctuating periods.

For those subjects that showed a trend in their response, we can further recognize:

- *Slow increase in response* (e.g., subjects 1-2, 2-7, 1C-6, 2C-2, 2C-5, 2C-8). For experimental subjects, this is simply due to a slow learning rate, while the interpretation for control subjects is less obvious. Perhaps the unpredictability of

the US was a factor increasing the response, as observed also by Kaye and Pearce (1984).

- *Slow decrease in response* (e.g., subjects 1-1, 1-7, 1C-1, 1C-7, 2C-7). This phenomenon is related to the presentation of the stimuli and their mutual association. This is not short-term habituation, which is a non-associative process occurring relatively quickly (only a few sessions) (Çevik, 2014; Thompson, 2009). Moreover, short-term habituation is faster for weaker stimuli, which we did not see here. However, it is not long-term habituation either, which also occurs in a relatively short time span (a few sessions, although it depends on the experiment and the subject species) before any plateau in the response (Ornitz and Guthrie, 1989; Packer and Siddle, 1987; Plaud et al., 1997). Here one might rather talk about a very long-term habituation, occurring because animals are presented with the same stimulus in all trials of all sessions. In the next sections, we will make a more in-depth analysis of the individuals’ data.

## Discussion

Summarizing the conclusions obtained from the above results:

- The experimental design has been validated as a viable

tool of generation and control of Pavlovian conditioning.<sup>4</sup> The subjects discriminated between the different chances of getting the US during the tone CS (simultaneous conditioning) with respect to when the tone was absent. The response was much higher during the CS than before or after. The definitory criterion for successful discrimination is the ratio between pre-CS and CS licking. Post-CS response, seldom discussed in the literature, was much larger than pre-CS response due to a natural inertia in the licking behavior but, still, it was much smaller than the response during the CS.

- While taking the average of raw data is useful for between-groups comparisons (absolute value of the asymptotes), error bars are reduced when considering the average of data with normalized asymptote of learning. Normalizing also the learning rate of individuals does not add much information and is a strongly model-dependent procedure.

- Although we did observe long-range (i.e., spanning several sessions) fluctuations in the average subjects response, the error bars due to individual differences are large enough to conclude that these fluctuations are not significant. Hull model (5) is a good description of the average learning curve in Pavlovian conditioning.

- The main average effects of overtraining are an extremely slow decrease of the post-CS response and a fast extinction. Fast extinction points out that the response of the animals during the experiment was not driven by habit, contrary to what one might expect in long training histories (Gür et al., 2018).

We can compare our findings with those in the literature of post-peak depression or inhibition by reinforcement cited in the *Introduction*. In general, our subjects reached the asymptote of learning after 15 to 20 sessions. While gradients in response have been registered on as short a scale as trial-by-

trial or session-by-session intervals, large-scale (i.e., spanning many sessions) fluctuations characterized all the plateau after acquisition. In some cases, we did see a response decrease, but much later than acquisition. Even granting that aversive conditioning may be faster than appetitive one, this leads us to believe that this decrease is a long-range phenomenon different from the post-peak depression observed in experiments employing only a few hundred CS-US pairings, in contrast with our almost four thousand trials each with an average of two CS-US pairings. The latter could be a transient phenomenon corresponding to the first fluctuation peak just after acquisition, when present. Such interpretation is corroborated by past evidence on the non-robustness of inhibition by reinforcement when extending the duration of the experiment (Dukhayil and Lyons, 1973).

In general, observations of individual differences were not accompanied by attempts to explain them quantitatively (see, however, Urcelay et al., 2012). In the following sections we want to do just that. It should be made absolutely clear that the fact that Hull model is a good fit of data does *not* mean that individual differences and response fluctuations are mere statistical phenomena to be treated as unwanted errors. Different subjects do respond very differently to stimuli and their response does change erratically trial after trial and session after session. The issue then is whether we can find a theoretically motivated model (not just an *ad hoc* fitting curve, which is not hard to concoct) better than Hull model in explaining the data, in particular, the long-range response decrease observed in some subjects (not to be confused with the post-peak depression effect in the literature, as already said above).

## DYNAMICAL MODELS OF INDIVIDUAL BEHAVIOR

### Motivation: least-action principle and fine tuning

The simplicity of Hull model makes it the ideal example where to introduce all the main ingredients of a dynamical reinterpretation of Pavlovian conditioning processes. By *dynamical*, we mean a very precise concept, superior to any casual use of the term in the loose sense of “evolving” or “interacting”. Namely, we postulate that any conditioning process can be described by a quantity called *action* and that the change of the association strength during conditioning happens in such a way that the action is minimized. Let us introduce the rationale behind this view.

As a global, externally observable phenomenon, Pavlovian learning has been described through models such as Rescorla–Wagner’s (1972) and others (Le Pelley, 2004; Mackintosh, 1975b; Pearce and Hall, 1980; Wagner, 1981; Wagner & Vogel, 2009). In general, the essence underlying these models appeals to psychological aspects such as the surprisingness or novelty or predictiveness of the stimuli.

---

<sup>4</sup>It is inevitable that the procurement of saccharin in the present preparation implies licking at the bottle spout, thus establishing an operant contingency between licking and obtaining the reinforcer. Furthermore, given that the US occurred at random times within the CS, this is an ideal condition for the maintenance of superstitious licking. Despite this being correct (Killeen and Pellón, 2013; Pellón et al., 2018; Pellón and Killeen, 2015), lick suppression has been accepted as Pavlovian under an experimental paradigm similar to the current one, when the consequence is aversive or has been devalued (e.g., Jozefowicz et al., 2011). By analogy, lick enhancement might have those same characteristics as the reduction of the response, not to mention that after extended training it has been generally accepted that behavior shifts control from the consequence to the antecedent stimulus (Dickinson and Balleine, 2002), a case in which the results that will be modeled here might fall. Additionally, even if we accept that licking in the present experiment has an operant contribution to its installment, which is true, we believe that the theoretical analysis applied in the present paper is not really affected if an event stimulus is replaced by a response (see also section *General conclusions*).

However, it is not unreasonable to believe that an alternative conceptualization is possible where, despite behavioral errors by the subject, the learning process is a naturally efficient one and, so to speak, minimizes the biological adaptation effort. At a biological level, learning can be viewed as a sequence of events modifying some of the synaptic connections of the brain. This modification does not happen in a disordered way since, as associative models already highlighted, there exist laws (learning curves) applicable to statistically significant samples. Going a bit beyond the macroscopic view of traditional associative models, but without attempting a microscopic quantitative description of neural plasticity, we postulate that the brain mechanics of a subject change through learning from an initial state A to a final state B efficiently. Operationally, a most effective way to describe this minimization of effort is through the action. If we depict the learning process in time  $t$  as a path from A to B in an abstract space parametrized by the association strength  $v$ , the profile  $v(t)$  describing the evolution in the association strength minimizes the path from point  $v(t_A)$  to point  $v(t_B)$ . A similar statement could be made about the energy spent in changing the internal state, but both are described by the same quantity, the action. The action  $S$  is a function of the association strength  $v$  and it is minimized when its variation with respect to  $v$  is zero:<sup>5</sup>

$$\frac{\delta S}{\delta v} = 0. \quad (8)$$

This is the principle of least action. It has been applied successfully in physics and our aim now is to use it also in psychology. From physics we will get guidance about what  $S$  is and this guidance will prove itself correct because it will immediately recover not only Hull's, but also Rescorla-Wagner's model as special cases.

The main idea is to reinterpret the learning curve of any associative model as the trajectory of one or more small balls (pointwise *particles*) rolling up and down a hill (a *potential*). The way a particle moves along its potential is called dynamics. In the case of the Hull model, there is only one particle whose trajectory is shown in Fig. 1 and whose potential  $U(v)$  is depicted in Fig. 9 (top). The proof of this statement is given in Appendix A, while the dynamics corresponding to multicue or variable-salience conditioning models is discussed in Appendix B. In excitatory conditioning with just one cue, the particle rolls down the slope from the point  $v = 0$  to the bottom at  $v = \lambda$ , where it unnaturally stops.

At this point, one appreciates the first major advantage of the least-action principle. If the latter is true, then it is very hard to understand why a particle placed on the slope of the potential well would roll down and stop exactly at its bottom.

<sup>5</sup>At the maxima and minima of a function, its first derivative vanishes.

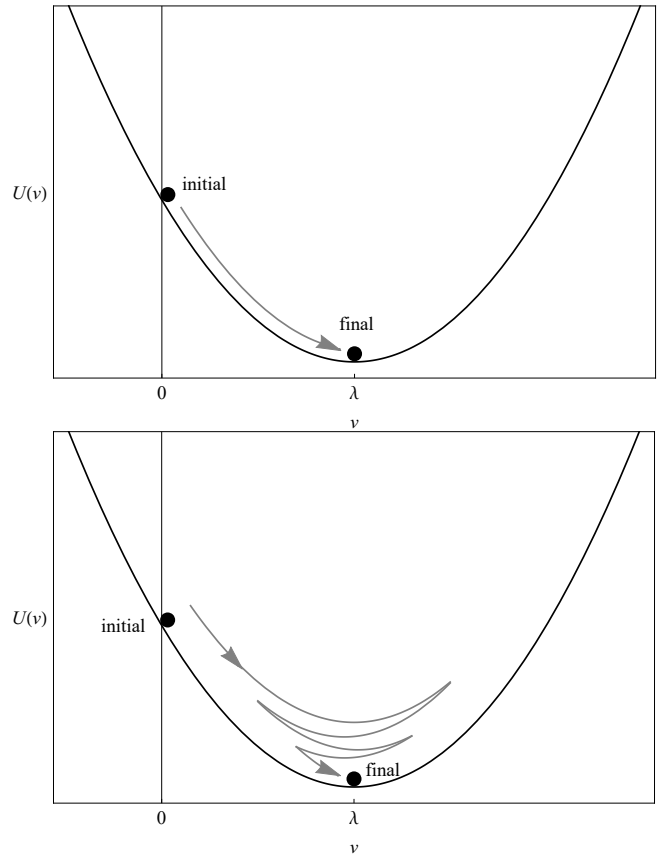


Figure 9. Top: the potential  $U(v)$  of Hull's model (24) for  $\lambda = 1$  and  $\alpha\beta = 1$ . Compare with the solution (3) in Fig. 1. Bottom: the potential  $U(v)$  of the dynamical model (29) for  $\lambda = 1$  and  $(\alpha\beta)^2 + \mu^2 = 1$ . Compare with the solution (9) in Fig. 10. In both cases, the particle rolling down the potential represents the change in the associative strength. The direction of "motion" in excitatory conditioning is represented by a gray arrow.

The least-action principle tells us that we must fine tune the initial conditions (position and velocity) of the particle to infinite precision in order to achieve such a behavior. If some latitude in the choice of initial conditions is allowed (as it should in a natural biological setting), then in general the particle will oscillate up and down the well until reaching a final stop at the bottom, as shown in the bottom plot of Fig. 9.

We decided to use tools borrowed from physics because, in the long run, they carry two major advantages. First, as said above, they allow one to modify Pavlovian models in a natural way that would result rather obscure in the traditional approach, and that can be contrasted with experiments. Second, they are the basis from which we will construct a predictive theory of individual short-scale response variability, presented in section *Quantum Hull model*. Ultimately, revisiting conditioning models as dynamical models amounts

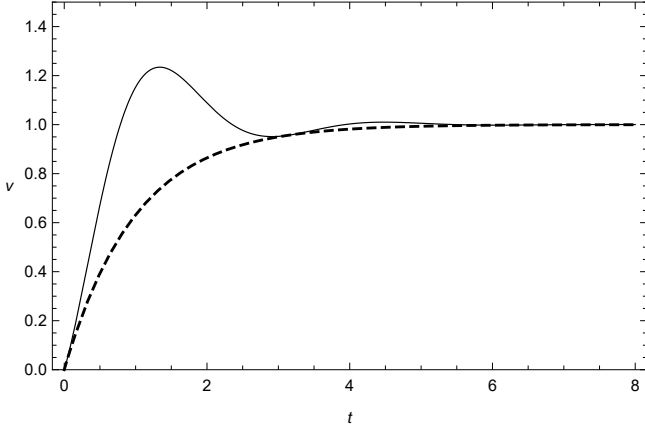


Figure 10. The learning curve (9) (solid) with periodic oscillations with  $\mu = 2$  and  $A = 0$ , compared with Hull's learning curve (4) (dashed). Here  $\lambda = 1 = \alpha\beta$ .

to a new paradigm of doing model-building in psychology, where qualitative reasonings leading to quantitative formulæ are replaced by a rigorous sequence of logical steps. As in any model building, arbitrariness is not removed, but it will be pinpointed and put under a higher degree of control.

### Theory

The catchword is “unnatural.” The way the particle moves along its potential in the case of the Hull model is very special because it reduces to the simple equation (2). When it rolls down the slope, the particle experiences some resistance (*friction*) from the floor, but not so much as to brake completely. This happens, by sheer coincidence, exactly at the bottom of the slope. In a more general situation, we would expect the particle to oscillate up and down the bottom, if the friction is moderate, until it reaches a complete stop (Fig. 9, bottom). If we abandon the rigid setting of Hull's dynamics and allow for such a scenario, much more natural from a dynamical point of view, we obtain a different trajectory, i.e., a different learning curve (Appendix A):

$$v(t) = \lambda \left[ 1 - e^{-\alpha\beta t} (\cos \mu t + A \sin \mu t) \right], \quad (9)$$

where  $\mu$  and  $A$  are constants. When  $\mu = 0$ , this reduces to Hull model (4) of excitatory conditioning. When  $\mu \neq 0$ , learning is subject to a friction force with progressively damped oscillations around zero. The learning curve is modified as in Fig. 10. This profile features oscillations of fixed frequency  $\mu$  and decreasing amplitude above and below the asymptote, which we can look for in data. In particular, it predicts a first response peak above the subsequent asymptote.

Notice that  $v(t)$  is not positive definite at small times unless  $A$  is sufficiently small. To avoid this problem and to remove a free parameter from the model, we will pay special

attention to the case  $A = 0$ . Data will show that the  $A \neq 0$  is disfavored anyway.

Reverting back to discrete time, we can recast Eq. (30) as a law for the association strength  $v_n$  at the beginning of trial (or session)  $n$ . The first and second-order derivatives  $\dot{v}$  and  $\ddot{v}$  correspond, respectively, to the forward finite differences  $v_n - v_{n-1}$  and  $v_{n+1} - 2v_n + v_{n-1}$ , so that the analogue of Eq. (1) is

$$v_{n+1} - (1 - 2\alpha\beta)(2v_n - v_{n-1}) = (\alpha^2\beta^2 + \mu^2)(\lambda - v_{n-1}). \quad (10)$$

Unless  $\mu = 0$ , it is not possible to write a simple incremental law as Hull's, and the association strength at the beginning of trial  $n + 1$  is predicted by that of the previous *two* trials  $n$  and  $n - 1$ , instead of just the one immediately preceding as in Hull model (1).

### Data analysis: comparison with Hull model

In order to assess the goodness of fit of the dynamical proposal with respect to the traditional Hull model, we should take into account that the first has more free parameter than Hull's. Having more parameters clearly gives an intrinsic flexibility in data fitting that more rigid theories do not have, and one should balance this factor against the actual capabilities of the new models to accommodate observations. This is the typical situation where comparative statistics such as the Bayesian (or Schwarz) Information Criterion (BIC) and the Akaike Information Criterion (AIC) can be extremely useful, as advocated by Witnauer et al. (2017).

Let  $\sigma_e^2 := \sum_{n=1}^N [y_n - f(t_n)]^2 / N$  be the error variance of the fit, the averaged sum of squared residuals (also known as residual sum of squares or sum of squared errors), where  $N$  is the number of data,  $y_n$  is the experimental datum at the  $n$ -th session and  $f(t_n)$  is the value predicted by the theoretical model. (The error variance  $\sigma_e^2$  is not the estimated variance  $\sigma^2$  of the fits discussed above. They are related to each other by  $\sigma_e^2 = N\sigma^2 / (N - p)$ , where  $p$  is the number of free parameters of the function  $f$ .) The BIC is defined as (Schwarz, 1978)

$$\text{BIC} := N \ln \sigma_e^2 + p \ln N, \quad (11)$$

while the AIC is (Akaike, 1974)

$$\text{AIC} := N \ln \sigma_e^2 + 2p. \quad (12)$$

The first term in Eqs. (11) and (12) quantifies the badness of the fit (the greater the error variance, the worse the fit), while the second term increase linearly with  $p$ . The BIC and AIC penalize model complexity slightly differently. For each theoretical model, one can compute the BIC and the AIC: the model with smaller criteria is to be preferred. Calling the difference  $\Delta := |(\text{IC model 1}) - (\text{IC model 2})|$  for the Bayes or Akaike IC, one finds weak evidence if  $\Delta < 2$ , positive evidence if  $2 \leq \Delta < 6$ , strong evidence if  $6 \leq \Delta < 10$ ,

and very strong evidence if  $\Delta > 10$  (Jeffreys, 1961; Kass and Raftery, 1995). We will use the term “moderate” to indicate cases where evidence is positive in one criterion but weak in the other.

While Hull model has two free parameters ( $\lambda$  and  $\alpha\beta$ ), the oscillatory model (9) has four ( $\lambda$ ,  $\alpha\beta$ ,  $\mu$ , and  $A$ ). Setting  $A = 0$ , we are left with three free parameters, which can give more flexibility with respect to Hull model but are more penalized in the Information Criteria when fitting session-by-session individual data (Tab. 3).

We can divide the subjects in three groups: those for which the Hull model is clearly favoured, those for which the  $A = 0$  oscillatory model is clearly favored, and those where the Hull and oscillatory models are about equally favored by the Information Criteria.

- As one can see from the table, Hull best fit is favored for subjects 1-1, 1-2, 1-3, 1-4, 1-5, 1-6, 2-2, 2-6, and 2-7 (weak to positive evidence,  $1 \leq \Delta \leq 5$ ). However, here we are not comparing two independent models but a model and its extension by one ( $\mu$ ) or two ( $\mu, A$ ) extra parameters. Therefore, we have to interpret with care the meaning of the cases where Hull is favored. For subjects 1-1, 1-2, 1-5, 2-2, and 2-7, the estimated  $\mu$  in the oscillatory best fit is compatible with zero (1-1:  $\mu = -0.13 \pm 0.17$ ; 1-2:  $\mu = 10^{-11} \pm 10^7$ , 1-5:  $\mu = 6 \pm 10^5$ ; 2-2:  $\mu = 10^{-6} \pm 10^4$ ; 2-7:  $\mu = 10^{-4} \pm 6$ ). Therefore, there is no statistically significant smooth oscillation of the type (9) in their response. For subject 1-4 (weak evidence in favor of Hull according to the AIC,  $\Delta = 1$ ),  $\mu$  is nonzero at the 68% confidence level but zero at the 99% confidence level ( $\mu = 0.45 \pm 0.21$ ). In the case of subjects 1-3 and 1-6,  $\mu$  is significantly nonzero at the 99% confidence level but is very high (1-3:  $\mu = 12.61 \pm 0.04$ ; 1-6:  $\mu = 6.23 \pm 0.02$ ), meaning that data are fitted with densely packed oscillations. We regard this as an artifact and thus discard these oscillatory fits as unviable and consider the  $\mu = 0$  case as the best fit. Finally, in the case of subject 2-6  $\mu$  is significantly nonzero at the 99% confidence level and is not high ( $\mu = 0.04 \pm 0.01$ ), but the BIC and AIC are larger than for the Hull model. From this discussion, we conclude that, of these nine cases, *only one* (subject 2-6) sees Hull model as the favorite when considered as independent of (alternative to, opponent of) the oscillatory model, although evidence is just positive according to the BIC ( $\Delta = 3$ ) and weak according to the AIC ( $\Delta = 1$ ). While in all the other cases Hull’s primacy should be regarded simply as the fact that, for these subjects, the parameter  $\mu$  is close to zero.

- The data of subjects 1-7, 2-3, 2-4, and 2-8 favor the  $A = 0$  oscillatory model with, respectively, very strong, moderate, strong, and moderate evidence. Restoring  $A$  as a free parameters, we get an even better fit for subject 1-7.

- The case of subjects 2-1 and 2-5 is less clear-cut: the  $A = 0$  oscillatory model (2-1:  $\mu = 0.17 \pm 0.03$ ; 2-5:  $0.56 \pm 0.04$ ) is slightly more favored than Hull model in the

AIC, while the  $A \neq 0$  model is worse than the  $A = 0$  one in both the BIC and the AIC. Since the difference is about 1% of the value of the criteria and evidence in favor or against is weak ( $\Delta = 1$ ), we cannot decide whether  $\mu = 0$  or  $\mu \neq 0$  for these subjects.

The best-fit parameter values of subjects 1-7, 2-3, 2-4, and 2-8 for the three models are given in Tab. 4 and the best-fit curves are shown in Fig. 11. Since the favored best fits with  $A \neq 0$  are not particularly strong (the parameter  $A$  is always zero at the 95% confidence level), we can conclude that the model with  $A = 0$  is sufficient to explain the data of these subjects deviating from Hull’s behavioral trend.

## Discussion

Overall, the Hull model is favored (but only moderately) for only one out of the 15 experimental subjects, the oscillatory model with  $A = 0$  and  $\mu \neq 0$  is strongly favored in two subjects and moderately favored in two more, the oscillatory model with  $A = 0$  and  $\mu = 0$  is a good fit of eight more subjects (and it coincides with Hull model), and there is no preference for either model in two more subjects. The fact that the Hull model is favored (and moderately so) only in 7% of the experimental subjects justifies the present and future interest in the  $A = 0$ ,  $\mu \neq 0$  oscillatory model (9).

The conclusion is that, if we insist in considering Hull model as the correct description of the learning curves, then we can explain at most 73% of the data ( $1+8+2 = 11$  subjects out of 15), while if we postulate the least-action principle we obtain a model that includes Hull as a special case and can explain 93 – 100% of the data. Therefore, this extension of Hull model is both natural and viable.

## COLORED STOCHASTIC MODEL OF INDIVIDUAL BEHAVIOR

### Motivation and spectral analysis

The first aspect drawing one’s attention to the individuals’ data is the generalized presence of large fluctuations in the response, translating into an unstable inter-trial and inter-session associative strength. These fluctuations are present even in those very few subjects with relatively small inter-session variability, such as 2-7. Since there seems to be no qualitative change with the time scale (trial-by-trial compared with session-by-session; see Fig. 12), fluctuations might be assumed to plague the performance of the subjects at *any* scale. This means that it is quite natural to regard these data as a time series described by a nowhere-differentiable pattern instead of a smooth learning curve. This is the motivation to replace (1) with an evolution equation for the associative strength encoding a stochastic component.

The mathematics of stochastic processes is not a new tool in learning theories. In fact, the earliest conditioning models had an inherent element of randomness in their predic-

BIC, AIC ↘	1-1	1-2	1-3	1-4	1-5	1-6	1-7	1-8
Hull	<b>171, 163</b>	<b>43, 36</b>	<b>-32, -40</b>	<b>68, 60</b>	<b>-62, -69</b>	<b>13, 5</b>	116, 108	-
oscillations ( $A = 0$ )	175, 165	48, 38	-28, -38	71, 61	-57, -67	16, 6	104, 94	-
oscillations ( $A \neq 0$ )	179, 166	52, 40	-25, -38	75, 62	-55, -68	<b>18, 5</b>	<b>91, 78</b>	-
fractional	175, 165	80, 70	-28, -38	62, 52	-44, -54	41, 31	123, 113	-
BIC, AIC ↘	2-1	2-2	2-3	2-4	2-5	2-6	2-7	2-8
Hull	<b>64, 56</b>	<b>103, 95</b>	-3, -10	-27, -35	<b>84, 76</b>	<b>49, 41</b>	<b>-139, -147</b>	-75, -82
oscillations ( $A = 0$ )	65, <b>55</b>	107, 97	<b>-4, -14</b>	<b>-33, -43</b>	<b>85, 75</b>	52, 42	-135, -145	<b>-76, -86</b>
oscillations ( $A \neq 0$ )	69, 57	112, 99	-1, -13	-31, <b>-43</b>	91, 79	57, 45	-130, -143	-72, -84
fractional	68, 58	110, 100	5, -5	-16, -26	88, 78	52, 42	-64, -74	-70, -80

Table 3

BIC and AIC (approximated to zero decimals) of the best fits of session-by-session data with Hull model (4), the oscillatory model (9) with  $A = 0$ , the oscillatory model with  $A \neq 0$  (shown only for subjects significantly deviating from Hull's learning curve), and the fractional model (54) described in Appendix C. Favored models are in boldface, except the fractional model for subject 1-4 because it is a false positive.

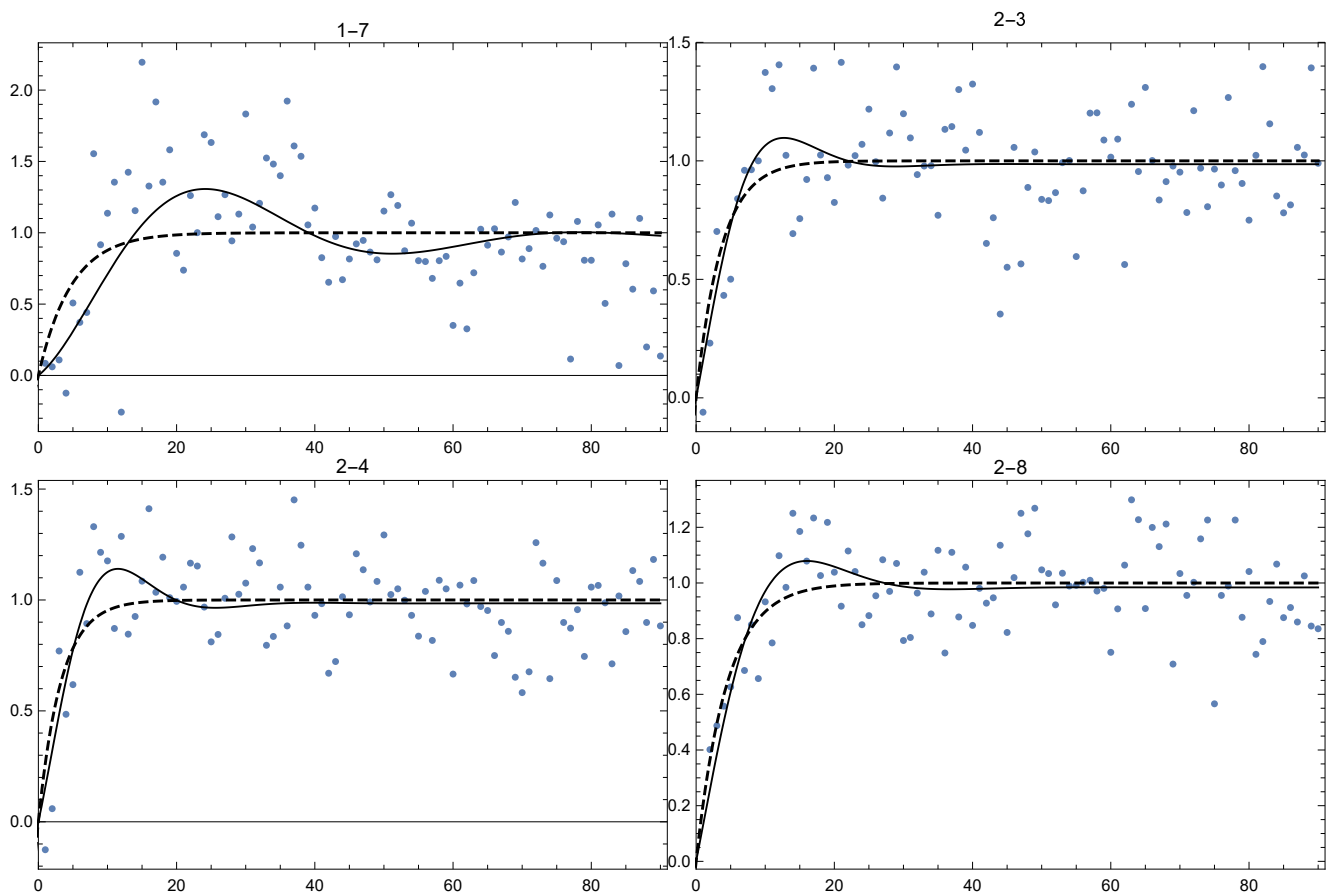


Figure 11. Best-fit of normalized data with Hull model (4) (dashed curve) and the oscillatory model (9) with  $A = 0$  with the parameter values of Tab. 4. Sessions are on the horizontal axis and normalized response is on the vertical axis.

Subject	Parameters	Hull	Oscillations ( $A = 0$ )	Oscillations ( $A \neq 0$ )
1-7	$\lambda$	1	$0.97 \pm 0.04$	<b><math>0.78 \pm 0.13</math></b>
	$\alpha\beta$	$0.21 \pm 0.09$	$0.04 \pm 0.01$	<b><math>0.04 \pm 0.01</math></b>
	$\mu$	0	$0.12 \pm 0.01$	<b><math>0.05 \pm 0.02</math></b>
	$A$	0	0	<b><math>-2.46 \pm 1.94</math></b>
	$\sigma$	0.43	0.40	<b>0.36</b>
2-3	$\lambda$	1	<b><math>0.99 \pm 0.02</math></b>	$0.99 \pm 0.02$
	$\alpha\beta$	$0.27 \pm 0.07$	<b><math>0.15 \pm 0.05</math></b>	$0.19 \pm 0.08$
	$\mu$	0	<b><math>0.19 \pm 0.04</math></b>	$0.30 \pm 0.07$
	$A$	0	<b>0</b>	$0.63 \pm 0.55$
	$\sigma$	0.22	<b>0.22</b>	0.22
2-4	$\lambda$	1	<b><math>0.98 \pm 0.02</math></b>	$0.99 \pm 0.02$
	$\alpha\beta$	$0.30 \pm 0.07$	<b><math>0.14 \pm 0.03</math></b>	$0.27 \pm 0.11$
	$\mu$	0	<b><math>0.22 \pm 0.03</math></b>	$0.38 \pm 0.07$
	$A$	0	<b>0</b>	$1.04 \pm 0.59$
	$\sigma$	0.20	<b>0.18</b>	0.18
2-8	$\lambda$	1	<b><math>0.98 \pm 0.02</math></b>	$0.98 \pm 0.02$
	$\alpha\beta$	$0.23 \pm 0.03$	<b><math>0.13 \pm 0.02</math></b>	$0.13 \pm 0.03$
	$\mu$	0	<b><math>0.15 \pm 0.02</math></b>	$0.15 \pm 0.05$
	$A$	0	<b>0</b>	$0.02 \pm 0.46$
	$\sigma$	0.15	<b>0.15</b>	0.15

Table 4

Best-fit values of the parameters of Hull model (4) and the oscillatory model (9) with  $A = 0$  and  $A \neq 0$  for those subjects whose data (normalized with respect to Hull's asymptote) favor at least one of the oscillatory models for both the BIC and the AIC.  $\sigma$  is the estimated standard error. The most favored model is in boldface.

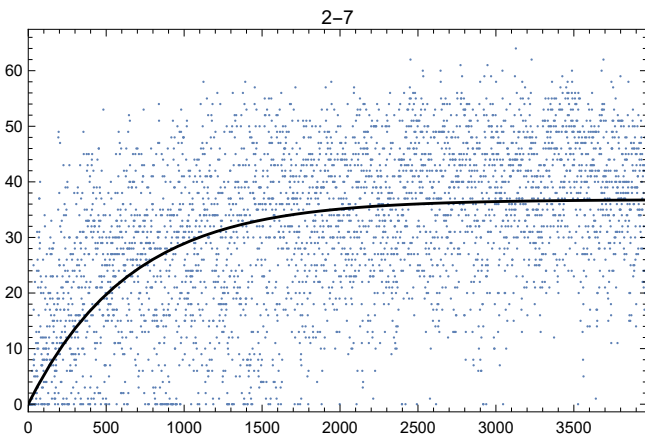


Figure 12. Trial-by-trial data of subject 2-7. The best-fit values for all subjects are given in Tab. 5. This example, where we chose the most normative subject at the session-by-session time scale, shows that data do not become smoother when changing the scale.

tions. The classic 1950s models were cast in the language of probability theory and one considered the probability  $p$  of a given conditioned response (CR) as a function of the trial number  $n$ ; see, e.g., the works by Estes (Estes, 1950; Estes and Burke, 1953), Bush and Mosteller (1951a; 1951b; 1953),

and the reviews by Mosteller (1958) and Bower (1994). Later on, the strength of association  $v$  was regarded as a better operational variable than the probability  $p$  (Rescorla and Wagner, 1972) and the focus was shifted to ideally deterministic predictions. More recently, stochastic processes played a role in the context of neural networks and their application to robotics and artificial intelligence. In particular, a path integral can describe a learning process of a neural network as a finite-temperature stochastic process (Balakrishnan, 2000). Path integrals have also been applied to control theory and reinforcement learning (Braun et al., 2011; Farshidian and Buchli, 2013; Kappen, 2007; Pan et al., 2014; 2015; Theodorou, 2011; Theodorou et al., 2010a; 2010b; 2011; van den Broek et al., 2008). In all these cases, the problem is to minimize the cost of a learning process or of an action by an agent.

Despite some remote similarities, these approaches differ from ours, as we will see below. First, however, we have to introduce some indispensable tools to carry out a spectral analysis. The latter is an analysis of the frequency modes constituting the noise in data. If data predominantly oscillate on a long time scale, then the noise dominates the small frequencies of the spectrum. On the other hand, if oscillations mainly occur on a very short time scale, then the spectrum is more noisy at large frequencies. The noise in learning data corresponds to the second case.

	<b>1-1</b>	<b>1-2</b>	<b>1-3</b>	<b>1-4</b>
$\lambda$	$8.9 \pm 0.2$	$14.7 \pm 0.3$	$21.8 \pm 0.2$	$11.9 \pm 0.1$
$\alpha\beta$	$0.00832 \pm 0.00213$	$0.00155 \pm 0.00015$	$0.00298 \pm 0.00022$	$0.02458 \pm 0.00595$
$\sigma$	12.1	13.5	12.8	9.1
	<b>1-5</b>	<b>1-6</b>	<b>1-7</b>	<b>1-8</b>
$\lambda$	$22.2 \pm 0.3$	$13.4 \pm 0.2$	$9.7 \pm 0.1$	–
$\alpha\beta$	$0.00273 \pm 0.00018$	$0.00264 \pm 0.00025$	$0.00677 \pm 0.00097$	–
$\sigma$	12.4	10.5	8.1	–
	<b>2-1</b>	<b>2-2</b>	<b>2-3</b>	<b>2-4</b>
$\lambda$	$10.3 \pm 0.1$	$15.7 \pm 0.2$	$19.7 \pm 0.3$	$19.8 \pm 0.2$
$\alpha\beta$	$0.00688 \pm 0.00095$	$0.00696 \pm 0.00111$	$0.00793 \pm 0.00115$	$0.00865 \pm 0.00119$
$\sigma$	8.2	14.3	15.5	14.2
	<b>2-5</b>	<b>2-6</b>	<b>2-7</b>	<b>2-8</b>
$\lambda$	$7.5 \pm 0.1$	$17.0 \pm 0.4$	$36.8 \pm 0.3$	$21.0 \pm 0.2$
$\alpha\beta$	$0.77470 \pm 1.21695$	$0.00103 \pm 0.00008$	$0.00154 \pm 0.00006$	$0.00632 \pm 0.00066$
$\sigma$	6.6	11.8	12.7	13.2

Table 5

Hull-model best-fit parameters of trial-by-trial data.  $\sigma$  is the estimated standard error. There is greater dispersion than in binned data (session-by-session, Tab. 1).

In essence, the variability of the response of a subject is encoded in the frequencies  $\omega$ , distributed in the so-called power spectral density  $S(\omega)$ , obtained from the response  $v(t)$ . If the response is perfectly stable from trial to trial, then all frequencies are equally represented in  $S(\omega)$  and the power spectral density is constant. If the response varies gradually as in the ideal learning curve of Hull model, then  $S(\omega)$  is a smooth function. If, however, the response varies erratically from trial to trial, as in actual data, then  $S(\omega)$  becomes very ragged and this raggedness is what we call *noise*. The basics of spectral analysis and theoretical shape of the power spectral density for the Hull model without and with noise are presented in Appendix D. Here we only note that noise alone is usually represented by the power spectral density

$$S_a(\omega) = \frac{1}{\omega^a}, \quad (13)$$

where  $a$  is a constant. When  $a = 0$ , noise is said to be *white*, while it is *colored* if  $a \neq 0$ .

The nature of the noise source in data can be discriminated by the large-frequency region of the power spectral density. If all noise comes from statistical error, then this region is flat in the log-log plane. However, if this region is not flat and exhibits a positive or negative average slope, then it is possible that some other random noise-generating mechanism, of cognitive-behavioral origin, is in action.

## Theory

Hull model with colored noise admits a straightforward mathematical treatment as a stochastic process. Let us go back to the original equation (1) for the change in associative strength from one trial to the next:  $\Delta v_n = \alpha\beta(\lambda - v_{n-1})$ ,

which we can also write as  $v_n = (1 - \alpha\beta)v_{n-1} + \lambda\alpha\beta$ . Now we promote  $v_n$  to a random variable  $V_n = v_n + \xi_n$ , where  $v_n$  and  $\xi_n$  are, respectively, the deterministic and stochastic parts. This is tantamount to consider the stochastic version of the previous equation, with an added random noise source  $\eta_n$ :

$$V_n = (1 - \alpha\beta)V_{n-1} + \lambda\alpha\beta + \eta_n, \quad (14)$$

where  $\eta_n = \xi_n - (1 - \alpha\beta)\xi_{n-1}$ . This is called a first-order autoregressive process (ARP) with drift  $\lambda\alpha\beta$  and colored noise  $\eta_n$ . When  $\eta_n$  has a normal distribution (white noise) and in the limit  $\alpha\beta \rightarrow 0$ , this reduces to a random walk (Brownian motion). In the case of Pavlovian conditioning, it would correspond to a baseline random behavior in the presence of non-salient stimuli.

What is the source of the noise  $\eta_n$ ? In our psychological interpretation of this signal, we can draw inspiration from the “1/f noise” cognitive literature, where the variability in human response in memory tasks, reaction tasks, mental rotation, word naming, and so on, is characterized by a colored noise (Dixon et al., 2010; 2012; Eke et al., 2002; Farrell et al., 2006; Gilden, 2001; Gilden et al., 1995; Holden, 2005; 2013; Holden et al., 2009; 2011; Kello et al., 2007; 2008; Ihlen and Vereijken, 2010; 2013; Likens et al., 2015; Stephen et al., 2009a; 2009b; Van Orden et al., 2003; 2005; Thornton and Gilden, 2005; Wagenmakers et al., 2004; 2005; 2012; see Calcagni, 2018, for a brief account, and Kello et al., 2010, and Riley and Holden, 2012, for reviews). There are three interpretations of this phenomenon. In the so-called *idiosyncratic* view, this noise is regarded as the intrinsic uncertainty, possibly due to an internal estimation error, in the formation of representations in the mind, such as the reproduction of

spatial or temporal intervals in human memory (Gilden et al., 1995). Different cognitive systems may have different types of uncertainty, all combining to accidentally give an overall noise term which is not a general, fundamental (i.e., endogenous, intrinsic to mind and body) property of human behavior (Farrell et al., 2006; Wagenmakers et al., 2004; 2005; 2012). In the *nomothetic* view, the stochastic component may be due not to specific cognitive systems, nor to the mere sum of their noises, but to a more fundamental mechanism such that cognition would happen as the emergence of patterns in a self-organizing complex dynamical system (Dixon et al., 2010; 2012; Gilden, 2001; Gilden et al., 1995; Holden, 2013; Ihlen and Vereijken, 2010; Riley and Holden, 2012; Stephen et al., 2009a; 2009b; Van Orden et al., 2003). In particular, the colored noise would be the collective expression of the metastable coordination of different cognitive and motor systems in the performance of a task (Kello et al., 2007). A third view intermediate between the idiosyncratic and the nomothetic was also considered (Likens et al., 2015).

Translating these considerations to the realm of non-human animal behavior, we can entertain the possibility (Calcagni, 2018) that, if nonwhite noise were detected in experiments of Pavlovian or operant conditioning, one would be observing a signal coming from the coordination of motor systems with the internal functioning of the subject's mind (either as an averaging of multiple cognitive subsystems or as an emergent collective manifestation of such coordination). We will come back to this cognitive perspective after analyzing the data.

### Data analysis: comparison with Hull model

Session-by-session data are a coarse-grained version of the full data set of trial points. Inevitably, this coarse graining can hide or distort stochastic signals present at all time scales. For this reason, we consider trial-by-trial data. It is not difficult to check that a similar analysis done with session-by-session data yield the same results, but with a much greater error in the fits.

Table 5 reports the parameters of the Hull model fitting trial-by-trial data, while Fig. 13 shows the power spectral density of the signal of some experimental subjects, calculated from each individual set of trial data points. See Figs. 10 and 11 of the *Supplemental Material* for the spectra of all experimental subjects. Due to failure of recordings, the total number of points of subjects 1-5, 1-6, and 1-7 is smaller than the maximum 3960: respectively, 3828, 3894, and 3916. This causes no problem since we have plenty of statistics. The exponential-dominated smooth region (plateaux near  $\omega = 0$ ) in Fig. D3 is not visible in these figures because they span a larger frequency range; however, one can check that the spectra at low frequencies are of the same form as the simulated white-noise spectrum in Fig. D3.

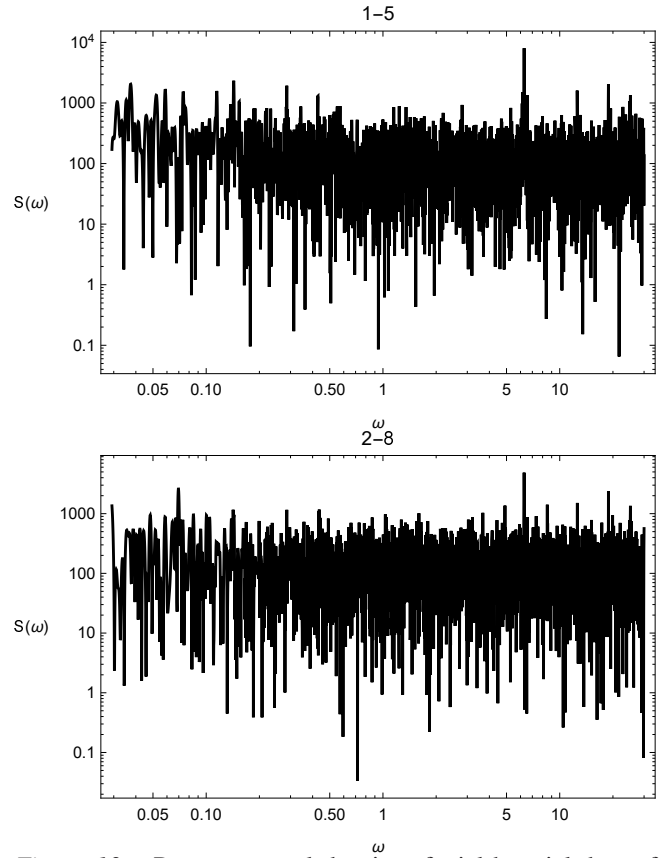


Figure 13. Power spectral density of trial-by-trial data of two representative subjects of Group 1 and Group 2. The onset of the spectra on the left agrees with the signal predicted by Hull model, while the noise band at higher frequencies extends indefinitely to the right.

We look for a fit of the type of (13) (times a constant which plays no role here) of the region of the spectral densities dominated by the stochastic noise, typically for  $\omega > 0.1$ . Fitting the power spectra from  $\omega = 0.1$  to  $\omega = 30$ , we get the results of Tab. 6.<sup>6</sup>

The parameter  $a$  is zero within the experimental uncertainty at the  $1\sigma$ -level for all subjects except 1-1, 1-3, and 2-3, where  $a$  vanishes at the  $2\sigma$ -level. In all cases, the best-fit value of  $a$  is very close to zero, at least in one part over one hundred. Therefore, all subjects of both groups display white noise.

Note that the spectral analysis of the noise signal occurs

<sup>6</sup>For the nonlinear fit, we used a sampling of frequencies of  $\Delta\omega = 0.001$ , but we checked that a sampling ten times coarser does not change the results significantly. Also, if one fits up to a smaller maximum, e.g.,  $\omega = 5$  or  $\omega = 10$ , one does obtain a nonvanishing  $a$  for several subjects. However, this may be due to considering a region of frequencies where the negative slope of the background profile in Fig. D1 still dominates over the noise signal.

$S_a(\omega) = \omega^{-a}$	1-1	1-2	1-3	1-4
$a$	$0.016 \pm 0.011$	$-0.003 \pm 0.010$	$-0.016 \pm 0.014$	$0.003 \pm 0.010$
Color	white*	white	white*	white
	1-5	1-6	1-7	1-8
$a$	$-0.011 \pm 0.016$	$-0.007 \pm 0.010$	$-0.010 \pm 0.013$	–
Color	white	white	white	–
	2-1	2-2	2-3	2-4
$a$	$0.010 \pm 0.010$	$-0.001 \pm 0.010$	$0.021 \pm 0.012$	$0.007 \pm 0.008$
Color	white	white	white*	white
	2-5	2-6	2-7	2-8
$a$	$0.002 \pm 0.007$	$-0.009 \pm 0.023$	$-0.044 \pm 0.051$	$-0.006 \pm 0.008$
Color	white	white	white	white

Table 6

Type of noise in the noise spectrum  $S_a(\omega)$  of individual trial-by-trial data, analyzed between  $\omega = 0.1$  and  $\omega = 30$ . The error is one standard deviation. Asterisks denote conclusions valid within two standard deviations.

in a frequency region unaffected by whether the background model is Hull's or the oscillatory one, Eqs. (4) and (9). The power spectral density of the latter would only differ in the position of the right end of the plateau in Fig. D1 and in an extra bump just at the onset of the slope. When fitting high-frequency data, these details are subdominant with respect to the main noise trend and, in fact, they do not appear in Fig. 13.

## Discussion

Having checked the presence of white noise in individual subjects, we turn to the psychological interpretation of these results. From a strictly behaviorist point of view, the question of whether this noise comes from a naive sum over different cognitive systems or arises as an emergent phenomenon is immaterial. These data cannot tell us anything about either alternative. However, we observe the same noise in all subjects and this noise is *white*. The simplest explanation is that its origin is statistical and implies no fundamental property of the "rat mind." If there were an underlying motor-cognitive mechanism (naive interference or emergent phenomenon) depending on the individual, on the task, and on the relevance of the stimuli for the subject and its learning history, one would see these differences in the noise trend. Although we cannot exclude this possibility, our data do not yield support to it. In particular, they exclude the cognitive function of *attention* as the main responsible for colored noise. In fact, the main processes involved in this Pavlovian experiment are motor and attentional, and the only source of a colored signal could come from attention alone (or its interference with motor processes; idiosyncratic view) or as an emergent phenomenon from the combination of attention and motor processes (nomothetic view). The conclusion is that higher-order cognitive functions, absent in this experiment but present in those of human response, may be the

main source of colored noise.

Talking about response variability in the learning curve, Gallistel et al. (2004) conjectured that data of conditioning experiments might bear a trace of a colored noise. We do not confirm this conjecture here and, on the other hand, we also insist on the existence, at a significant confidence level, of a learning asymptote, which was questioned by the same authors.

We also stress that the cognitive-noise hypothesis is descriptive but not predictive. To the best of our knowledge, no explicit model of the "internal working of the mind" predicting the observed diversity of noise spectra has been proposed. In the section *Quantum Hull model*, we will advance a quantitative theory giving this type of prediction.

## QUANTUM HULL MODEL

Having described, in section *Dynamical models of individual behavior*, several well-known models of Pavlovian conditioning in terms of the classical mechanics of pointwise particles, we make a new step: we quantize them. In physics, "quantization" is a mathematical procedure that uses a classical system as the basis to construct a physically different system governed by the law of quantum mechanics. These laws are still governed by the least-action principle, they describe the behavior of microscopic objects and recover the classical system in a certain limit. In the present context of behavioral psychology, we want to quantize the learning system not just "because we can," but because we want to check whether the dynamical paradigm can also explain quantitatively the response fluctuations observed in experiments.

Thus, a classical pointwise particle moving along a smooth trajectory  $x(t)$  becomes, upon quantization, a wavefunction  $\Psi(x, t)$  which indicates the probability to find the particle at position  $x$  at time  $t$ . It is not our purpose to introduce the reader to the main notions of quantum mechanics.

What matters here is to understand what happens if we quantize conditioning models: do these models predict phenomena in animal behavior not contemplated by standard learning? The answer is in the affirmative.

In “classical” learning, the response is predicted deterministically by the learning curve, so that at time  $t$  after the onset of training the CS-US association strength will exactly be  $v(t)$ ; this association strength is then identified with the amount of response of the subject, for instance, the number of licks. Experimental uncertainty forbids to take this picture too literally, and exact predictions must be checked against data with error bars. However, in “quantum” learning the prediction itself is not deterministic and we cannot claim that at time  $t$  the subject will respond with strength  $v$ . Instead, we can only give a probability distribution  $\mathcal{P}(v, t)$  saying what the chance is that at time  $t$  the subject will respond with strength  $v$ . This uncertainty is *not* due to experimental errors and it will be there even in the most unrealistic case of an error-free observation. In other words, it is intrinsic to the behavior of the animal. Whether this feature is of motor or cognitive origin is a problem one might want to understand after checking the theory experimentally. What matters here is that we can predict the exact shape of the probability distribution  $\mathcal{P}(v, t)$  if we follow the quantization procedure so successful in physics. The point-particle trajectory  $v(t)$  is replaced by a wave-function  $\Psi(v, t)$ , solution to the quantum dynamics, that can spread throughout the whole domain  $0 < v < \lambda$ . The probability to have a certain association strength  $v$  at time  $t$  is given by  $\mathcal{P}(v, t) = |\Psi(v, t)|^2$ . The characteristic of these *quantum* models of Pavlovian conditioning is that they have no way to maintain perfect conditioning (i.e.,  $v = \lambda$ ) indefinitely. After some sojourn time determined by the salience of the stimuli, the subject can exhibit a nonoptimal or even overoptimal association strength away from perfect conditioning, even if the CS-US pair is presented in each trial. We will describe these effects with the simplest available example: the quantum Hull model.

## Theory

In the classical Hull model, at time  $t$  we can determine with absolute accuracy the strength  $v(t)$  and, from Eq. (2), the velocity of learning or learning rate  $\dot{v}(t) = \alpha\beta[\lambda - v(t)]$ . After quantizing this model with the procedure described in Appendix E, as a result we can no longer determine  $v(t)$  and  $\dot{v}(t)$  with arbitrary accuracy. Curiously, the uncertainty  $\Delta v$  on the association strength  $v$  is limited by the uncertainty  $\Delta \dot{v}$  on the learning rate  $\dot{v}$ , in such a way that, in general, if we measure  $v$  with very good accuracy there will be a large uncertainty on a  $\dot{v}$  measurement, and vice versa. In other words, if we force  $\Delta v$  to get as close to zero as possible, then  $\Delta \dot{v}$  will increase, and vice versa. This relative minimum uncertainty, present even in an error-free ideal experiment, is governed

by the relation

$$\Delta v \Delta \dot{v} \geq \frac{\hbar}{2}, \quad (15)$$

where  $\hbar$  is a strictly positive constant, a fundamental parameter of the theory. In the classical model,  $\hbar = 0$  and we can measure  $v$  and  $\dot{v}$  with infinite accuracy (in an error-free experiment) simultaneously.

*A priori*, the subject has infinitely many ways to reach optimal learning  $v = \lambda$  starting from complete ignorance  $v = 0$  at  $t = 0$ . While in the classical model there exists only one single learning curve  $v(t)$  connecting the points  $v(0) = 0$  and  $v(\text{large } t) \simeq \lambda$ , in the quantum model all the possible trajectories are realized simultaneously and in such a way that they interfere with one another. The net effect is the uncertainly relation (15). The interested reader may consult Appendix E for more details about this perspective, which goes under the name of path-integral quantization.

The quantum model gives rise to several prediction.

- *Prediction 1.* The asymptote of learning is not a durable achievement. There exists an intrinsic source of variability in the subject response, not due to statistical errors or unpredictability of individual behavioral quirks. Only three situations as possible: (i) response variability is too slow to be detected, (ii) it only happens between training sessions, or (iii) it happens on a trial-by-trial basis.

- *Prediction 2.* There exists a special quantum state following a Gaussian distribution such that response fluctuations do not decrease in time. Initially, the system evolves almost classically and one can determine with good accuracy the association strength of the subject, but at later trials there is a nonzero chance that the subject display a nonoptimal conditioning level, even if the highest probability is at the asymptotic value  $v = \lambda$ . Quantum fluctuations increase to indefinitely large values.

- *Prediction 3.* There exists a quantum state such that response fluctuations are large and almost constant throughout the whole experiment. This state minimizes the uncertainly principle (15), so that  $\Delta v \Delta \dot{v} = \hbar/2$  at all times. The amplitude  $\delta v$  of quantum fluctuations is of order of the uncertainty  $\Delta v$ , which in turn is of order of the classical asymptote of learning:

$$\Delta v \sim \delta v = O(\lambda). \quad (16)$$

- *Prediction 4.* The universal constant  $\hbar$  can be determined by experiments and reads

$$\hbar \simeq 2\alpha\beta(\Delta v)^2. \quad (17)$$

- *Prediction 5.* Response variability is described by white noise.

Again, we refer to Appendix E for a top-down derivation of these claims. Here we comment on a central aspect relevant to their empirical check. The first prediction is a consequence of the inequality (15). At any given time (i.e., trial), the uncertainty  $\Delta v$  on the association strength can be interpreted as

the fact that the association between the CS and the US continuously varies in strength and is subject to what we may call *quantum fluctuations*. After reaching the asymptote at  $v = \lambda$ , the subject will not keep the maximal response  $\lambda$  because, due to these quantum fluctuations, the association strength will be shifted by some amount  $\delta v > 0$ . Therefore, the actual response at any given time fluctuates as  $\lambda \pm \delta v$ . After some characteristic *sojourn time*  $t_*$  since reaching the point  $v = \lambda$ , the subject shows signs of “unlearning” (if the fluctuation is negative and  $\lambda \rightarrow \lambda - \delta v$ ) or even of “overlearning” (if the fluctuation is positive and  $\lambda \rightarrow \lambda + \delta v$ )!

Therefore, at times  $t > t_*$ , the subject can display either of two behaviors: (A) it loses the incentive even if the US is presented at each subsequent trial and the probability to show a conditioned response upon presentation of the CS starts to decrease; or, (B) its response increases beyond the learning asymptote. Neither situation (A) nor (B) lasts forever because once the particle rolls down back or across the hill-top (under- or over-response by the subject), the presentation of new trials pushes the association strength back to the asymptote. Once reached the asymptote again at a time  $t_1 > t_*$ , the subject will stay there for another period of duration  $\sim t_*$ , after which another fluctuation will happen at a time  $\sim t_* + t_1$  since the beginning of the experiment. And so on.

What do we expect to observe then? In an ideal experiment of quantum physics, one prepares the particle at the unstable maximum at time  $t = 0$  and asks what the probability is to find the particle at the same state after some time  $t$ . However, pointwise measurements and continuous observation of unstable systems (Fonda et al., 1978) can give rise to very different outcomes. Persistence at the maximum can be extended if the system is measured too often or continuously (i.e., observed) and not left to evolve naturally a sufficiently long time (Sudbery, 1984). If one observes the system at a time  $t < t_*$ , most likely one will not detect any change with respect to the initial state, while at times  $t > t_*$  decay from the unstable state will be observed more likely. In the context of comparative psychology, this distinction is less clear. The natural time evolution of the system corresponds to unobservable cognitive processes taking place in the subject after training, away from the experimenter and the conditioning box, while measuring the response of the subject in an experiment yields an empirical estimate of the otherwise unobservable associative strength. However, separating the natural evolution from measurement is a tricky business because “measuring” also means making the system evolve by training. One might change interpretation and insist that “natural evolution” is equivalent to training and a “measurement” corresponds to testing the result of training at the last trial, but this distinction would be quite artificial because the measurement procedure does not depend on whether the US is presented or not. Therefore, each time the subject is trained the association strength evolves *and* is measured at the same

time. As a consequence, we can identify three situations, depending on whether  $t_*$  is greater or smaller than the inter-trial and inter-session intervals.

- (i)  $t_* > \Delta t_{\text{session}} > \Delta t_{\text{trial}}$ . If  $t_*$  is greater than the duration of a trial  $\Delta t_{\text{trial}}$ , the phenomenon of sojourn time is altered, and in fact reset, each time a break in conditioning is taken. In this case, once the subject reaches the asymptote of learning we should observe a constant response at  $v = \lambda$ , at all trials. If  $t_*$  is also greater than the inter-session interval, then the response is stable both on a trial-by-trial and on a session-by-session time scale. The learning curve would be identical to the classical one in both time scales.

- (ii)  $\Delta t_{\text{trial}} < t_* < \Delta t_{\text{session}}$ . If  $t_*$  were greater than the trial duration  $\Delta t_{\text{trial}}$  but smaller than the inter-session interval  $\Delta t_{\text{session}}$ , then we should observe a change in response between sessions, rapidly restored to maximal learning after the first trials of the session. The trial-by-trial learning curve would then display a long plateau marked by local “pulses” or fluctuations lasting only the first few trials of each session.

- (iii)  $t_* < \Delta t_{\text{trial}}$ . If  $t_*$  is smaller than the duration of a trial, then we should observe decay, to the left (under-response) or to the right (over-response), from the learning asymptote. The overall picture after the acquisition phase is neither that of a constant, stable maximal response (as in the classical Hull model or when  $t > \Delta t_{\text{session}}$ ) nor a sudden decrease or increase in the response some time after reaching the asymptote (as it would happen in a physics experiments), nor a sudden decrease or increase of response at the beginning of each session (as when  $\Delta t_{\text{trial}} < t < \Delta t_{\text{session}}$ ). Rather, there would be a never-ending series of trial-by-trial oscillations above and below the asymptote.

### Empirical evidence of predictions

1. Our observations clearly fall into case (iii). Response variations occur on a trial-by-trial time scale  $t_* < \Delta t_{\text{trial}}$ .

2. If the system were described by a Gaussian state, response fluctuations should increase in time. This prediction is not met. If one starts from a nearly classical state with a spread width  $b$  close to zero, late-time fluctuations may become compatible with data, but then early variations of the response are too small relative to those actually observed. Roughly speaking, the problem is that, regardless the absolute size of the fluctuations, we did not observe any relative change in them during the experiment. There are two alternative meanings we can attach to this outcome. Either the Gaussian state is a valid description but  $b$  is so small (i.e., the initial state is so sharply peaked at the classical solution) that we cannot see an appreciable spread of the distribution of the association strength  $v$  in the total time scale of the experiment; or we must exclude the Gaussian state (75) as a viable initial condition. The second possibility does not rule out the theory as a whole because one can choose other states, usually constructed from the non-normalizable energy

eigenstates of the inverted oscillator (see Barton, 1986). In general, however, these will not minimize the uncertainty principle, and they will suffer from the same problem of fast spreading in time. Due to the quantum uncertainty in the rate of change of the association strength, the association strength can acquire different velocities and so get further and further displaced from the classical value.

3. The prediction (16) is compatible with what we found in the experiment. Identifying the amplitude of fluctuations with the estimated standard deviation of the fits with Hull model,

$$\delta v \stackrel{?}{=} \sigma, \quad (18)$$

we get  $\sigma \sim 0.1 - 0.6\lambda$ : the uncertainty of the association strength is between 10% and 60% the value of the asymptote, depending on the subject, for an average of about one third of the asymptote. This is true not only for the session-by-session data (Tab. 2), but also for the trial-by-trial ones (Tab. 5). Using trial-by-trial data, the average of the variance  $\sigma^2$  for each group and for all experimental subjects together is

$$\text{Group 1: } \quad \bar{l}^2 \simeq \sigma_{\text{avg}}^2 = 129.2 \pm 40.5, \quad (19a)$$

$$\text{Group 2: } \quad \bar{l}^2 \simeq \sigma_{\text{avg}}^2 = 154.0 \pm 63.9, \quad (19b)$$

$$\text{Group 1+2: } \quad \bar{l}^2 \simeq \sigma_{\text{avg}}^2 = 142.5 \pm 55.6. \quad (19c)$$

The value obtained in each group separately is the same within the experimental error. We can improve this result by recalling that the quantum model we are testing is based on the inverted harmonic oscillator associated with Hull classical model. However, we saw that at least subjects 1-7, 2-3, 2-4, and 2-8 follow an oscillatory learning curve. Therefore, strictly speaking the quantum Hull model does not apply to these animals. On the other hand, developing a quantum theory over the oscillatory classical model (9) can be more difficult than for the Hull model (4) because one cannot recast the model as a simple inverted harmonic oscillator and one has to deal with the dissipative forces of a damped model. As a simple way to obviate this problem, we discard the data of subjects 1-7, 2-3, 2-4, and 2-8 from the estimates of  $\bar{h}$ . The result is a decrease in the error uncertainty:

Group 1 (no 1-7):

$$\bar{l}^2 \simeq \sigma_{\text{avg}}^2 = 139.8 \pm 33.6, \quad (20a)$$

Group 2 (no 2-3, 2-4, 2-8):

$$\bar{l}^2 \simeq \sigma_{\text{avg}}^2 = 123.2 \pm 59.7, \quad (20b)$$

Group 1+2 (no 1-7, 2-3, 2-4, 2-8):

$$\bar{l}^2 \simeq \sigma_{\text{avg}}^2 = 132.3 \pm 48.0. \quad (20c)$$

Thus, the typical response oscillation is similar for all subjects and is large despite the quantum state being very close to classicality.

Subject	Group 1	Group 2
1	2.4	0.9
2	0.6	2.8
3	1.0	3.8
4	4.1	3.5
5	0.8	<i>67.5</i>
6	0.6	0.3
7	0.9	0.5
8		2.2
Average	1.5 ± 1.2	10.2 ± 21.7
Corr. average		2.0 ± 1.3

Table 7

Estimate (17) of  $\bar{h}$  for the individual subjects and in average. In the corrected average of Group 2, the datum of subject 2-5 (in italics) has been removed.

4. Applying the estimate (18) to Eq. (17) yields  $\bar{h} \simeq 2\alpha\beta\sigma^2$ . This expression is crude and can only give generic qualitative indications about the viability of the model. Plugging the values of  $\alpha\beta$  and  $\sigma^2$  for each subject individually, we get a rather heterogeneous set of values, reported in Tab. 7.

One of the data is especially off the average, namely, subject 2-5. This is due to its extremely high value of  $\alpha\beta \approx 0.77$ . Removing this datum, the average of Group 2 is comparable with that of Group 1. The grand average is  $1.7 \pm 1.3$ . The uncertainty is of order of the central value and, although the latter is different from zero within one standard deviation, it does not constitute a compelling evidence of the validity of the model.

5. Recalling that there is no trace of color in our data and that the descriptive stochastic model with white noise is the best fit, we immediately conclude that the quantum theory, which also predicts a white-noise spectrum of fluctuations, adequately describes the signal of all subjects.

## Discussion

Holden et al. (2011) and Van Orden et al. (2010) suggested the hypothesis that response variability could be analogous to that produced by quantum fluctuations in quantum mechanics. This parallelism was partially motivated by the fact that human behavior can be affected by its measurement, just like a quantum system is modified by the act of measuring with an apparatus. Here we took the analogy *ad litteram* and, after having defined the quantum system rigorously, checked whether it is experimentally viable. We found that response variability *could* be interpreted as quantum fluctuations of the size

$$\delta v \sim \sqrt{\frac{\bar{h}}{2\alpha\beta}}. \quad (21)$$

Any other model predicting an  $\alpha\beta$ -dependent  $\delta v$  with a differ-

ent trend in (and magnitude of) the amplitude of fluctuations would hardly find a subject-independent constant  $\bar{h}$  to a significant confidence level. Combining the estimate on  $\bar{h}$  with the prediction on white noise, we can conclude that data *are* compatible with the quantum theory. However, we cannot go beyond a moderate optimism regarding its validity, since the error associated with the estimates (19) is rather large, about 30 to 40% of the value. The error in the corrected estimates (20) is slightly smaller. This uncertainty is due to the estimation of the amplitude of fluctuations by the rough guess (18). Moreover, statistical white noise can obviously accommodate data with a flat stochastic signal. Another potential source of white noise is the experimental design itself. The delivery of the US with a uniform distribution during the CS already introduces a random component that should reflect in the subjects' response. Therefore, one would expect white noise even in the total absence of any "cognitive" or "quantum" mechanism. This random component is already taken into account in the statistical error, which, as we just noted, dominates the relation (17) and the estimates (19) and (20).

### GENERAL CONCLUSIONS

By assuming minimization of the action as a guiding principle, we have constructed a new framework of models of Pavlovian conditioning. The simplest of these models is a natural extension of Rescorla–Wagner model with one cue (Hull model in short). Looking at data, we saw that the oscillatory classical model (9) with  $A = 0$  and  $\mu \neq 0$  is favored over Hull's in 27% to 40% of the experimental cases. The estimated dispersion of the session-by-session individual data with respect to the theoretical curve is about the same for the Hull and oscillatory models in all the cases where the latter is clearly favored (Tab. 4). In all the other cases, the parameter  $\mu$  is close to zero and Hull model and its extension coincide. Therefore, all data can be explained by the extension of Hull model. At a biological level, the explanation of why  $\mu$  takes different values in different subjects (for some, as we have seen,  $\mu$  is close to zero) might reside in individual differences in brain configuration. Different dynamical adaptations of synaptic connections during learning would give rise to a different damping rate of the oscillations. Regardless of whether this microscopic interpretation has a basis in reality or not, the least-action principle states that learning is a naturally effective process that minimizes the internal changes in the subject. These changes are observable and can be quantified through the behavioral laws stated here.

We have also analyzed the quantum theory using Hull model as the classical layer and found that it could describe response fluctuations, although we could not find conclusive evidence. Quantizing the oscillatory model will probably clarify this open question.

In parallel, using individual trial-by-trial data we have

checked for the presence of colored noise in the frequency spectrum of the subjects' response. We found no evidence of color and all subjects showed a flat (white) noise spectrum (Tab. 6). The origin of this white noise can be simply statistical, but we also considered two quantitative models accounting for it. One is a descriptive model implementing stochastic fluctuations in the subject's individual response; speculations about the origin of this noise may find inspiration in the " $1/f^\alpha$ " cognitive literature, albeit in that case there is established evidence of a colored spectrum. The other model is not only descriptive, but also predictive, and interprets response variability as a manifestation of a process obeying the laws of quantum mechanics. We tested the predictions of the theory with data and we found agreement, although the error bars on the estimates of the "Planck" constant  $\bar{h}$  are too conspicuous to conclude that the model is correct.

Although data show that individual responses are far from following the textbook smooth learning curve, they do not show an "abrupt acquisition" phenomenon either, as sometimes claimed in the literature (see Gür et al., 2018, and references therein). Some subjects do show something that could be described as an abrupt acquisition, but response variability is too large throughout the experiment to make this conclusion meaningful when, to put it simply, a sharp initial rise in response is yet another random fluctuation around the ideal average curve (see Figs. 2 and 4 in the *Supplemental Material*). Precisely for the same reason, although it is true that traditional associative models do not predict abrupt changes in behavior, our findings do not support representational or model-based models either (Gür et al., 2018). Response variability is so fine grained that its random, nowhere-differentiable nature is, in our opinion, unquestionable. We have offered two interpretations about these behavioral fluctuations, stochastic (from cognitive noise component in the underlying model) or quantum (from a model affected by quantum uncertainties). Both cases go beyond standard associationism, but are based on it nevertheless: associative learning still is an adequate description of averaged data.

The psychological interpretation of the quantum theory remains open. The idea that quantum mechanics can play a role in brain processes and in the emergence of consciousness is almost as old as the discipline (see Stanford Encyclopedia of Philosophy, 2015, for an account) and fostered debate among psychologists, physicists and philosophers, sometimes leading to original collaborations between authorities in their respective fields (Beck and Eccles, 1992; Bohm, 1990, 2002; Jung and Pauli, 1952; Penrose, 1989; Ricciardi and Umezawa, 1967; Stapp, 2009; Wigner, 1967). Recently, there has been interest in applying quantum mechanics to human cognition and decision making (Bruza et al., 2009a; 2015; Busemeyer and Bruza, 2012; Busemeyer et al., 2006; 2009; 2011; 2014; Pothos and Busemeyer, 2011; Pothos et al., 2017; Trueblood and Busemeyer, 2012; Years-

ley and Busemeyer, 2015), reinforcement learning (Fakhari et al., 2013), as well as in the general field of artificial intelligence (Bruza et al., 2009b; Busemeyer et al., 2012). The role of quantum physics at the time scale of brain processes ( $\sim 10 - 100$  ms) is still controversial (Hagan et al., 2002; Tegmark, 2000) and it is not clear whether and how it affects cognition and behavior. Our main concern here is not the origin of quantum cognitive or behavioral phenomena, but the collection of empirical evidence (or the lack of it) in their favor in the context of animal learning, novel with respect to the above literature. We may come back to the psychological interpretation of the quantum Hull model only after better evidence is gathered. Our results regarding this model are insufficient to validate it but, at the same time, we hope they are suggestive enough to elicit the researcher’s curiosity further.

A difficulty in testing the model in the future may come from the fact that the constant  $\hbar$  is dimensionful. Above, we always omitted this information, but all values of  $\hbar$  in this paper should be quoted in units of (association strength)<sup>2</sup> per time unit or, more specifically, “(licks)<sup>2</sup>/trial.” Clearly, these units become cumbersome when trying to compare values obtained in different experiments with different dependent variables and trial duration. At any rate, the priority should be to verify the constancy of  $\hbar$  with independent data, leaving the cross-experimental determination of the actual value of  $\hbar$  as a next-step problem. In particular, one should investigate whether response fluctuations remain large, constant, and with a white-noise spectrum also when the US/reinforcer is presented on a more regular strictly deterministic schedule.

Finally, a word about replicability and applicability. Since all the models we have presented in the main text of this paper are foundational extensions of the *simplest* conditioning process involving simple associations between stimuli and responses, it may not be necessary to conduct *ad hoc* experiments to test their validity. The long-range oscillations of the dynamical model, the spectral properties of response variations, and all the main features the quantum model can be checked in any experiment, past or future, that had a sufficient number of sessions (in the case of the dynamical model) or trials (in the case of the stochastic noise and of the quantum model) and whose design induced a simple conditioning process. In general, the condition of having many sessions is much more restrictive than that of having many trials, but it is not necessary to take or make experiments as lengthy as ours. Eventually, what one is looking for is cumulative evidence, and that is achievable with enough experiments of moderate length. Moreover, our models may obtain confirmation or be ruled out by extant or future data not only about Pavlovian conditioning, but also from the operant conditioning literature. In the second case, one invokes the possibility that associative models can also describe operant behavior (Killeen and Nevin, 2018).

**Supplemental material.** Additional figures and data are available at this [Dropbox link](#).

**Acknowledgments.** G.C. thanks Pedro Vidal for invaluable help in writing the PASCAL programs of the pilot experiments that eventually led to the program used in this paper and Esmeralda Fuentes, Gabriela E. López-Tolsa, Ana de Paz and Valeria E. Gutiérrez-Ferre for rat-related advice. All authors thank Ralph Miller for his many fruitful comments and suggestions about the experimental design, Antonio Rey for his outstanding handling of the lab schedule and of technical issues, and Vanessa Roldán for her involvement in the experiment and daily lab routine through part of this project. The experiment was run at the Animal Behavior Lab, Departamento de Psicología Básica I, Facultad de Psicología, Universidad Nacional de Educación a Distancia, Madrid, Spain, and was supported by grant PSI2016-80082-P from Ministerio de Economía y Competitividad, Secretaría de Estado de Investigación, Desarrollo e Innovación, Spanish Government (R.P. Principal Investigator).

## Appendix A

### DYNAMICAL HULL MODEL WITH FRICTION

Taking the time derivative of (2), we obtain

$$\ddot{v} + 2\alpha\beta\dot{v} + (\alpha\beta)^2(v - \lambda) = 0. \quad (22)$$

This equation can be derived from the action<sup>7</sup>

$$S_{\text{Hull}} = \int_0^T dt \tilde{\mathcal{L}}_{\text{Hull}}, \quad (23)$$

where the Lagrangian  $\mathcal{L}_{\text{Hull}}$  reads

$$\tilde{\mathcal{L}}_{\text{Hull}} = e^{2\alpha\beta t} \mathcal{L}_{\text{Hull}}, \quad \mathcal{L}_{\text{Hull}} = \frac{\dot{v}^2}{2} - U(v), \quad (24a)$$

$$U(v) = \frac{(\alpha\beta)^2}{2}(v - \lambda)^2. \quad (24b)$$

Let us explain all symbols and the procedure in detail.  $t$  is time and the integral runs from some initial time conventionally set to  $t = 0$  to the time  $t = T$  when the experiment ends.

<sup>7</sup>The action (23) is defined up to an overall normalization constant and we can choose such a constant so that the constant acceleration term in (22) is 1. In other words, if  $\lambda \neq 0$  we can rescale  $S_{\text{Hull}} \rightarrow -mS_{\text{Hull}}$ , where  $m := -(\lambda\alpha^2\beta^2)^{-1}$  is something we might call the “conditioning mass.” This is an intuitive measure of the inertia the subject experiences during learning. When the magnitude or salience of the US or the salience of the CS decrease, the mass  $|m|$  increases and the less efficient the conditioning will be. The heavier the mass, the longer the learning will take to reach a certain strength of association. Note that we have chosen the arbitrary rescaling of the action in such a way that the conditioning mass depends on all the parameters we would expect to affect the inertia of learning on empirical grounds. But for practical purposes, one can work with the original action (23).

The function  $v = v(t)$  is the association strength related to one CS. The ideal situation of maximal learning corresponds to  $T = +\infty$ . For instance, at the beginning of an excitatory conditioning the association strength will be  $v(0) = 0$  and its velocity  $\dot{v}(0) \neq 0$ , while at arbitrarily large times  $v(+\infty) = \lambda > 0$  (some asymptote determined by the magnitude of the US) and  $\dot{v}(+\infty) = 0$ .

In physics terminology, Eq. (24) corresponds to a nonrelativistic, classical particle with *kinetic energy*  $\dot{v}^2/2 \geq 0$  and *potential energy*  $U(v)$ . According to the variational principle in classical mechanics, the dynamical equation for a particle following a trajectory  $x(t)$  is obtained by varying an action  $S[x]$  with respect to a small fluctuation  $\delta x$  of the degree of freedom  $x(t)$  and imposing that the action is stationary against this fluctuation ( $\delta S = 0$ ) when the latter vanishes at the boundary of the integration domain,  $\delta x(0) = 0 = \delta x(T)$ . This means that the motion  $x(t)$  solving the dynamics minimizes the path from point  $x(0)$  to point  $x(T)$ . For this reason, the variational principle (8) is also called the principle of least action. For an action  $S[v]$  depending on one degree of freedom  $v$ , the equation of motion (8) is equivalent to the Euler–Lagrange equation

$$\frac{d}{dt} \frac{\partial \tilde{\mathcal{L}}}{\partial \dot{v}} - \frac{\partial \tilde{\mathcal{L}}}{\partial v} = 0. \quad (25)$$

It is easy to check that Eq. (22) is given by (25) when applied to (24). For a generic potential, the equation of motion reads  $\ddot{v} + 2\alpha\beta\dot{v} + U'(v) = 0$ , where the prime is a derivative with respect to  $v$  and the *friction* term  $2\alpha\beta\dot{v}$  is generated by the prefactor  $\exp(2\alpha\beta t)$  in the action. Friction terms can arise in very different contexts in physics. One is in the dynamics of fields in curved spacetimes. In that case, the prefactor  $\exp(2\alpha\beta t)$  would correspond to the volume density factor  $\sqrt{-g}$  of space(time). The other way to get friction is by the conventional non-variational approach to classical mechanics, where the Lagrangian does not depend explicitly on time. By definition in this case, the equation of motion is not (25) but

$$\frac{d}{dt} \frac{\partial \mathcal{L}}{\partial \dot{v}} - \frac{\partial \mathcal{L}}{\partial v} = Q, \quad Q = -2\alpha\beta\dot{v}, \quad (26)$$

where  $Q$  is the friction force. The final result is the same, Eq. (22). A third way to obtain Hull model, without friction but with an inverted potential, can be found in section *Quantum Hull model*.

The Lagrangian (24a) has a clear interpretation in physics: it describes the one-dimensional dynamics of a nonrelativistic particle with positive mass and in a potential  $U(v)$ . The particle, or worldline  $v(t)$ , is nonrelativistic because of the form of the kinetic term  $m\dot{v}^2/2$ . It has a positive mass because, in our case,  $m = +1$ . The potential  $U(v)$  (Fig. 9) has a quadratic part, a linear part and a constant term, but it is just quadratic when expressed in terms of the variable

$$x := \lambda - v. \quad (27)$$

This is the potential of a *damped harmonic oscillator*, i.e., a particle with trajectory  $x(t)$  attached to a spring with positive spring constant  $k = (\alpha\beta)^2$  and subject to friction. The classical equation of motion (22) is rewritten as

$$\ddot{x} + 2\Omega\dot{x} + \Omega^2 x = 0, \quad \Omega := \alpha\beta, \quad (28)$$

where we introduced a “frequency”  $\Omega$  proportional to the salience of the US and of the CS. In excitatory conditioning, the particle rolls down the potential well from the point  $x = \lambda$  ( $v = 0$ ) to the global minimum at  $x = 0$  ( $v = \lambda$ ), where it stops due to the finely tuned friction with damping coefficient  $2\alpha\beta$  (Fig. 9). In extinction, the minimum is shifted to the origin but the particle behavior is similar, rolling from  $v = \lambda$  down to  $v = 0$ .

The potential (24b) in the Lagrangian (24a) gives rise to the equation of motion (28), which is very special: the damping coefficient  $2\Omega$  is exactly twice the frequency of the oscillator. In general, this would be considered as a fine tuning of the parameters of the model because the friction term makes the particle stop precisely at the bottom of the potential. If we relax this condition but still allow for friction, the most natural outcome will be that the particle will start to oscillate around the minimum of the potential, eventually sitting on top of it when its kinetic energy is exhausted. This is achieved simply by changing Eq. (24b) as

$$U(v) = \frac{(\alpha\beta)^2 + \mu^2}{2}(v - \lambda)^2 \quad (29)$$

where  $\mu$  is a constant. Equation (22) is then replaced by

$$\ddot{v} + 2\Omega\dot{v} + (\Omega^2 + \mu^2)(v - \lambda) = 0, \quad \Omega = \alpha\beta, \quad (30)$$

whose solution is Eq. (9). This profile has concrete realizations in electronic engineering and signal processing and is called “step response” in that context (the oscillatory pattern is called “ringing”). When  $\mu \neq 0$ , the particle is subject to a friction force  $Q$  given by plugging Eq. (9) into Eq. (26).

## Appendix B

### MULTI-CUE AND VARIABLE-SALIENCE MODELS

For future explorations, we note that it is possible to recast any model of Pavlovian conditioning as a dynamical system described by the action

$$S = \int_0^T dt \left[ \sum_{i=1}^N \frac{\dot{v}_i^2}{2} - \sum_{i=1}^N U_i(v_i) - W(v_1, \dots, v_N) \right], \quad (31)$$

where the functions  $v_i = v_i(t)$  are the association strengths related to  $N$  conditioned stimuli ( $N$  “particles”),  $U_i$  is the potential energy of each particle, and the term  $W(v_1, \dots, v_N)$  is an interaction describing how the particles affect one another by cross-terms. The total potential energy of the system is  $\sum_i U_i + W$ .

Having already discussed the Hull model for a single CS (Hull, 1943), we now consider the Rescorla–Wagner model generalizing Hull model to many stimuli (Rescorla and Wagner, 1972; Wagner and Rescorla, 1972), the Mackintosh attentional model (Mackintosh, 1975b), and a nonlinear approximation to Mackintosh model recently proposed by one of the authors (Calcagni, 2018). Notice that, in some cases, it may be more convenient to recast the system with different variables (if available) than the association strength in (31).

### Classical dynamics of the Rescorla–Wagner model

The Rescorla–Wagner model (Rescorla and Wagner, 1972; Wagner and Rescorla, 1972) is an extension of Hull model to many conditioned stimuli. The trial-by-trial change in each strength of association  $v_n^{(i)}$ ,  $i = 1, \dots, N$ , is

$$\Delta v_n^{(i)} = \alpha_i \beta \left[ \lambda - \sum_{j=1}^N v_{n-1}^{(j)} \right], \quad (32)$$

which, in the continuum limit, translates to the differential equations

$$\dot{v}_i = \alpha_i \beta \left( \lambda - \sum_{j=1}^N v_j \right), \quad i = 1, \dots, N, \quad (33)$$

$$\ddot{v}_i = \alpha_i \left( \sum_{j=1}^N \alpha_j \right) \beta^2 \left( \sum_{k=1}^N v_k - \lambda \right). \quad (34)$$

The latter stems from the multiparticle action (31) with

$$U_i(v_i) = -\frac{1}{2} \alpha_i \left( \sum_j \alpha_j \right) \beta^2 (v_i - \lambda)^2, \quad (35)$$

$$\begin{aligned} W(v_1, \dots, v_N) &= - \left( \sum_j \alpha_j \right) \beta^2 \left( \sum_i \alpha_i v_i \right) \sum_{k \neq i} v_k \\ &= - \left( \sum_j \alpha_j \right) \beta^2 \sum_i \sum_{k \neq i} (\alpha_i + \alpha_k) v_i v_k, \end{aligned} \quad (36)$$

as one can check from Eq. (25) for each  $v_i$ . In physics, this would correspond to a system of interacting, inverted harmonic oscillators (see section *Quantum Hull model* for the single inverted oscillator). It is easy to check that the energy of each inverted oscillator is not conserved individually due to interactions.

### Classical dynamics of the Mackintosh model and its nonlinear approximation

For one CS, the attentional model by Mackintosh is described by

$$\Delta v_n = \alpha_{n-1} \beta (\lambda - v_{n-1}), \quad \Delta \alpha_n = \gamma (\lambda - v_{n-1}). \quad (37)$$

In the continuum,

$$\dot{v} = \beta \alpha (\lambda - v), \quad \dot{\alpha} = \gamma (\lambda - v), \quad (38)$$

which can be combined as  $\partial_t [v - \beta \alpha^2 / (2\gamma)] = 0$ . Therefore,  $v$  and  $\alpha$  are related by

$$v(t) = \frac{\beta}{2\gamma} \alpha^2(t) + \lambda - c, \quad (39)$$

where  $c$  is a constant. Plugging this back into (38), one obtains two first-order equations decoupled in  $v$  and  $\alpha$ , with unique solutions

$$v(t) = \lambda - c \operatorname{sech}^2 \left( \sqrt{\frac{\gamma \beta c}{2}} t \right), \quad (40a)$$

$$\alpha(t) = \sqrt{\frac{2\gamma c}{\beta}} \tanh \left( \sqrt{\frac{\gamma \beta c}{2}} t \right). \quad (40b)$$

Since  $v(0) = \lambda - c$  and, for  $c > 0$ ,  $v(\pm\infty) = \lambda$ , excitatory conditioning is obtained for  $c = \lambda$ . Comparing with Eq. (3), one immediately sees that the learning curve of the continuous Mackintosh model is less steep at the beginning of the conditioning, a phenomenon we dubbed (we will presently see why) “uphill learning” in Calcagni (2018). Mackintosh’s model for two or more cues corresponds to a multi-particle system we will not write down here.

The construction of a Lagrangian is somewhat problematic for this model. In fact, *a priori* the strength of association  $v$  and the salience  $\alpha$  of the CS are independent variables and one should consider a Lagrangian  $\mathcal{L}[v, \alpha] = \dot{v}^2/2 + \dot{\alpha}^2/2 - U_1(v) - U_2(\alpha) - W(v, \alpha)$  which is varied with respect to the two degrees of freedom  $v$  and  $\alpha$ . However, there is no such action. From (38), we have

$$\ddot{v} = -\beta^2 \alpha^2 (\lambda - v) + \gamma \beta (\lambda - v)^2, \quad \ddot{\alpha} = \gamma \beta \alpha (\lambda - v). \quad (41)$$

If we ask to vary  $\mathcal{L}$  with respect to  $v$  and  $\alpha$  independently using the Euler–Lagrange equations (25), then the first equation in (41) suggests an interaction term  $W = \beta^2 \alpha^2 (\lambda v - v^2/2) + d$  for some constant  $d$ , while the second equation in (41) requires  $W = \gamma \beta \alpha^2 v/2$ . Even setting  $d = 0$ , these two expressions can never match because the first one has an extra  $O(\alpha^2 v^2)$  term. Therefore, if we insist in describing the model with a dynamical action, we must first use the relation (39) to recast Eq. (41) into a single nonlinear differential equation. Let us do this first for the association strength  $v$ . Equation (40a) can be recast as

$$\dot{v} = \pm \sqrt{-2U(v)}, \quad (42)$$

$$\begin{aligned} U(v) &= -\gamma \beta (v - \lambda + c)(v - \lambda)^2 \\ &= -\gamma \beta [(c - \lambda) \lambda^2 + (3\lambda - 2c) \lambda v - (3\lambda - c)v^2 + v^3]. \end{aligned} \quad (43)$$

Notice that the writing (42) is equivalent to  $\ddot{v} + U'(v) = 0$ . Then, the Lagrangian reads

$$\mathcal{L}_{\text{Mac}} = \frac{\dot{v}^2}{2} - U(v), \quad (44)$$

while the energy is

$$E_{\text{Mac}} = \gamma\beta(v - \lambda - c)(\lambda - v)^2 + U(v) = 0. \quad (45)$$

The potential (43) is understood as valid in the interval  $0 \leq v \leq \lambda$ , while outside this interval one should impose the infinite barriers as in (24).

Mathematically, the only but important difference with respect to Hull model is in the form of the potential: a polynomial of order 2 in the Hull case and of order 3 in the Mackintosh case, with the sign of the linear and quadratic terms flipped; see Fig. B1. While in the Hull model excitatory conditioning is represented by a particle rolling up the potential towards the absolute maximum, in the Mackintosh model the particle has first to roll down a trough (the local minimum in the figure) before climbing up the local maximum. Defining the action with an overall extra  $-$  sign, this motion consists in climbing up a hill before rolling down the local minimum; this is the dynamical description of “uphill” learning.

It may be more convenient to recast the system in terms of the variable  $\alpha$ . The problem of the potential in (44) is that it is unbounded from below. The solution (40a) is of “rolling” type, i.e., the particle moves from some initial position down to the local minimum or up to the local maximum. In order to avoid falling indefinitely down or climbing upwards the potential, we have imposed the initial conditions typical of a learning process. However, these initial conditions are rather unnatural inasmuch as they do not correspond to a local extremum of the potential: so to speak, the particle starts with non-zero velocity at a slope of the potential. This configuration is not suitable to describe quantum solutions of the quantum system, which should always begin from or end at a static configuration.

Such is the characteristic of the solution (40b). The second expression in (38) can be written as

$$\dot{\alpha} = \pm \sqrt{-2U(\alpha)}, \quad (46)$$

$$U(\alpha) = -\frac{1}{2} \left[ \gamma c - \frac{\beta}{2} \alpha^2 \right]^2, \quad (47)$$

corresponding to the Lagrangian

$$\tilde{\mathcal{L}}_{\text{Mac}} = \frac{\dot{\alpha}^2}{2} - U(\alpha). \quad (48)$$

The potential  $U(\alpha) \leq 0$  is quartic and is bounded from above (Fig. B2). For  $c > 0$ , its two maxima are at  $\alpha = \pm \sqrt{2\gamma c/\beta}$ . In particular, to reach the asymptotic value  $\alpha = 1$  it must be  $\gamma = \beta/(2c)$ . The solution (40b) is a *kink* interpolating

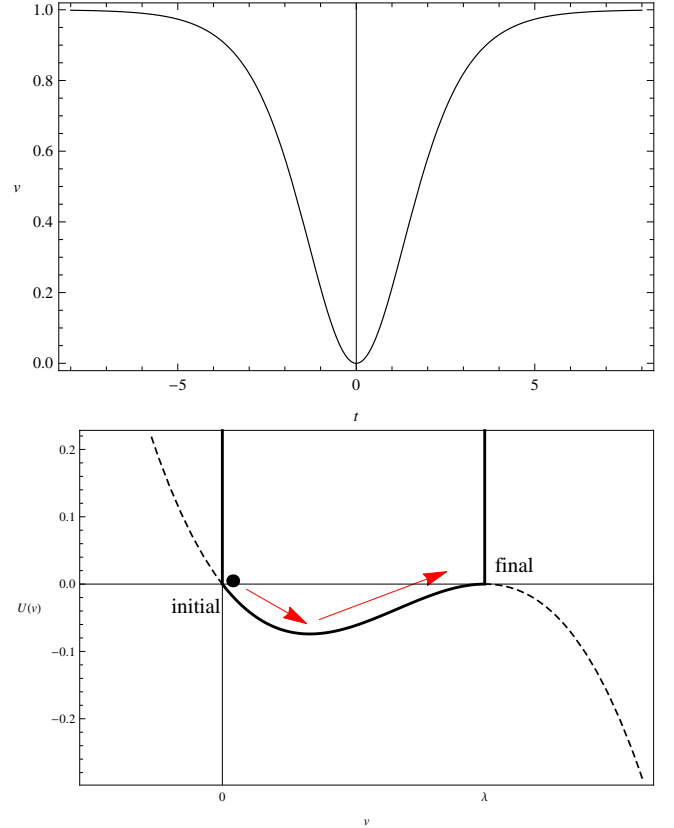
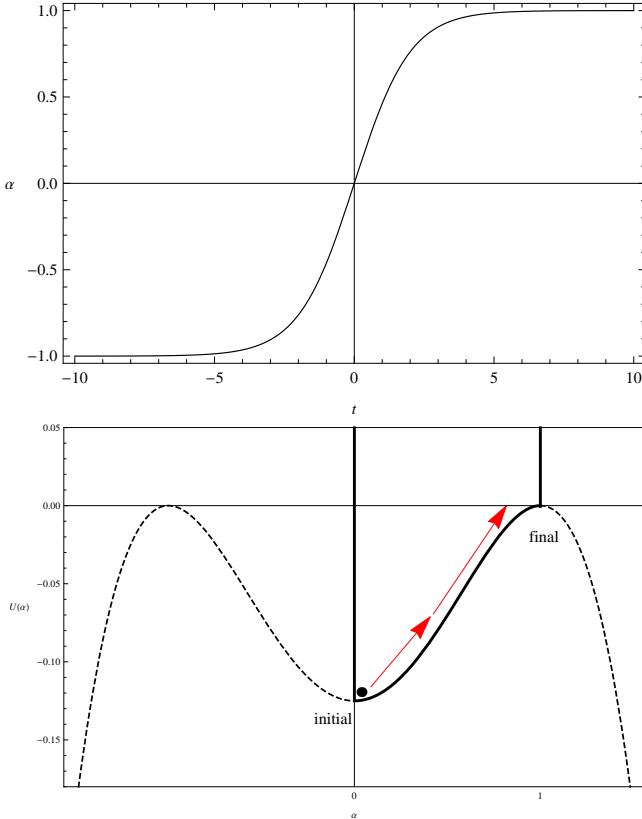


Figure B1. Top panel: the solution (40a) of Mackintosh conditioning model (44) for  $c = \lambda = 1$ ,  $\beta = 1$  and  $\gamma = 1/2$ . Bottom panel: the potential  $U(v)$  (43) for  $c = \lambda = 1$  and  $\beta\gamma = 1/2$ . The particle rolling down the potential represents the change in the associative strength. The direction of “motion” in excitatory conditioning is represented by a red arrow.

between these maxima. In the present case, however,  $t \geq 0$  and the solution runs from the local minimum at  $\alpha = 0$  to the positive maximum. This corresponds, in particular, to the excitatory case  $c = \lambda$ .

Let us pause for a moment and discuss a caveat. To get an extinction curve, one should have  $v(0) = \lambda$  as initial condition and  $v(\pm\infty) = 0$ . Then, setting  $\lambda = 0$  one would have to impose  $c < 0$ ; for this range of values,  $v$  and  $\alpha$  remain real valued but become periodic,  $v \propto \cos^{-2}$  and  $\alpha \propto \tan$ . This behavior does not correspond to extinction. Another possibility is to consider the branch  $t \in (-\infty, 0]$  that we ignored in all the other models. Since  $v$  is even in time, following  $v(t)$  from the infinite past until  $t = 0$  corresponds to decrease the association strength from  $\lambda$  to 0 (Fig. 12). However, this is a solution of the equations of motion with a nonvanishing parameter  $\lambda$ , which means that the US is offered at the end of each trial. Clearly, this does not correspond to a realistic extinction experiment. Rather, it is a sort of “rewinding” of an excitatory experiment backwards



*Figure B2.* Top panel: the solution (40b) of Mackintosh conditioning model (48) for  $c = \lambda = 1$ ,  $\beta = 1$  and  $\gamma = 1/2$ . Bottom panel: the potential  $U(\alpha)$  (47) for  $c = \lambda = 1$  and  $\beta\gamma = 1/2$ . The particle rolling down the potential represents the change in the salience of the CS. The direction of “motion” in excitatory conditioning is represented by a red arrow.

in time or, conversely, an excitatory process with a different parametrization of time ( $t$  running from 0 to  $-\infty$ ). The latter interpretation can also be reached by taking the Mackintosh proposal as an approximate model and assuming  $\alpha$  to sit at the maximum at  $\alpha = -\sqrt{2\gamma c}/\beta$ . In that case, for  $c = \lambda$  we would have a Hull model with  $t \rightarrow -t$  and the negative branch would be physically the same as the positive branch.

We conclude this section with a side remark. The system of differential equations (38) could be solved exactly, while the treatment of the discrete system (37) is more complicated. This motivated one of the authors to propose a nonlinear model approximating Mackintosh’s when the parameter  $\gamma$  is very small (Calcagni, 2018). Given two parameters  $0 < \alpha_{\min} < \alpha_{\max} \leq 1$  representing the minimum and maxi-

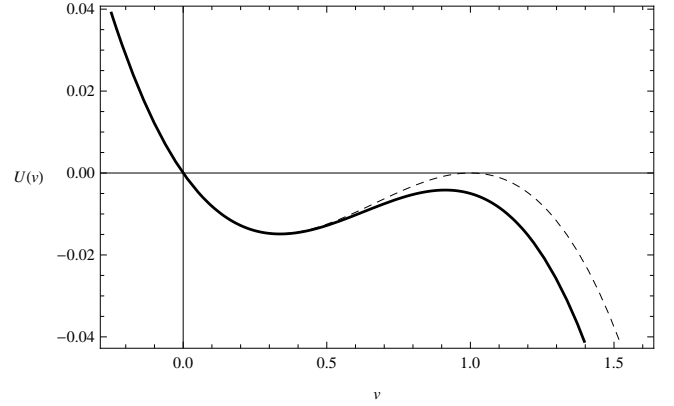


*Figure B3.* The quartic potential in (51) (solid curve) compared with (43) (dashed curve), for  $\lambda = c = 1$ ,  $\beta = 1$  and  $\gamma = 0.1$ .

imum value of the salience of the CS, this model is

$$\alpha_n = \alpha_{\min} + (\alpha_{\max} - \alpha_{\min}) \frac{v_n}{\tilde{\lambda}}, \quad (49)$$

$$\begin{aligned} \Delta v_n &= \alpha_{n-1} \beta (\lambda - v_{n-1}) \\ &= \beta \left[ \alpha_{\min} + (\alpha_{\max} - \alpha_{\min}) \frac{v_{n-1}}{\tilde{\lambda}} \right] (\lambda - v_{n-1}) \\ &= A - Bv_{n-1} - Cv_{n-1}^2, \end{aligned} \quad (50)$$

where  $A = \beta\alpha_{\min}\lambda$ ,  $B = \beta(\alpha_{\max} - C\lambda)$ ,  $C = (\alpha_{\max} - \alpha_{\min})/\tilde{\lambda}$ . In the continuum, we have  $\dot{v} = A - Bv - Cv^2$ , i.e.,

$$\ddot{v} = -AB + (B^2 - 2AC)v + 3BCv^2 + 2C^2v^3. \quad (51)$$

The profile  $U(v)$  is the same as in Fig. 9 when  $\gamma = O(10^{-2})$ , while for larger  $\gamma$  the local maximum is lowered (Fig. B3).

If we compare Eqs. (51) and (42), we immediately see that this nonlinear model collapses to Mackintosh’s model when the cubic term is negligible,  $C \ll 1$ , which happens if  $\alpha_{\max} \approx \alpha_{\min} \approx \alpha$ . All the coefficients can be mapped easily into one another. For instance, the  $O(v^2)$  terms in Eqs. (51) and (42) match if  $C \approx \gamma/\alpha$ .

## Appendix C

### OTHER MODELS OF FLUCTUATING RESPONSE Fractional stochastic model

We want to explore the possibility of a long-range effect in data or, more precisely, whether the time series of responses has long-memory correlations. The previous model accounts for local fluctuations in the response but does not contemplate the chance that, for whatever reason, the learning history of the subjects can affect future response more heavily than predicted by Hull model, in either its deterministic or stochastic version. This situation is described, for instance, by an autoregressive fractionally integrated moving average (ARFIMA) process. Without entering into many details, we can model this process as follows.

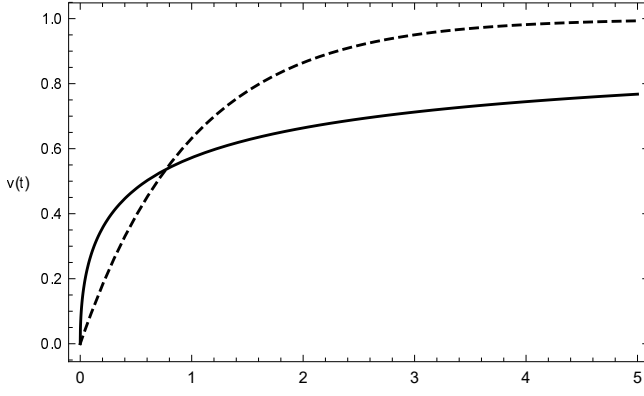


Figure C1. Learning curve (54) (solid) with  $\gamma = 0.5$ , compared with Hull's curve (4) (dashed), for  $\lambda = 1 = \alpha\beta$ .

In the continuous-time limit, the AR process with drift and colored noise (14) takes the form  $\dot{V}(t) = \alpha\beta[\lambda - V(t)] + \eta(t)$ . A random ARFIMA-like process with long memory would be described by

$$\partial_t^\gamma V(t) = \alpha\beta[\lambda - V(t)] + \eta(t), \quad (52)$$

where  $\partial_t^\gamma$  is a fractional derivative of order  $\gamma$  (Kilbas et al., 2006). There are many definitions of fractional derivative; here we will take the left Caputo derivative  $(\partial^\gamma f)(t) := [\Gamma(1 - \gamma)]^{-1} \int_0^t dt' (t - t')^{-\gamma} \partial_{t'} f(t')$ , where  $\Gamma$  is Euler function and  $0 < \gamma < 1$ . Fractional derivatives are commonly employed in statistical, financial, or physical systems with memory.

In this descriptive model, the biggest impact on behavior is given by the fractional derivative rather than the noise term. For this reason, we can ignore  $\eta$  and consider the deterministic equation

$$\partial_t^\gamma v = \alpha\beta(\lambda - v), \quad (53)$$

whose solution is the Mittag-Leffler function (Haubold et al., 2011):

$$v(t) = \lambda[1 - E_\gamma(-\alpha\beta t^\gamma)]. \quad (54)$$

When  $\gamma = 1$ ,  $E_1(-\alpha\beta t) = \exp(-\alpha\beta t)$  and one recovers (4). The learning curve (54) is shown in Fig. C1. Compared with Hull's curve, (54) is steeper at early times and increases much slower at late times.

The BIC and AIC of the best fit of normalized session-by-session individual data is shown in Tab. 3. The fractional model is unfavored by all subjects except 1-4, which is a false positive:  $\gamma = 1$  within the error uncertainty. In fact, all fits select  $\gamma = 1$  as the value of the fractional exponent. Since the deterministic model (53) does not work, we can also exclude the stochastic version (52), which exhibits the same global trend.

## Random-fractal model

Calcagni (2018) noted that, instead of a learning curve, the set of points of the association strength in a Pavlovian conditioning process can be described by a fractal, a somewhat peculiar set defined recursively whose points can be totally disconnected from one another and whose dimension can be noninteger. A learning process is then represented as a ‘‘hopping’’ on a fractal, each trial or session corresponding to an iteration level of the set. This reinterpretation, applied to the Hull, Rescorla–Wagner, Mackintosh, and Pearce–Hall models, does not change the prediction of any of these deterministic (i.e., not involving probabilities) learning models, but it offers a geometric way to characterize not the efficiency of a training program *per se*, but for a given subject.

For instance, a so-called Cantor set is associated with Hull model and its dimension (more precisely, Hausdorff dimension) is  $d_H(C) = d_C(C) = -\ln 2 / \ln(1 - \alpha\beta)$ . We can calculate this quantity from the individual session-by-session fits of Tab. 1. There is great variability in the dimension. 1-1:  $d_H \approx 2.4$ , 1-2:  $d_H \approx 13.1$ , 1-3:  $d_H \approx 6.1$ , 1-4:  $d_H \approx 0.6$ , 1-5:  $d_H \approx 7.5$ , 1-6:  $d_H \approx 7.5$ , 1-7:  $d_H \approx 2.9$ ; 2-1:  $d_H \approx 2.8$ , 2-2:  $d_H \approx 4.0$ , 2-3:  $d_H \approx 2.2$ , 2-4:  $d_H \approx 1.9$ , 2-5:  $d_H \approx 0.5$ , 2-6:  $d_H \approx 19.6$ , 2-7:  $d_H \approx 11.7$ , 2-8:  $d_H \approx 2.7$ . The large the saliences  $\alpha\beta$ , the smaller the dimension (the fractal set becomes a collection of disconnected sparse points) and the more efficient the conditioning, i.e., fewer the sessions needed to reach the asymptote of learning. Such is the case of subjects 1-4 and 2-5, which maintained a steady response already in the first 10 sessions. On the other hand, the larger the dimension the longer it took to reach the asymptote, as was the case of subjects 1-2, 2-6, and 2-7, all of which showed a slow steady increase almost until the end of the experiment.

This description, alternative to the usual one, may be interesting by itself, but the fractal interpretation does more than that when a random element is introduced. The deterministic model can be extended to a probabilistic one when the saliences  $\alpha\beta$  take a random value in a given distribution with support between 0 and 1. This can happen in different situations, from a controlled experimental design of partial reinforcement with randomized schedule (the CS or the US can be either present or absent at any given trial) to the natural environment of the subject with everchanging stimuli. Or, according to the hypotheses put forward in the *1/f* cognitive literature (section *Colored stochastic model of individual behavior – Theory*), random variations of  $\alpha\beta$  may happen due to the internal flickering of the subject's cognitive modules.

In all cases, because of the characteristics of the geometric interpretation, one expects these random fluctuations to be relatively *small* with respect to the absolute asymptote of learning and progressively *damped* (Calcagni, 2018). Neither feature is seen in the data: behavioral fluctuations are not damped in time can be as large as  $O(\lambda)$  and go well above or

below the theoretical asymptote found with the best fit. This finding does not rule out the fractal picture because, as we said, it is a repackaging of Hull model in terms of a geometric language. However, it does limit the scope of application of random fractals, at least in experimental designs like this where the US is not presented on a deterministic schedule: random variations of  $\alpha\beta$  do not describe observed and observable response instabilities but, rather, some subdominant and perhaps undetectable effect.

#### Appendix D SPECTRAL ANALYSIS

Assume that a completely noise-free learning curve were described by Hull model (4). This curve is smooth at all times and this should reflect in its frequency decomposition. To see this, we take its cosine *Fourier transform*:

$$\begin{aligned}\tilde{v}(\omega) &= \mathcal{F}[v(t)] := 2 \int_0^{+\infty} dt \cos(\omega t) v(t) \\ &= -\frac{2\lambda\alpha\beta}{(\alpha\beta)^2 + \omega^2} + 2\pi\lambda\delta(\omega),\end{aligned}\quad (55)$$

where  $\omega$  is the frequency and  $\delta$  is the Dirac delta distribution (identically equal to zero for  $\omega \neq 0$  and to  $\infty$  at  $\omega = 0$ ). We employ the cosine Fourier transform, typically used in signal processing, because we want a real-valued results and  $v(t)$  has support only in  $t \geq 0$ . Without loss of information, we can remove the zero mode  $\omega = 0$  and restrict the frequency range to  $\omega > 0$  ( $\tilde{v}(-\omega) = \tilde{v}(\omega)$  is even in  $\omega$ ), so that the delta term drops out. The *power spectral density* is then defined as the modulus square of the Fourier transform of the signal:

$$S(\omega) := |\tilde{v}(\omega)|^2 = \frac{4(\lambda\alpha\beta)^2}{[(\alpha\beta)^2 + \omega^2]^2}. \quad (56)$$

This profile is depicted in Fig. D1 in a log-log scale. Short frequencies have a constant power up to some point  $\omega_0 = (4\lambda\alpha\beta)^{-2}$ ,<sup>8</sup> where the spectral density drops steadily to zero. This means that the profile  $v(t)$  is mainly made of frequencies  $\omega \lesssim \omega_0$ , while frequencies  $\omega \gg \omega_0$  are not important. These large frequencies correspond to small-scale details of  $v(t)$  but, since  $v(t)$  is completely smooth, its small-scale structure is empty: zooming into it does not give more information. This signal is further distorted by the limited size of the data sample, by small but smooth ripples. Thus, if data follow a smooth learning curve different from Hull's, then a spectral analysis should find an  $S(\omega)$  different from that shown in Fig. D1. By itself, this should draw our interest in determining the power spectral density of data.

However, the spectral analysis can uncover much more. In general, data are noisy. This noise can come from

<sup>8</sup>The first derivative of (56) is proportional to  $\omega/\omega_0$  and is therefore small (i.e.,  $S(\omega)$  is approximately constant) when  $\omega/\omega_0 \ll 1$ .

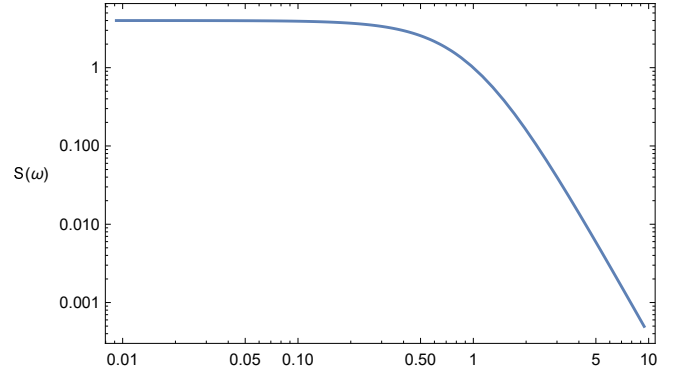


Figure D1. Power spectral density (56) of the ideal learning curve (4) for  $\alpha\beta = 1 = \lambda$ .

statistical error or from intrinsic sources. Statistical error has a Gaussian distribution and is therefore *white noise*. White noise is a random signal with a uniform probability distribution of frequencies (Fig. D2). In general, random signals called *colored noise* can be characterized by the power spectral density (13) (up to an overall constant), where  $a$  is a constant exponent (usually denoted as  $\alpha$  in the literature; to avoid confusion with the CS salience, we change notation here). White noise corresponds to  $a = 0$ , while other popular cases are *pink noise* ( $a = 1$ ,  $S_1$  decreases linearly with the frequency), *Brownian noise* ( $a = 2$ ,  $S_2$  decreases quadratically), *blue noise* ( $a = -1$ ,  $S_{-1}$  increases linearly with the frequency), and so on (Fig. D2). The spectrum (13) is better visualized in log-log plot, since in that case the parameter  $a$  is nothing by the slope of the line  $\log S_a = -a \log \omega$ . As we said above, experimental data of associative learning processes are usually noisy at small time scales, i.e., the trial-by-trial response variation is usually greater than any long-term variation around the asymptote of learning. Therefore, the spectral density of a realistic learning curve following Hull model should be of the form of Fig. D1 with a noise signal superposed and dominating those frequencies where  $S(\omega)$  drops. In other words, the total signal  $S_{\text{tot}}(\omega) = S(\omega) + S_a(\omega)$  is approximately equal to  $S_{\text{tot}}(\omega) \simeq S(\omega)$  (Eq. (56)) at small frequencies  $\omega \lesssim \omega_0$ , while  $S_{\text{tot}}(\omega) \simeq S_a(\omega)$  at large frequencies  $\omega \gg \omega_0$ . Simulated signals of this kind are shown in Fig. D3. Here we can also appreciate the distortion (smooth ripples) coming from the limited size of the data sample.

#### Appendix E CONSTRUCTION OF THE QUANTUM HULL MODEL Preliminaries: classical setting

Since the friction term in (22) can introduce unnecessary complications, we first recast the classical model as an *inverted harmonic oscillator*. Taking the time derivative of (2) but replacing  $\dot{v}$  with its explicit expression, we obtain the

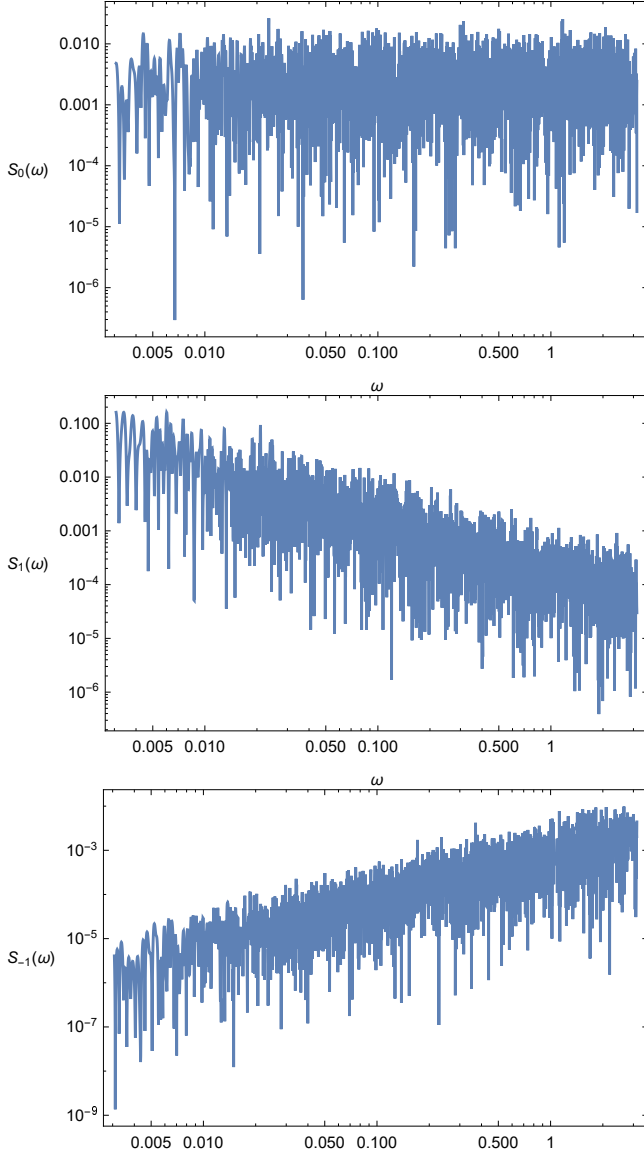


Figure D2. Power spectral density (13) of white noise (top,  $a = 0$ ), pink noise (middle,  $a = 1$ ), and blue noise (bottom,  $a = -1$ ), simulated with the AudioGenerator of Mathematica.

equation of motion

$$\ddot{v} - (\alpha\beta)^2 v + \lambda(\alpha\beta)^2 = 0, \quad (57)$$

which can be derived from the action

$$S_{\text{Hull}} = \int_0^T dt \mathcal{L}_{\text{Hull-inv}}, \quad (58)$$

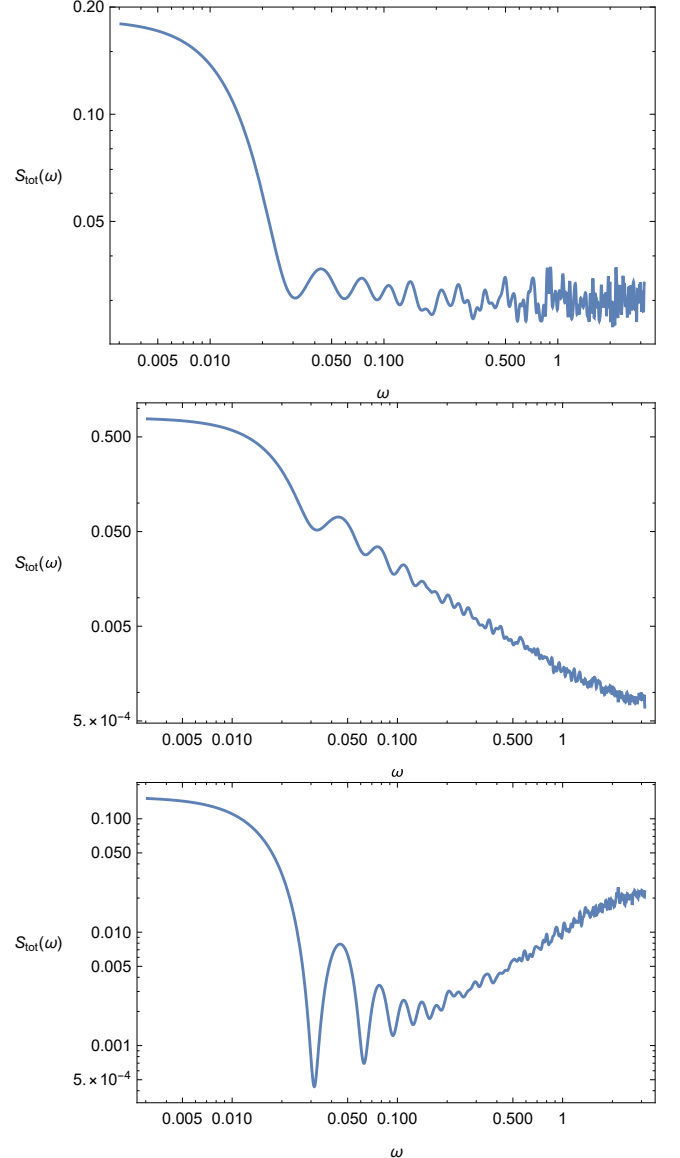


Figure D3. Total power spectral density  $S_{\text{tot}}(\omega) = S(\omega) + S_a(\omega)$  with white noise (top,  $a = 0$ ), pink noise (middle,  $a = 1$ ), or blue noise (bottom,  $a = -1$ ), simulated with Mathematica. Here  $\alpha\beta = 1 = \lambda$  and we used a sample size of 200 data points.

where

$$\mathcal{L}_{\text{Hull-inv}} = \frac{\dot{v}^2}{2} - U(v), \quad (59a)$$

$$U(v) = \begin{cases} -\frac{(\alpha\beta)^2}{2}(v - \lambda)^2 & (0 \leq v \leq \lambda) \\ +\infty & (v < 0 \text{ or } v > \lambda) \end{cases} \quad (59b)$$

In excitatory conditioning, the particle rolls up its hill-top potential from the global maximum  $v = 0$  to the point  $v = \lambda$  at which we placed an infinite potential barrier. This barrier is simply a way to force the dynamics into the interval

$0 \leq v \leq \lambda$ .

Applying the variational principle, the Euler–Lagrange equations (25) yield (57). This time, the particle is attached to a spring with negative spring constant  $k = -(\alpha\beta)^2 < 0$ . In terms of the variable (27),

$$\ddot{x} - \Omega^2 x = 0, \quad \Omega = \alpha\beta. \quad (60)$$

The energy of the particle is a constant of motion and it vanishes. Since (2) is equivalent to  $\dot{v} = \sqrt{-2U(v)}$ ,

$$E_{\text{Hull}} := \frac{\dot{v}^2}{2} + U(v) = 0. \quad (61)$$

Therefore, no matter what type of conditioning process enforced, the initial and final state will have equal energy. The energy found in (61) vanishes but one can always shift the potential by a constant that does not appear in the equation of motion, so that  $E$  can take positive or negative values. For the particle to climb the potential up to the maximum, the initial kinetic energy  $E_{\text{kin}} = [\dot{v}(0)]^2/2$  must be positive in order to cancel the negative contribution  $U(0) = -(\alpha\beta\lambda)^2/2$  of the potential. At the final point,  $E_{\text{kin}} = 0 = U$ . Thus, comparing with the friction model, the hill-top model has the disadvantage of needing a potential barrier and requiring a somewhat unnatural initial condition (the particle starts exactly at the point on the slope which ensure it reaches the hill-top asymptotically), but on the other hand it is a conservative system.

In preparation for the quantum analysis, we recast the Hull model in Hamiltonian formalism. Defining the momentum

$$p := \frac{\delta S_{\text{Hull}}}{\delta \dot{x}} = \dot{x}, \quad (62)$$

the classical *Hamiltonian*  $H := p\dot{x} - \mathcal{L}$  from (24) is

$$H = \frac{1}{2}(p^2 - \Omega^2 x^2). \quad (63)$$

This expression is valid within the well  $0 \leq x \leq \lambda$ . The variables  $p$  and  $x = \lambda - v$  are said to be canonically conjugate and their Poisson bracket  $\{A, B\} := (\partial A/\partial x)(\partial B/\partial p) - (\partial A/\partial p)(\partial B/\partial x)$  is

$$\{x, p\} = 1. \quad (64)$$

The general classical solution of the equation of motion (28) is

$$x(t) = x_0 \cosh(\Omega t) + \frac{p_0}{w} \sinh(\Omega t), \quad (65)$$

where  $x_0 = x(0)$  and  $p_0 = p(0)$  and the hyperbolic functions are defined by  $\cosh z := (e^z + e^{-z})/2$  and  $\sinh z := (e^z - e^{-z})/2$ . The energy is  $E_{\text{Hull}} = H[x(t), p(t)] = (p_0^2 - \Omega^2 x_0^2)/2$ .

## Quantization

As we just saw, the usual Hull model is nothing but the classical inverted harmonic oscillator. The quantum inverted oscillator is also well known because it is one of the

few cases that admit a fully analytic treatment (Barton, 1986; Kemble, 1935; Shimbori and Kobayashi, 2000; Shimbori, 2000; Yuce et al., 2006). We will rely mainly on the results of Barton (1986), which we will review first and then interpret them in the fresh context of learning by conditioning. The starting point is the classical Hamiltonian formalism given by the Hamiltonian (63) and the Poisson bracket (64) for the canonical variables  $x$  and  $p$ . We promote the latter to operators  $\hat{x}$  and  $\hat{p}$  acting on a Hilbert space whose states  $\Psi(x, t)$ , also denoted by  $\langle x|\Psi\rangle$ , are called wave-functions. The position operator  $\hat{x}$  in the Schrödinger picture can be chosen to act multiplicatively and the momentum operator  $\hat{p}$  as a first-order partial differential derivative (this choice is called position representation):

$$x \rightarrow \hat{x} := x, \quad p \rightarrow \hat{p} := -i\bar{h} \frac{\partial}{\partial x}, \quad (66)$$

where  $\bar{h}$  is a constant. In physics, this would be Planck constant  $\hbar$  (“ $h$  bar”) but in psychology we do not know yet its magnitude and we call it with another symbol ( $\bar{h}$ , “bar  $h$ ”). The Poisson bracket (64) is converted into the commutator

$$\{\cdot, \cdot\} \rightarrow \frac{1}{i\bar{h}}[\cdot, \cdot], \quad (67)$$

where  $[\hat{A}, \hat{B}] := \hat{A}\hat{B} - \hat{B}\hat{A}$ . Consequently,

$$[\hat{x}, \hat{p}] = i\bar{h}. \quad (68)$$

Denoting by  $\langle \hat{A} \rangle = \langle \Psi|\hat{A}|\Psi\rangle$  the expectation value of an operator  $\hat{A}$  on a state  $|\Psi\rangle$ , one defines the standard deviation  $\Delta A = \sqrt{\langle \hat{A}^2 \rangle - \langle \hat{A} \rangle^2}$ . Then, for any quantum state and any two canonically conjugate operators  $\hat{A}$  and  $\hat{B}$  it is easy to prove Heisenberg uncertainty principle

$$\Delta A \Delta B \geq \frac{\bar{h}}{2}, \quad (69)$$

stating that one cannot have arbitrarily small standard deviations for both operators at the same time. In the case of the inverted harmonic oscillator and for symmetric states such that  $\langle \hat{x} \rangle = 0 = \langle \hat{p} \rangle$ , we have

$$\langle \hat{x}^2 \rangle \langle \hat{p}^2 \rangle \geq \frac{\bar{h}^2}{4}. \quad (70)$$

If one forces the quantum particle into a state sharply peaked at a certain position  $x$ , then the expectation value of the momentum cannot be determined with arbitrary accuracy.

To determine how the wave-function  $\Psi(x, t)$  evolves in time and position (association strength), we have to specify an equation for its dynamics. This is achieved in a standard way by replacing  $x$  and  $p$  in Eq. (63) with the operators (66), yielding the quantum Hamiltonian

$$\hat{H} = \frac{1}{2}(\hat{p}^2 - \Omega^2 \hat{x}^2) = -\frac{1}{2}(\bar{h}^2 \partial_x^2 + \Omega^2 x^2). \quad (71)$$

Then, the dynamics of  $\Psi(x, t)$  is defined by the Schrödinger equation

$$(i\hbar\partial_t - \hat{H})\Psi(x, t) = 0, \quad (72)$$

with boundary conditions to be established later. A first possibility, appealing because it can allow for a probabilistic interpretation of the wave-function, is to choose boundary conditions such that the wave-function vanishes at the walls  $x_1$  and  $x_2$  of the potential barrier. However, it is easy to check that this configuration is not viable (see Appendix F). Intuitively, a wave-function vanishing at  $v = 0$  and  $v = \lambda$  would never be able to recover the classical behavior in any limit, since it would prescribe the absence of the particle at the initial and final point of the evolution (in other words, such a wave-function would not describe a conditioning process approaching the asymptote  $v = \lambda$  starting from  $v = 0$ ). From now on, we consider the case without potential barriers where the Hamiltonian is given exactly by (71) for all  $x \in \mathbb{R}$ .

It is important to note that there is no quantum notion of a particle at a position  $x$  at time  $t$ . Given a square-integrable wave-function  $\Psi(x, t)$  such that  $\int_{-\infty}^{+\infty} dx |\Psi(x, t)|^2 = 1$ , the density  $|\Psi(x, t)|^2$  determines the probability to find the particle at a position  $x$  at time  $t$ . This probabilistic description of the particle dynamics is not due to our ignorance about the fine details of the experimental setting or of the theory: it is an intrinsic indeterminacy of Nature which has been verified in countless observations in physics. In the case of learning by conditioning models, we propose a similar setting, where the strength of association  $v$  at any given trial can be determined only probabilistically by a distribution  $|\Psi(v, t)|^2$ .

Since, as is well known, the Schrödinger procedure is equivalent to the path-integral quantization, one can explain these findings by interpreting “quantum” conditioning as the superposition, weighted by the classical action (58), of all possible learning curves from  $t = 0$  to  $t = T$ . Many of these trajectories do not reach optimal learning at  $t = T$  and they interfere with the classical trajectory with optimal learning producing the above-mentioned effect.

To find the most general solution of (72), we need the *Green function*  $G(x, x'; t)$ , which is the only solution of the Schrödinger equation that describes a point-wise source at  $t = 0$ . It is easy to check that

$$G(x, x'; t) = \sqrt{\frac{\Omega}{2\pi i\hbar \sinh(\Omega t)}} \exp\left\{\frac{i\Omega}{2\hbar \sinh(\Omega t)} \times [(x^2 + x'^2) \cosh(\Omega t) - 2xx']\right\} \quad (73)$$

is solution of  $(i\hbar\partial_t - \hat{H})G = 0$  with Hamiltonian (71), such that  $G(x, x'; 0) = \delta(x - x')$  (Barton, 1986). Then, the general solution of (72) is given by the propagation of any wave-function  $\Psi(x, 0)$  in time via G:

$$\Psi(x, t) = \int_{-\infty}^{+\infty} dx' G(x, x'; t) \Psi(x', 0). \quad (74)$$

In fact,  $(i\hbar\partial_t - \hat{H})\Psi(x, t) = \int dx' [(i\hbar\partial_t - \hat{H})G]\Psi(x', 0) = 0$ .

## Predictions

*Prediction 1: The asymptote of learning is not a durable achievement.* A notable consequence of Heisenberg uncertainty principle (70) is that equilibrium configurations cannot last forever. Suppose, for instance, that we set the initial conditions of the inverted oscillator solution (65) such that to reproduce excitatory conditioning in Hull model:  $x_0 = -p_0/\Omega = \lambda$ ,  $x(t) = \lambda e^{-\Omega t}$ . The classical system evolves from  $x(0) = \lambda$  up to the maximum of the potential at  $x(+\infty) = 0$ . Although  $x = \lambda - v = 0$  is reached asymptotically in time, in a real situation the subject gets close to this point in a finite time and, according to the classical theory, achieves full conditioning. This means that the subject cannot learn anything more about the association between the CS and the US: once reached the maximum of the potential, it will stay there forever. The maximum is a point of unstable equilibrium, i.e., by “perturbing the particle” a bit (in the psychological interpretation, this means to stimulate the subject with some means) it would fall down the potential again (the subject would “unlearn” the S-S association). Since the classical model has no such perturbations incorporated, this occurrence never happens in the usual Hull model. However, in the quantum Hull model the point of unstable equilibrium cannot be maintained due to quantum fluctuations and, after some characteristic *sojourn time*  $t_*$ , the particle is displaced away from the maximum and the subject shows signs of “unlearning” (if it falls back to the  $v < \lambda$  side of the hill) or even of “overlearning” (if it falls down on the  $v > \lambda$  side of the hill).

*Prediction 2: There exists a quantum state such that response fluctuations do not decrease in time.* Let us look for wave-functions peaked at the classical trajectory (Barton, 1986). Consider the  $t = 0$  Gaussian state

$$\Psi(x, 0) = \frac{1}{(\pi b^2)^{1/4}} \exp\left[-\frac{(x - x_0)^2}{2b^2} + \frac{i}{\hbar} p_0 x\right], \quad (75)$$

centered at  $x = x_0$  and where  $b$  is the distribution width. This profile minimizes the uncertainty principle (69). In fact, the expectation values of position and momentum on this state are

$$\langle \hat{x} \rangle = \int_{-\infty}^{+\infty} dx x |\Psi(x, 0)|^2 = x_0, \quad (76a)$$

$$\langle \hat{x}^2 \rangle = \int_{-\infty}^{+\infty} dx x^2 |\Psi(x, 0)|^2 = x_0^2 + \frac{b^2}{2}, \quad (76b)$$

$$\langle \hat{p} \rangle = -i\hbar \int_{-\infty}^{+\infty} dx \Psi^*(x, 0) \partial_x \Psi(x, 0) = p_0, \quad (76c)$$

$$\begin{aligned} \langle \hat{p}^2 \rangle &= -\hbar^2 \int_{-\infty}^{+\infty} dx \Psi^*(x, 0) \partial_x^2 \Psi(x, 0) \\ &= p_0^2 + \frac{\hbar^2}{2b^2}, \end{aligned} \quad (76d)$$

so that an estimate of the size of quantum fluctuations in position is given by  $\Delta x = \sqrt{\langle \hat{x}^2 \rangle - \langle \hat{x} \rangle^2} = b/\sqrt{2}$ ; then,  $\Delta p = \sqrt{\langle \hat{p}^2 \rangle - \langle \hat{p} \rangle^2} = \hbar/(\sqrt{2}b)$  and

$$\Delta x \Delta p = \frac{\hbar}{2}. \quad (77)$$

States saturating Heisenberg principle are called coherent. Calculating (74) and taking the square, one finds the probability density

$$|\Psi(x, t)|^2 = \frac{1}{\sqrt{\pi B^2(t)}} \exp\left\{-\frac{[x - x(t)]^2}{B^2(t)}\right\}, \quad (78)$$

where  $x(t)$  is the classical trajectory (65) and

$$B^2(t) = b^2 \cosh^2(\Omega t) + \frac{\hbar^2}{b^2 \Omega^2} \sinh^2(\Omega t). \quad (79)$$

Thus, the wave packet maintains the Gaussian form and it saturates Heisenberg principle at all times. At short times,  $B^2(t) = b^2 + (b^2 \Omega^2 + \hbar^2 b^{-2})t^2 + O(t^4)$ , while at late times  $B^2(t) \simeq [b^2 + \hbar^2(b\Omega)^{-2}]e^{2\Omega t}/4$ . Since  $B$  increases with  $t$ , the peak of probability follows the classical trajectory and it spreads exponentially as time goes by. Therefore, initially the system evolves almost classically (if  $b$  is small enough) and one can determine with good accuracy the association strength  $v = \lambda - x$  of the subject, but at later trials there is a nonzero chance that the subject display a non-optimal conditioning level, even if the highest probability is at the asymptotic value  $v = \lambda$ . Quantum fluctuations increase from the initial value  $b/\sqrt{2}$  to indefinitely large values  $\Delta x = B(t)/\sqrt{2} \simeq be^{\Omega t}/2^{3/2}$ , if  $\hbar \ll b\Omega$ . The probability density for the Hull model is shown in Fig. E1.

*Prediction 3: There exists a quantum state such that response fluctuations are large and almost constant.* A sharply peaked coherent state can be characterized by almost constant fluctuations. To see how, we make a few steps back and reflect on a basic property of the quantum model, doing a micro-analysis of the fluctuations. In order to understand the typical time scale involved in quantum fluctuations, one can calculate the sojourn time  $t_*$  in several but mutually agreeing ways which differ from one another by the level of rigorousness (Barton, 1986). Here we choose a semi-heuristic method based on an estimate of  $\langle \hat{x}^2(t) \rangle$ , the expectation value of the operator  $\hat{x}^2$  in the so-called Heisenberg picture on a real-valued state  $|\Psi_l\rangle$  that minimizes Heisenberg's uncertainty principle and maximizes  $t_*$  for a given length scale  $l$ .

In the Heisenberg picture, states are independent of  $t$  and operators evolve in time by the action of the quantum Hamiltonian. In particular, the position operator  $\hat{x} = \hat{x}(0)$  becomes  $\hat{x}(t) = e^{i\hat{H}t} \hat{x} e^{-i\hat{H}t}$ , and a similar expression holds for  $\hat{p}(t)$ . The criterion defining the sojourn time is established by the condition

$$\langle \Psi_l | \hat{x}^2(t) | \Psi_l \rangle \leq l^2, \quad 0 \leq t \leq t_*. \quad (80)$$

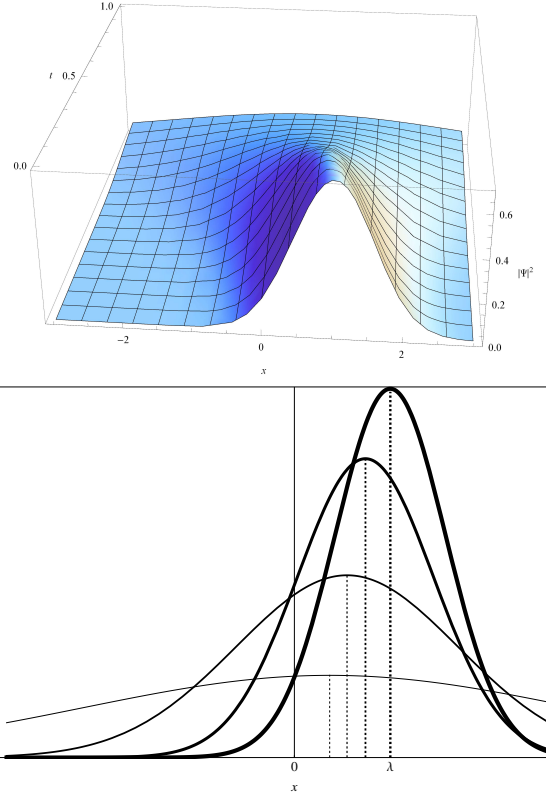


Figure E1. Top: the probability density (78) for the Hull model with  $\lambda = 1$ ,  $\Omega = 1$  and  $b = 0.9$ , as a function of  $x = \lambda - v$  and  $t$ . Bottom: snapshots of the probability density at  $t = 0, 0.3, 0.6, 1$  (decreasing thickness) for the same values of the parameters. Dashed lines indicate the position of the peak  $x(t)$  [Eq. (65) with  $x_0 = -p_0 = \lambda$ ].

The state  $|\Psi_l\rangle$  is such that  $\langle \hat{x}^2(0) \rangle = l^2$  [maximum value of  $\langle \hat{x}^2(t) \rangle$  at  $t = 0$ ],  $\langle \hat{x}^2(t) \rangle$  reaches a minimum at  $t = t_*/2$  and grows again to  $l^2$  at  $t = t_*$ . Regarding (65) as the solution in the Heisenberg picture, we can replace it into (80) and, if we also require  $\Psi(x) = \langle x | \Psi \rangle$  to be real, get  $\langle \hat{x}_0 \hat{p}_0 + \hat{x}_0 \hat{p}_0 \rangle = 0$  and

$$\langle \Psi_l | \hat{x}_0^2 \cosh^2(\Omega t) + \frac{\hat{p}_0^2}{\Omega^2} \sinh^2(\Omega t) | \Psi_l \rangle \leq l^2. \quad (81)$$

A further assumption we make is that  $|\Psi_l\rangle$  saturates Heisenberg principle (70) (which is valid also in the Heisenberg picture), so that  $\Delta x(t) \Delta p(t) = \hbar/2$  for all  $t$ . This is easily achieved by a wave packet analogous to (75), but now with a width constant at all times. Concretely, a minimum-uncertainty state for the oscillator peaked at some  $x = \bar{x}$  is the wave packet

$$\Psi_l(x) = \langle x | \Psi_l \rangle = \frac{1}{(\pi \hbar b_l^2)^{1/4}} \exp\left[-\frac{(x - \bar{x})^2}{2 \hbar b_l^2}\right], \quad (82)$$

where the constant  $b_l$  depends on  $l$  (here  $\hbar b_l^2$  plays the role of  $b^2$ ). In particular, for  $\bar{x} = 0$  calculations identical to

those in (76) yield  $\langle \hat{x}(t) \rangle = 0$ ,  $\langle \hat{x}^2(t) \rangle = \bar{h}b_l^2/2$ ,  $\langle \hat{p}(t) \rangle = 0$ ,  $\langle \hat{p}^2(t) \rangle = \bar{h}/(2b_l^2)$ , so that Heisenberg principle is saturated for all  $t$ :

$$\langle \hat{x}^2(t) \rangle \langle \hat{p}^2(t) \rangle = \frac{\bar{h}^2}{4}, \quad (83)$$

just as in the Schrödinger-picture relation (77).

We can make a crude estimate of  $l$  by recalling that, classically,  $x_0 = \lambda$ . Then, if the system is close to classicality at the beginning of the experiment,  $l^2 = \langle \hat{x}^2(0) \rangle = O(\lambda^2)$ , where “ $O$ ” means “of order of.” Thus, the typical fluctuation has a size of order of the asymptote,  $l = \delta v = O(\lambda)$ .

*Prediction 4: There is a universal constant  $\bar{h}$  that can be determined by experiments.* Saturating inequality (81) at  $t = t_*$  and using the identity  $\cosh^2 z - \sinh^2 z = 1$ , we can invert (81) and get

$$t_* = \frac{1}{2\Omega} \operatorname{arccosh} z, \quad z = \frac{2l^2 - \langle \hat{x}_0^2 \rangle + \langle \hat{p}_0^2 / \Omega^2 \rangle}{\langle \hat{x}_0^2 \rangle + \langle \hat{p}_0^2 / \Omega^2 \rangle}$$

where  $\operatorname{arccosh} z = \ln(z + \sqrt{z^2 - 1})$  is the inverse hyperbolic cosine. Therefore,  $z = (1 + 4l^2\Omega^2 b_l^2 / \bar{h} - \Omega^2 b_l^4) / (1 + \Omega^2 b_l^4)$ . Since  $\operatorname{arccosh} z$  increases monotonically in  $z$ ,  $t_*$  is maximized when  $z$  attains its maximum value  $z = \sqrt{1 + 4l^4\Omega^2 / \bar{h}^2}$  at  $b_l^2 = (\sqrt{1 + 4l^4\Omega^2 / \bar{h}^2} - 1) / (2l^2\Omega^2 / \bar{h})$ . Combining these expressions with the definition in (28), the final result reads

$$t_* = \frac{1}{2\alpha\beta} \ln \left[ \frac{2l^2\alpha\beta}{\bar{h}} + \sqrt{1 + \frac{(2l^2\alpha\beta)^2}{\bar{h}^2}} \right]. \quad (84)$$

The sojourn time increases monotonically with  $l$ : consistently with the first prediction, it takes longer to see larger quantum fluctuations. The greater the magnitude of the US, the greater  $t_*$ . This is somewhat intuitive: if the amount of US at each trial is high, the subject will tend to stay in the state of maximal conditioning longer. If we present the subject with 10 drops of saccharin solution, the state of maximal conditioning will decay *slower* than when presented with only one drop per trial.

However, for a fixed  $\lambda$  the sojourn time *decreases* with the saliences of the CS and of the US. This bizarre result may find a rationale if we admit that the total duration of the acquisition stage may affect the sojourn time at the asymptote of learning. Higher CS and US saliences lead to faster learning and the subjects reach the asymptote early, thus increasing the chance of response fluctuations of the trials. Conversely, the longer the conditioning process the lower the chance for the subject to move away from optimal conditioning once reached.

The magnitude of this effect is determined by the constant  $\bar{h}$ , which we assumed to be independent of the stimuli. Let us consider trial-by-trial individual data, which are those with better time resolution. The constant  $\bar{h}$  (the analogue of

Planck constant  $\hbar$  in quantum mechanics) is an external input that can be determined experimentally once the other parameters are known. While data allow us to find the best-fit values of  $\alpha\beta$  and  $\lambda$ , we only have an upper limit on  $t_*$  coming from the fact that responses vary considerably already from one trial to the next:

$$t_* \lesssim \Delta t_{\text{trial}} = 1, \quad (85)$$

which translates into a lower bound on  $\bar{h}$ . To find this bound, we must approximate Eq. (84). The values of  $\alpha\beta$  can be read from Tab. 1 for session-by-session data and from Tab. 5 for trial-by-trial data. In the first case,  $\alpha\beta \sim 10^{-2} - 10^{-1}$ , while in the second it is even smaller,  $\alpha\beta \sim 10^{-3} - 10^{-2}$ . Therefore, the approximation  $\alpha\beta \ll 1$  holds regardless of the magnitude of the ratio  $\bar{h}/l^2$ . If this ratio is of order unity, an expansion of Eq. (84) in  $\alpha\beta \ll 1$  yields  $t_* \simeq 2l^2\alpha\beta/\bar{h}$ , hence  $\bar{h} \simeq 2l^2\alpha\beta/t_* \gtrsim 2l^2\alpha\beta$ . If instead  $\bar{h} \ll l^2$ , an expansion in  $l^2\alpha\beta/\bar{h} \gg 1$  gives  $t_* \simeq (2\alpha\beta)^{-1} \ln(2l^2\alpha\beta/\bar{h})$ , hence  $\bar{h} \simeq 2l^2\alpha\beta \exp(-2\alpha\beta t_*) \gtrsim 2l^2\alpha\beta \exp(-2\alpha\beta) \simeq 2l^2\alpha\beta$ . In both cases, we find the same lower limit (17), which is also consistent with the following argument. We can get a simple estimate of  $\bar{h}$  by assuming that the Gaussian wave packet is an appropriate description of the association strength ( $v$ ) of the subject. As said above, this state saturates the uncertainty principle, Eq. (77). On the other hand, we have not seen an appreciable spread of the distribution of  $v$  values during the experiment, which means that the wave packet is sharply peaked at the classical trajectory. Therefore, we can take the classical evolution equation (2) ( $\dot{x} = -\alpha\beta x$ ) and the classical momentum (62) ( $p = \dot{x} = -\alpha\beta x$ ) to get a rough estimate of the momentum fluctuations  $\Delta p \sim \alpha\beta \Delta x$  (here absolute values are understood), so that Eq. (77) implies (17):  $\bar{h} \sim 2\alpha\beta(\Delta x)^2 \sim 2\alpha\beta l^2 \sim 2\alpha\beta \sigma^2$ .

*Prediction 5: Response variability is described by white noise.* The spectrum of the quantum fluctuations described by the state (82) is Gaussian. In fact, a Gaussian distribution is such that all even-order correlations can be expressed in terms of the two-point correlation function (Adler, 1981; Adler and Taylor, 2007). In our case, odd higher-order momenta vanish identically  $\langle \hat{x}^{2n+1} \rangle = 0$ , while even momenta are

$$\langle \hat{x}^{2n} \rangle = (2n-1)!! \left( \frac{\bar{h}b_l^2}{2} \right)^n = (2n-1)!! \langle \hat{x}^2 \rangle^n, \quad (86)$$

where “ $!!$ ” is the double factorial:  $N!! = N(N-2)(N-4)\dots$ . Thus,  $n = 1$  is the second-order correlation (76b) (with  $x_0 = 0$  and  $b^2 = \bar{h}b_l^2$ ),  $\langle \hat{x}^4 \rangle = 3\langle \hat{x}^2 \rangle^2$ , and so on. A Gaussian distribution of random fluctuations is precisely white noise.

## Appendix F

### POTENTIAL WITH INFINITE BARRIERS

To determine the general solution of the Schrödinger equation (72) with potential barriers, we use the procedure of

Yuce et al. (2006). Plugging the expression  $\Psi(x, t) = \exp[i\Omega x^2/(2\hbar) - \Omega t/2]\Phi(x, t)$  into (72) with (71), one gets  $i\dot{\Phi} + i\Omega x\partial_x\Phi + (\hbar/2)\partial_x^2\Phi = 0$ . After the variable redefinition  $x = \exp(\Omega t)y$  and a few manipulations, the equation of motion becomes  $ie^{2\Omega t}\dot{\Phi} + (\hbar/2)\partial_y^2\Phi = 0$ . Separating the variables as  $\Phi(y, t) = \phi(y)b(t)$  with  $b(t) = \exp(ie^{-2\Omega t}a/\Omega)$  and  $a$  some constant, one obtains  $(\partial_y^2 + 4a/\hbar)\phi(y) = 0$ , solved by  $\phi(y) = A \sin(2\sqrt{a/\hbar}y) + B \cos(2\sqrt{a/\hbar}y)$ . Overall, the general solution is

$$\Psi(x, t) = \mathcal{N} \exp\left(i\frac{\Omega x^2}{2\hbar} + ie^{-2\Omega t}\frac{a}{\Omega} - \frac{\Omega t}{2}\right) \times \left[ A \sin\left(2\sqrt{\frac{a}{\hbar}}e^{-\Omega t}x\right) + B \cos\left(2\sqrt{\frac{a}{\hbar}}e^{-\Omega t}x\right) \right], \quad (87)$$

where  $\mathcal{N}$  is a normalization constant.

For the wave-function (87) to vanish at  $x_1 = 0$  ( $v = \lambda$  the asymptote of learning), it must be  $B = 0$ . We also set  $A = 1$ , since there is an overall constant  $\mathcal{N}$ . On the other hand, at the beginning of conditioning ( $x_2 = \lambda$ ,  $v = 0$ ) one has  $\Psi(\lambda, 0) = 0$  only when the sine vanishes, which happens when  $2\lambda\sqrt{a/\hbar} = n\pi$ . This fixes the constant  $a$  introduced earlier:

$$a = \hbar \left(\frac{n\pi}{2\lambda}\right)^2, \quad n \in \mathbb{N}. \quad (88)$$

To fix also  $\mathcal{N}$ , we note that the wave-function  $\Psi$  is normalizable only if the position of one of the boundaries moves as  $x_2 = \lambda e^{\Omega t}$ . Therefore, in order to have a probabilistic interpretation of the wave-function we assume that one of the walls is dynamical. Consequently, integrating  $|\Psi|^2$  between  $x_1$  and  $x_2$  and imposing the result to be 1, we get

$$\int_0^{\lambda e^{\Omega t}} dx |\Psi(x, t)|^2 = \mathcal{N}^2 \frac{\lambda}{2} = 1 \quad \Rightarrow \quad \mathcal{N} = \sqrt{\frac{2}{\lambda}}. \quad (89)$$

The final result for the square-integrable wave-function of the quantum inverted oscillator in a box with moving walls is

$$\Psi_n(x, t) = \sqrt{\frac{2}{\lambda}} \exp\left[i\frac{\Omega x^2}{2\hbar} + ie^{-2\Omega t}\frac{\hbar}{\Omega}\left(\frac{n\pi}{2\lambda}\right)^2 - \frac{\Omega t}{2}\right] \times \sin\left(n\pi e^{-\Omega t}\frac{x}{\lambda}\right), \quad x = \lambda - v. \quad (90)$$

The probability distribution of values  $v$  is

$$|\Psi_n(v, t)|^2 = \frac{2}{\lambda} e^{-\Omega t} \sin^2\left(n\pi e^{-\Omega t}\frac{\lambda - v}{\lambda}\right). \quad (91)$$

Unfortunately, the moving-wall configuration is unviable in our context. The probability density  $|\Psi|^2$  is characterized by  $n$  periodic peaks in the interval  $\lambda(1 - e^{\Omega t}) \leq v \leq \lambda$ . As time increases, the peaks spread in the region  $-v \gg 0$ , which has no meaningful interpretation in the context of Pavlovian learning. Therefore, we must abandon the moving-wall case.

## References

- Adler, R.J. (1981). *The Geometry of Random Fields*. London, UK: Wiley.
- Adler, R.J., & Taylor, J. (2007). *Random Fields and Geometry*. New York, NY: Springer.
- Akaike, H. (1974). A new look at the statistical model identification. *IEEE Trans. Autom. Control* *19*, 716.
- Ayres, J.J.B., Berger-Gross, P., Kohler, E.A., Mahoney, W.J., & Stone, S. (1979). Some orderly nonmonotonicities in the trial-by-trial acquisition of conditioned suppression: Inhibition with reinforcement?. *Anim. Learn. Behav.* *7*, 174.
- Balakrishnan, J. (2000). Neural network learning dynamics in a path integral framework. *Eur. Phys. J. B* *15*, 679 [arXiv:cond-mat/0308503].
- Barton, G. (1986). Quantum mechanics of the inverted oscillator potential. *Ann. Phys. (N.Y.)* *166*, 322.
- Beck, F., & Eccles, J. (1992). Quantum aspects of brain activity and the role of consciousness. *Proc. Nat. Acad. Sci. USA* *89*, 11357.
- Bernal, S.Y., Dostova, I., Kest, A., Abayev, Y., Kandova, E., Touzani, K., Sclafani, A., & Bodnar, R.A. (2008). Role of dopamine D1 and D2 receptors in the nucleus accumbens shell on the acquisition and expression of fructose-conditioned flavor-flavor preferences in rats. *Behav. Brain Res.* *190*, 59.
- Bian, X., Tu, P., Chi, L., Gao, B., Ru, H., & Lu, K. (2017). Saccharin induced liver inflammation in mice by altering the gut microbiota and its metabolic functions. *Food Chem. Toxicol.* *107*, 530.
- Blanco, F., & Moris, J. (2017). Bayesian methods for addressing long-standing problems in associative learning: The case of PREE. *Q. J. Exper. Psychol.*, in press.
- Bohm, D. (1990). A new theory of the relationship of mind and matter. *Philos. Psychol.* *3*, 271.
- Bohm, D. (2002). *Wholeness and the Implicate Order*. Hoboken, NJ: Routledge.
- Bouton, M., Frohardt, R., Sunsay, C., Waddell, J., & Morris, R. (2008). Contextual control of inhibition with reinforcement: Adaptation and timing mechanisms. *J. Exp. Psychol. Anim. Behav. Process* *34*, 223.
- Bower, G.H. (1994). A turning point in mathematical learning theory. *Psychol. Rev.* *101*, 290.
- Braun, D.A., Ortega, P.A., Theodorou, E., & Schaal, S. (2011). Path integral control and bounded rationality. *2011 IEEE Symposium on Adaptive Dynamic Programming and Reinforcement Learning (ADPRL)*, 202–209.
- Bruza, P., Busemeyer, J.R., & Gabora, L. (2009). Introduction to the special issue on quantum cognition. *J. Math. Psychol.* *53*, 303.
- Bruza, P., Sofge, D., Lawless, W., van Rijsbergen, C.J., & Klusch, M. (Eds.) (2009). *Quantum Interaction. Third*

- International Symposium, QI 2009*. Heidelberg, Germany: Springer-Verlag
- Bruza, P.D., Wang, Z., & Busemeyer, J.R. (2015). Quantum cognition: a new theoretical approach to psychology. *Trends Cog. Sci.* 19, 383.
- Busemeyer, J.R., & Bruza, P.D. (2012). *Quantum Models of Cognition and Decision*. Cambridge, UK: Cambridge University Press.
- Busemeyer, J.R., Pothos, E.M., Franco, R., & Trueblood, J.S. (2011). A quantum theoretical explanation for probability judgment errors. *Psychol. Rev.* 118, 193.
- Busemeyer, J.R., Dubois, F., Lambert-Mogiliansky, A., & Melucci, M. (2012) *Quantum Interaction. Sixth International Symposium, QI 2012* Springer-Verlag Heidelberg Germany.
- Busemeyer, J.R., Wang, Z., Khrennikov, A., & Basieva, I. (2014). Applying quantum principles to psychology. *Phys. Scr.* T163, 014007.
- Busemeyer, J.R., Wang, Z., & Lambert-Mogiliansky, A. (2009). Empirical comparison of Markov and quantum models of decision making. *J. Math. Psychol.* 53, 423.
- Busemeyer, J.R., Wang, Z., & Townsend, J.T. (2006). Quantum dynamics of human decision-making. *J. Math. Psychol.* 50, 220.
- Bush, R.R., & Mosteller, F. (1951a). A mathematical model for simple learning. *Psychol. Rev.* 58, 313; reprinted in Mosteller (2006), pp. 221–234.
- Bush, R.R., & Mosteller, F. (1951b). A model for stimulus generalization and discrimination. *Psychol. Rev.* 58, 413; reprinted in Mosteller (2006), pp. 235–250.
- Bush, R.R., & Mosteller, F. (1953). A stochastic model with applications to learning. *Ann. Math. Stat.* 24, 559.
- Calcagni, G. (2018). The geometry of learning. *J. Math. Psychol.* 84, 74 [arXiv:1605.00591].
- Çevik, M.Ö. (2014). Habituation, sensitization, and Pavlovian conditioning. *Front. Integr. Neurosci.* 8, 13.
- Dickinson, A., & Balleine, B.W. (2002). The role of learning in the operation of motivational systems.. In C.R. Gallistel (Ed.), *Stevens' Handbook of Experimental Psychology. Vol. 3. Learning, Motivation and Emotion* (pp. 497–533). New York, NY: Wiley.
- Dixon, J.A., Stephen, D.G., Boncoddio, R.A., & Anastas, J. (2010). The self-organization of cognitive structure. *Psychol. Learn. Motiv.* 52, 343.
- Dixon, J.A., Holden, J.G., Mirman, D., & Stephen, D.G. (2012). Multifractal dynamics in the emergence of cognitive structure. *Topics Cogn. Sci.* 4, 51.
- Dukhayil, A., & Lyons, J.E. (1973). The effect of overtraining on behavioral contrast and the peak-shift. *J. Exp. Anal. Behav.* 20, 253.
- Eke, A., Herman, P., Kocsis, L., & Kozak, L.R. (2002). Fractal characterization of complexity in temporal physiological signals. *Physiol. Meas.* 23, R1.
- Estes, W.K. (1950) Toward a statistical theory of learning. *Psychol. Rev.* 57, 94.
- Estes, W.K. (1956). The problem of inference from curves based on group data. *Psychol. Bull.* 53, 134.
- Estes, W.K., & Burke, C.J. (1953). A theory of stimulus variability in learning. *Psychol. Rev.* 60, 276.
- Fakhari, P., Rajagopal, K., Balakrishnan, S.N., & Busemeyer, J.R. (2013). Quantum inspired reinforcement learning in changing environment. *New Math. Nat. Comp.* 9, 273.
- Farrell, S., Wagenmakers, E.-J., & Ratcliff, R. (2006). 1/f noise in human cognition: is it ubiquitous, and what does it mean?. *Psychon. Bull. Rev.* 13, 737.
- Farshidian, F., & Buchli, J. (2013). Path integral stochastic optimal control for reinforcement learning (unpublished).
- Finger, F.W. (1942). The effect of varying conditions of reinforcement upon a simple running response. *J. Exper. Psychol.* 30, 53.
- Fonda, L., Ghirardi, G.C., & Rimini, A. (1978). Decay theory of unstable quantum systems. *Rep. Prog. Phys.* 41, 587.
- Fujita, Y., Wideman, R.D., Speck, M., Asadi, A., King, D.S., Webber, T.D., Haneda, M., & Kieffer, T.J. (2009). Incretin release from gut is acutely enhanced by sugar but not by sweeteners in vivo. *Am. J. Physiol. Endocrinol. Metab.* 296, E473.
- Gallistel, C.R. (2012). On the evils of group averaging: Commentary on Nevin's "Resistance to extinction and behavioral momentum.". *Behav. Proc.* 90, 98.
- Gallistel, C.R., Fairhurst, S., & Balsam, P. (2004). The learning curve: implications of a quantitative analysis. *Proc. Nat. Acad. Sci. USA* 101, 13124.
- Gilden, D.L. (2001). Cognitive emissions of 1/f noise. *Psychol. Rev.* 108, 33.
- Gilden, D.L., Thornton, T., & Mallon, M.W. (1995). 1/f noise in human cognition. *Science* 267, 1837.
- Glautier, S. (2013). Revisiting the learning curve (once again). *Front. Psychol.* 4, 982.
- Gür, E., Duyan, Y.A., & Balcı, F. (2018). Spontaneous integration of temporal information: implications for representational/computational capacity of animals. *Anim. Cogn.* 21, 3.
- Hagan, S., Hameroff, S.R., & Tuszyński, J.A. (2002). Quantum computation in brain microtubules: decoherence and biological feasibility. *Phys. Rev. E* 65, 061901 [arXiv:quant-ph/0005025].
- Haubold, H.J., Mathai, A.M., & Saxena, R.K. (2001). Mittag-Leffler functions and their applications. *J. Appl. Math.* 2011, 298628 [arXiv:0909.0230].
- Hayes, K.J. (1953). The backward curve: a method for the study of learning. *Psychol. Rev.* 60, 269.
- Hearst, E. (1971). Contrast and stimulus generalization

- following prolonged discrimination training. *J. Exp. Anal. Behav.* **15**, 355.
- Holden, J.G. (2005). Gauging the fractal dimension of response times from cognitive tasks. In M.A. Riley & G.C. Van Orden (Eds.), *Contemporary Nonlinear Methods for Behavioral Scientists: A Webbook Tutorial* (pp. 267–318).
- Holden, J.G. (2013). Cognitive effects as distribution rescaling. *Ecol. Psychol.* **25**, 256.
- Holden, J.G., Van Orden, G.C., & Turvey, M.T. (2009). Dispersion of response times reveals cognitive dynamics. *Psychol. Rev.* **116**, 318.
- Holden, J.G., Choi, I., Amazeen, P.G., & Van Orden, G. (2011). Fractal  $1/f$  dynamics suggest entanglement of measurement and human performance. *J. Exp. Psychol. Hum. Percept. Perform.* **37**, 935.
- Hull, C.L. (1943). *Principles of Behavior*. New York, NY: Apple-Century-Crofts.
- Ihlen, E.A.F., & Vereijken, B. (2010). Interaction-dominant dynamics in human cognition: beyond  $1/f^\alpha$  fluctuation. *J. Exp. Psychol. Gen.* **139**, 436.
- Ihlen, E.A.F., & Vereijken, B. (2013). Multifractal formalisms of human behavior. *Hum. Mov. Sci.* **32**, 633.
- Jaksic, H., Vause, T., Frijters, J.C., & Feldman, M. (2018). A comparison of a novel application of hierarchical linear modeling and nonparametric analysis for single-subject designs. *Behav. Anal. Res. Prac.* **18**, 203.
- Jeffreys, H. (1961). *Theory of Probability (3rd edition)*. Oxford, UK: Oxford University Press.
- Jozefowicz, J., Witnauer, J.E., & Miller, R.R. (2011). Two components of responding in Pavlovian lick suppression. *Learn. Behav.* **39**, 138.
- Jung, C.G., & Pauli, W. (1955). *Naturerklärung und Psyche*. Zürich, Switzerland: Rascher. Translated by P. Silz in *The Interpretation of Nature and the Psyche*. Pantheon New York NY 1955.
- Kappen, H.J. (2007). An introduction to stochastic control theory, path integrals and reinforcement learning. *AIP Conf. Proc.* **887**, 149.
- Kass, R.E., & Raftery, A.E. (1995). Bayes Factors. *J. Amer. Stat. Assoc.* **90**, 773.
- Kaye, H., & Pearce, J.M. (1984). The strength of the orienting response during Pavlovian conditioning. *J. Exp. Psychol. Anim. Behav. Process.* **10**, 90.
- Kello, C.T., Beltz, B.C., Holden, J.G., & Van Orden, G.C. (2007). The emergent coordination of cognitive function. *J. Exp. Psychol. Gen.* **136**, 551.
- Kello, C.T., Anderson, G.G., Holden, J.G., & Van Orden, G.C. (2008). The pervasiveness of  $1/f$  scaling in speech reflects the metastable basis of cognition. *Cogn. Sci.* **32**, 1217.
- Kello, C.T., Brown, G.D.A., Ferrer-i-Cancho, R., Holden, J.G., Linkenkaer-Hansen, K., Rhodes, T., & Van Orden, G.C. (2010). Scaling laws in cognitive sciences. *Trends Cogn. Sci.* **14**, 223.
- Kemble, E.C. (1935). A contribution to the theory of the B. W. K. method. *Phys. Rev.* **48**, 549.
- Kilbas, A.A., Srivastava, H.M., & Trujillo, J.J. (2006) *Theory and Applications of Fractional Differential Equations*. Amsterdam, The Netherlands: Elsevier.
- Killeen, P.R., & Nevin, J.A. (2018). The basis of behavioral momentum in the nonlinearity of strength. *J. Exp. Anal. Behav.* **109**, 4.
- Killeen, P.R., & Pellón, R. (2013). Adjunctive behaviors are operants. *Learn. Behav.* **41**, 1.
- Kimmel, H.D., & Burns, R.A. (1975). Adaptational aspects of conditioning. In W.K. Estes (Ed.), *Handbook of Learning and Cognitive Processes. Vol. 2* (pp. 99–142). Hillsdale, NJ: Erlbaum.
- Le Pelley, M.E. (2004). The role of associative history in models of associative learning: a selective review and a hybrid model. *Q. J. Exp. Psychol.* **57**, 193.
- Likens, A.D., Fine, J.M., Amazeen, E.L., Amazeen, P.G. (2015). Experimental control of scaling behavior: what is not fractal?. *Exp. Brain Res.* **233**, 2813.
- Mackintosh, N.J. (1975). A theory of attention: Variations in the associability of stimuli with reinforcement. *Psychol. Rev.* **82**, 276.
- Mazur, J.E., & Hastie, R. (1978). Learning as accumulation: A reexamination of the learning curve. *Psychol. Bull.* **85**, 1256.
- Merrill, M. (1931). The relationship of individual growth to average growth. *Hum. Biol.* **3**, 37.
- Millenson, J.R. (1963). Random interval schedules of reinforcement. *J. Exp. Anal. Behav.* **6**, 437.
- Mosteller, F. (1958). Stochastic models for the learning process. *Proc. Amer. Philos. Soc.* **102**, 53 (1958); [reprinted](#) in Mosteller (2006), pp. 295–307.
- Mosteller, F. (2006). S.E. Fienberg & D.C. Hoaglin (Eds.), *Selected Papers of Frederick Mosteller*. New York, NY: Springer.
- Newell, A., & Rosenbloom, P.S. (1981). *Mechanisms of Skill Acquisition and the Law of Practice*. Hillsdale, NJ: Erlbaum.
- Ornitz, E.M., & Guthrie, D. (1989). Long-term habituation and sensitization of the acoustic startle response in the normal adult human. *Psychophysiol.* **26**, 166.
- Overmier, J.B., Payne, R.J., Brackbill, R.M., Linder, B., & Lawry, J.A. (1979). On the mechanism of the post-asymptotic CR decrement phenomenon. *Acta Neurobiol. Exp. (Warsaw)* **39**, 603.
- Packer, J.S., & Siddle, D.A.T. (1987). The effects of signal value on short- and long-term habituation. *Biol. Psychol.* **24**, 261.
- Pan, Y., Theodorou, E.A., & Kontitsis, M. (2014). Model-based path integral stochastic control: a Bayesian non-

- parametric approach. Preprint [arXiv:1412.3038](https://arxiv.org/abs/1412.3038).
- Pan, Y., Theodorou, E.A., & Kontitsis, M. (2014). Sample efficient path integral control under uncertainty. Preprint [arXiv:1509.01846](https://arxiv.org/abs/1509.01846).
- Pavlov, I.P. (1927). *Conditioned Reflexes*. London, UK: Oxford University Press.
- Pearce, J.M., & Hall, G. (1980). A model for Pavlovian learning: variations in the effectiveness of conditioned but not of unconditioned stimuli. *Psychol. Rev.* *87*, 532.
- Pellón, R., Íbías, J., & Killeen, P.R. (2018). Delay gradients for spout-licking and magazine-entering induced by a periodic food schedule. *Psychol. Record* *68*, 151.
- Pellón, R., & Killeen, P.R. (2015). Responses compete and collaborate, shaping each other's distributions: Commentary on Boakes, Patterson, Kendig, and Harris (2015). *J. Exp. Psychol. Anim. Learn. Cogn.* *41*, 444.
- Penrose, R. (1989). *The Emperor's New Mind*. Oxford, UK: Oxford University Press
- Pickens, C.L., Golden, S.A., Adams-Deutsch, T., Nair, S.G., & Shaham, Y. (2009). Long-lasting incubation of conditioned fear in rats. *Biol. Psychiatry* *65*, 881.
- Plaud, J.J., Gaither, G.A., Amato Henderson, S., & Devitt, M.K. (1997). The long-term habituation of sexual arousal in human males: A crossover design. *Psychol. Record* *47*, 385.
- Pothos, E.M., & Busemeyer, J.R. (2011). Formalizing heuristics in decision-making: a quantum probability perspective. *Front. Psychol.* *2*, 289.
- Pothos, E.M., Busemeyer, J.R., Shiffrin, R.M., & Yearsley, J.M. (2017). The rational status of quantum cognition. *J. Exp. Psychol. Gen.* *146*, 968
- Rescorla, R.A., & Wagner, A.R. (1972). A theory of Pavlovian conditioning: variations in the effectiveness of reinforcement and nonreinforcement. In A.H. Black & W.F. Prokasy (Eds.), *Classical Conditioning II* (pp. 64–99). New York, NY: Appleton-Century-Crofts.
- Ricciardi, L.M., & Umezawa, H. (1967). Brain and physics of many-body problems. *Kibernetik* *4*, 44.
- Riley, M.A., & Holden, J.G. (2012). Dynamics of cognition. *WIREs Cogn. Sci.* *3*, 593.
- Schwarz, G. (1978). Estimating the dimension of a model. *Ann. Statist.* *6*, 461.
- Sclafani, A., & Ackroff, K. (1994). Glucose- and fructose-conditioned flavor preferences in rats: taste versus postingestive conditioning. *Physiol. Behav.* *56*, 399.
- Shimbori, T., & Kobayashi, T. (2000). Complex eigenvalues of the parabolic potential barrier and Gel'fand triplet. *Nuovo Cim. B* *115*, 325 (2000) [[arXiv:math-ph/9910009](https://arxiv.org/abs/math-ph/9910009)].
- Shimbori, T. (2000). Operator methods of the parabolic potential barrier. *Phys. Lett. A* *273*, 37 [[arXiv:quant-ph/9912073](https://arxiv.org/abs/quant-ph/9912073)].
- Sidman, M. (1952). A note on functional relations obtained from group data. *Psychol. Bull.* *49*, 263.
- Smith, P.L., & Little, D.R. (2018). Small is beautiful: in defense of the small-*N* design. *Psychon. Bull. Rev.* *xx*, xxx.
- Solomon, R.L., & Corbit, J.D. (1974). An opponent-process theory of motivation: I. Temporal dynamics of affect. *Psychol. Rev.* *81*, 119.
- Stanford Encyclopedia of Philosophy (2015). <https://plato.stanford.edu/entries/qt-consciousness>.
- Stapp, H.P. (2009). *Mind, Matter, and Quantum Mechanics*. Berlin, Germany: Springer
- Stephen, D.G., Dixon, J.A., & Isenhower, R.W. (2009a). Dynamics of representational change: entropy, action, and cognition. *J. Exp. Psychol. Hum. Percept. Perform.* *35*, 1811.
- Stephen, D.G., Boncoddò, R.A., Magnuson, J.S., & Dixon, J.A. (2009b). The dynamics of insight: mathematical discovery as a phase transition. *Memory Cogn.* *37*, 1132.
- Sudbery, A. (1984). The observation of decay. *Ann. Phys. (N.Y.)* *157*, 512.
- Swithers, S.E., & Hall, W.G. (1994). Does oral experience terminate ingestion?. *Appetite* *23*, 113.
- Tegmark, M. (2000). Importance of quantum decoherence in brain processes. *Phys. Rev. E* *61*, 4194 [[arXiv:quant-ph/9907009](https://arxiv.org/abs/quant-ph/9907009)].
- Terrace, H.S. (1966). Behavioral contrast and the peak-shift: effects of extended discrimination training. *J. Exp. Anal. Behav.* *9*, 613.
- Theodorou E.A., Iterative Path Integral Stochastic Optimal Control: Theory and Applications to Motor Control. PhD Thesis (U. Southern California, U.S.A., 2011).
- Theodorou E., Buchli J., & Schaal, S. (2010). Reinforcement learning of motor skills in high dimensions: a path integral approach. *Robotics and Automation (ICRA), 2010 IEEE International Conference on*, 2397–2403.
- Theodorou E., Buchli J., & Schaal, S. (2010). A generalized path integral control approach to reinforcement learning. *J. Machine Learn. Res.* *11*, 3137.
- Theodorou, E., Stulp, F., Buchli, J., & Schaal, S. (2011). An iterative path integral stochastic optimal control approach for learning robotic tasks. *IFAC Proc. Vol.* *44*, 11594.
- Thompson, R.F. (2009). Habituation: a history. *Neurobiol. Learn. Mem.* *92*, 127.
- Thornton, T.L., & Gilden, D.L. (2005). Provenance of correlations in psychological data. *Psychon. Bull. Rev.* *12*, 409.
- Trueblood, J.S., & Busemeyer, J.R. (2012). A quantum probability model of causal reasoning. *Front. Psychol.* *3*, 138.

- Urcelay, G.P., Witnauer, J.E., & Miller, R.R. (2012). The dual role of the context in postpeak performance decrements resulting from extended training. *Learn. Behav.* *40*, 476.
- van den Broek, B., Wiegerinck, W., & Kappen, B. (2008). Graphical model inference in optimal control of stochastic multi-agent systems. *J. Art. Int. Res.* *32*, 95.
- Van Orden, G.C., Holden, J.G., & Turvey, M.T. (2003). Self-organization of cognitive performance. *J. Exp. Psychol. Gen.* *132*, 331.
- Van Orden, G.C., Holden, J.G., & Turvey, M.T. (2005). Human cognition and  $1/f$  scaling. *J. Exp. Psychol. Gen.* *134*, 117.
- Van Orden, G.C., Kello, C.T., & Holden, J.G. (2010). Situated behavior and the place of measurement in psychological theory. *Ecol. Psychol.* *22*, 24.
- Wagenmakers, E.-J., Farrell, S., & Ratcliff, R. (2004). Estimation and interpretation of  $1/f^\alpha$  noise in human cognition. *Psychon. Bull. Rev.* *11*, 579.
- Wagenmakers, E.-J., Farrell, S., & Ratcliff, R. (2005). Human cognition and a pile of sand: a discussion on serial correlations and self-organized criticality. *J. Exp. Psychol. Gen.* *135*, 108.
- Wagenmakers, E.-J., van der Maas, H.L.J., & Farrell, S. (2012). Abstract concepts require concrete models: why cognitive scientists have not yet embraced nonlinearly coupled, dynamical, self-organized critical, synergistic, scale-free, exquisitely context-sensitive, interaction-dominant, multifractal, interdependent brain-body-niche systems. *Topics Cogn. Sci.* *4*, 87.
- Wagner, A.R. (1981). SOP: a model of automatic memory processing in animal behavior. In N.E. Spear & R.R. Miller (Eds.), *Information Processing in Animals: Memory Mechanisms* (pp. 5–47). Hillsdale, NJ: Erlbaum.
- Wagner, A.R., & Rescorla, R.A. (1972). Inhibition in Pavlovian conditioning: applications of a theory. In M.S. Halliday & R.A. Boakes (Eds.), *Inhibition and Learning* (pp. 301–336). London, UK: Academic Press.
- Wagner, A.R., & Vogel, E.H. (2009). Conditioning: theories. *Encyclopedia of Neuroscience* *3*, 49.
- Wigner, E.P. (1967). Remarks on the mind-body question. In E.P. Wigner (Ed.), *Symmetries and Reflections* (pp. 171–184). Bloomington, IN: Indiana University Press.
- Witnauer, J.E., Hutchings, R., & Miller, R.R. (2017). Methods of comparing associative models and an application to retrospective reevaluation. *Behav. Proc.* *144*, 20.
- Yearsley, J.M., & Busemeyer, J.R. (2015). Quantum cognition and decision theories: a tutorial. *J. Math. Psychol.* *74*, 99.
- Young, M.E. (2018). A place for statistics in behavior analysis. *Behav. Anal. Res. Prac.* *18*, 193.
- Yuce, C., Kilic, A., & Coruh, A. (2006). Inverted oscillator. *Phys. Scr.* *74*, 114 [arXiv:quant-ph/0703234].